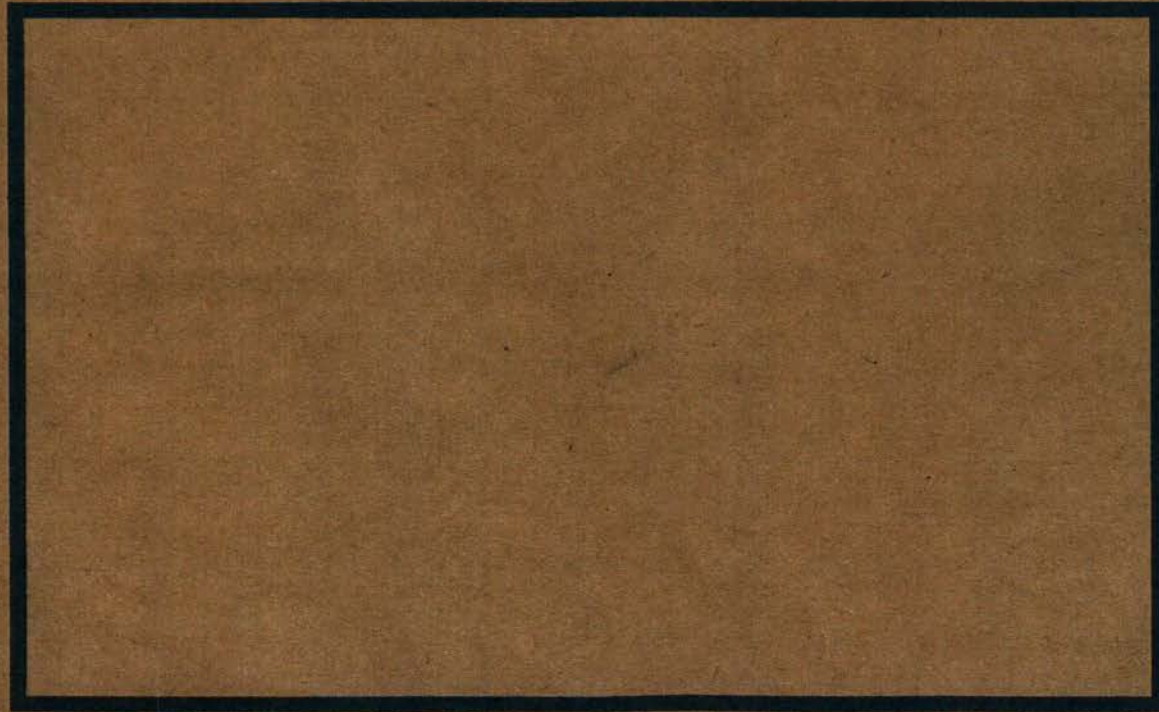


ENG 201-(EQC 1991/18)

**Behaviour of Reinforced Concrete Interior Beam-Column Joints
Designed Using High Strength Concrete and Steel**

*Xian Zuo Xin, supervised by R Park and H Tanaka, Department of
Civil Engineering, University of Canterbury*



RESEARCH REPORT

Behaviour of Reinforced Concrete Interior Beam-Column Joints Designed Using High Strength Concrete and Steel

Xian Zuo Xin

Supervised by R. Park and H. Tanaka

July 1992

92-3

Department of Civil Engineering

**University of Canterbury
Christchurch New Zealand**

**BEHAVIOUR OF REINFORCED CONCRETE
INTERIOR BEAM-COLUMN JOINTS
DESIGNED USING HIGH STRENGTH CONCRETE AND STEEL**

**A Research Report Based on the
Master of Engineering (Civil) Thesis**

of

XIAN ZUO XIN

Supervised by R Park and H Tanaka

This research project was supported by the Earthquake and War Damage Commission of New Zealand as Research Project 91/18 "Reinforced Concrete Beam-Column Joints of Building Frames".

**University of Canterbury
Christchurch, New Zealand**

July 1992

ACKNOWLEDGEMENTS

This research was carried out in the Department of Civil Engineering, University of Canterbury, New Zealand.

I wish to express my heartfelt emotion to Professor R. Park and Dr H. Tanaka for their valuable assistance and encouragement as supervisors of this project.

Professor T. Paulay is thanked for his interest and advice.

I am thankful to Messrs N.J. Hickey and P.A. Murphy for their enthusiasm and help during testing. Also acknowledged are Mr G.E. Hill for his assistance and arrangement, Mr H.H. Crowther for arranging the purchase of materials and Mr M. Roestenburg for his photographic work.

Thanks are extended to Messrs P.C. Cheung and J. Restrepo for their helpful suggestions.

The University Fees Scholarship provided by the University of Canterbury is gratefully acknowledged.

The research project was sponsored by the Earthquake and War Damage Commission (Project 91/18). That support is also gratefully acknowledged.

Finally, I would like to thank my wife and my parents and brother as well as my friends for their support and encouragement during the past two years.

ABSTRACT

This report deals with the behaviour of interior beam-column joints of reinforced concrete ductile frames using Grade 430 steel bar under simulated earthquake loading.

Six specimens with symmetrical or unsymmetrical longitudinal reinforcement from Grade 430 steel bar were tested to investigate the anchorage performance of the beam bars passing through the joint core. The experimental results indicated that the use of high-strength concrete was beneficial. The effect of the ratio of area of bottom steel to top steel was found to be significant when determining the anchorage length of beam bars in the joint core.

Based on the test results and other previous research works in the University of Canterbury, a recommendation was proposed for a limitation on the beam bar diameter of beam bar passing through an interior beam-column joint.

TABLE OF CONTENTS

	<u>Page</u>
ABSTRACT	
ACKNOWLEDGEMENTS	
TABLE OF CONTENTS	
NOTATION	
REFERENCES	
CHAPTER 1 : <u>BEAM-COLUMN JOINT</u>	1
1.1 INTRODUCTION	1
1.2 LITERATURE REVIEW	3
1.3 THE AIMS OF THIS PROJECT	6
CHAPTER 2 : <u>MODEL OF THE BEHAVIOUR INTERIOR</u>	8
<u>BEAM-COLUMN JOINTS</u>	
2.1 ACTIONS ON INTERIOR PLANE FRAME JOINTS	8
2.2 SHEAR RESISTING MECHANISMS FOR INTERIOR JOINTS	11
2.2.1 Diagonal Compression Concrete Strut Mechanism	13
2.2.2 Truss Mechanism	
2.2.3 Additional Sources of Shear Resistance	14
2.3 THE RELATIONSHIP OF BOND AND SHEAR RESISTING MECHANISMS IN THE JOINT	15
CHAPTER 3 : <u>CODE REQUIREMENTS FOR CONVENTIONAL</u>	24
<u>BEAM-COLUMN JOINTS</u>	
3.1 GENERAL	24

3.2	DESIGN ASSUMPTIONS	24
3.3	HORIZONTAL JOINT SHEAR	24
3.4	VERTICAL JOINT SHEAR	26
3.5	CONFINEMENT	27
3.6	BAR ANCHORAGE IN INTERIOR JOINTS	28
3.7	BAR ANCHORAGE AT EXTERIOR JOINTS	29
 CHAPTER 4 : <u>TEST PROGRAMME</u>		 31
4.1	INTRODUCTION	31
4.2	DESIGN OF UNITS	31
4.3	PROPERTIES OF MATERIALS	41
	4.3.1 Concrete	41
	4.3.2 Steel	43
4.4	FABRICATION OF THE UNITS	44
4.5	TEST RIG	45
4.6	INSTRUMENTATION	47
	4.6.1 General	47
	4.6.2 Load	47
	4.6.3 Displacements	48
	4.6.4 Joint Shear Distortion	48
	4.6.5 Beam Bar Slip	49
	4.6.6 Strains	49
	4.6.7 Observation of Cracking	51
4.7	LOADING SEQUENCE	51
 CHAPTER 5 : <u>TEST RESULTS OF UNIT 1</u>		 53
5.1	GENERAL OBSERVATIONS	53
	5.1.1 General	53
	5.1.2 Unit 1	53
	5.1.3 Unit 2	56
	5.1.4 Unit 3	59
	5.1.5 Unit 4	62
	5.1.6 Unit 5	65
	5.1.7 Unit 6	68

5.2	LOAD-DISPLACEMENT RESPONSE	71
5.3	BEAM BAR SLIP	75
5.4	COMPONENTS OF DISPLACEMENT	82
5.5	STRAIN VARIATION ALONG BEAM BAR	83
5.6	STRAIN VARIATION IN JOINT CORE HOOPS	83
 CHAPTER 6 : <u>DISCUSSION OF RESULTS</u>		105
6.1	UNITS WITH SYMMETRICAL LONGITUDINAL BEAM REINFORCEMENT	105
6.2	UNITS WITH UNSYMMETRICAL LONGITUDINAL BEAM REINFORCEMENT	106
6.3	COMPARISON OF THE RESULTS	108
6.4	BOND REQUIREMENT OF BEAM BAR IN AN INTERIOR BEAM-COLUMN JOINT	108
 CHAPTER 7 : <u>CONCLUSIONS AND SUGGESTIONS</u>		114
7.1	CONCLUSIONS	114
7.2	SUGGESTIONS FOR FUTURE RESEARCH	115
 APPENDIX A <u>THEORETICAL PREDICTION OF THE STRENGTH AND FIRST YIELD DISPLACEMENT OF TEST UNITS</u>		116
A.1	THEORETICAL STRENGTHS OF UNIT	116
A.2	CALCULATION OF FIRST YIELD DISPLACEMENT	117
A.3	THEORETICAL FIRST YIELD DISPLACEMENT	118
 APPENDIX B <u>ESTIMATED DEFORMATION OF THE BEAM</u>		120

NOTATION

A_b	area of gross section of beam
A_c	area of gross section of column
A_g	area of gross section of column
A_{sh}	total area of transverse bars with spacing s_h
A_s, A'_s	area of tension and compression longitudinal reinforcement of beam, respectively
A_{sc}, A'_{sc}	area of tension and compression reinforcement in one face of column
b_c	overall width of column
b_j	effective width of joint
b_w	web of width of beam
$C_c, C'_c, \text{ etc}$	compression stress resultant in concrete
C_j	joint shear participation factor = $V_{jh}/(V_{jx} + V_{jy})$
$C_s, C'_s, \text{ etc}$	compression stress resultant in reinforcement
d_b	reinforcing bar diameter
$d_{b,b}$	bottom beam bar diameter
$d_{b,t}$	top beam bar diameter
D_c	diagonal compression force resisted by concrete strut mechanism in joint core
D_s	diagonal compression force resisted by truss mechanism in joint core
E_c	modulus of elasticity of steel, MPa
f'_c	compressive strength of concrete, MPa
f_y	yield strength of reinforcement, MPa
f_{yh}	yield strength of horizontal joint reinforcement
f_{su}	ultimate strength of reinforcement, MPa

G	shear modulus of concrete
h''	dimension of the concrete core of the section measured perpendicular to the direction of the hoop bars to outside of the perimeter hoop
h_b	depth of beam
h_c	depth of column in the direction of horizontal shear to be considered
h'_c	reduce depth of column
$h_1...h_5$	distance between potentiometers above beam and beneath beam
I^b	moment of inertia about ideal centre axis of gross section of beam
I^c	moment of inertia of gross section of column
I^b_{cr}	moment of inertia of cracked beam section
I^c_{cr}	moment of inertia of cracked column section
k	factor to take into account the non-uniform distribution of shear stress
L_b	half of length of beam of test unit
L_c, L'_c	storey height of column between points of support of test unit
l_{db}	the basic development length of a deformed bar in compression
l_{dh}	the basic development length of a deformed bar in tension terminating
$l_1...l_5$	distance between centre-line of a beam sub-region and beam support point
M_1	positive beam moment at column face
M_2	negative beam moment at column face
P, P'	column axial load
P_e	minimum design axial load in compression on column
R_1, R_2	reaction force on beam support points
$S_1...S_5$	distance of a pair of potentiometers from column face or adjacent pair

s_h	centre to centre spacing of the hoop sets
s_r	the clear span of the bottom of ribs of steel bar
T, T', T'', T'''	tension force in reinforcement (subscripted)
u_0	unit bond force including overstrength of bar in tension
u_1, u_2	unit bond force
u_b	average bond stress
V	storey shear force
V_{b1}, V_{b2}	vertical shear force in beam
V_{ch}	horizontal joint shear strength provided by concrete strut mechanism
V_{col}, V_{col}'	design shear force
V_{cv}	vertical joint shear strength provided by concrete strut mechanism
V_{jh}	total horizontal shear force across a joint
V_{jv}	total vertical shear force across a joint
V_{jx}	total horizontal joint shear force in x direction
V_{jy}	total horizontal joint shear force in y direction
V_{sh}	ideal horizontal joint shear strength provided by horizontal joint shear reinforcement
V_{sv}	ideal vertical joint shear strength provided by vertical joint shear reinforcement
α	beam longitudinal steel overstrength factor
β	A_s'/A_s
β_i^b	a modification factor for the flexural rigidity of beam to include the effect from shear deformation
β_i^c	a modification factor for the flexural rigidity of column to include the effect from shear deformation
θ	an angle of the diagonal compression field to the horizontal
γ	distortion angle of joint core

Δ	storey displacement
Δ_y	yield storey displacement
$\Delta_b, \Delta_c, \Delta_j$	storey displacement from beam, column and joint deformations, respectively
$\Delta S_1 \dots \Delta S_5$	changes in distance of $S_1 \dots S_5$
$\Delta_{yb}, \Delta_{yc}, \Delta_{yj}$	yield storey displacement from beam, column and joint deformations respectively
Δ_{y1}, Δ_{y2}	storey displacement along pushing or pulling direction at three-quarters of theoretical horizontal ultimate load
$\Delta_{y,m}$	measured first yield displacement
$\Delta_{y,t}$	theoretical first yield displacement
$\Delta T_c, \Delta T'_c, \Delta T''_c$	the bond force transmitted from the beam and etc column longitudinal reinforcing to the concrete within the strut
δ, δ'	deformation of joint diagonal
ϵ_y	yield strain
ϵ_{sh}	strain at the commencement of strain hardin
ρ_t	area ratio of total column longitudinal reinforcement
ϕ	strength reduction factor

REFERENCES

1. Park, R. and Paulay, T., "Reinforced Concrete Structures", John Willy & Sons, New York, 1975, 769p.
2. CND/EERI, "EL-Asnam, Algeria Earthquake of October 10, 1980", Reconnaissance and Engineering Report, Earthquake Engineering Research Institute, Berkeley, California, January 1983.
3. Paulay, T. and Park, R., "Joints in Reinforced Concrete Frames Designed for Earthquake Resistance", Research Report 84-9, Department of Civil Engineering, University of Canterbury, Christchurch, 1984, 71p.
4. Hanson, N.W. and Conner, H.W., "Seismic Resistance of Reinforced Concrete Beam-Column Joints", Proceedings of the Structural Division, American Society of Civil Engineering, Vol.93, No.ST5, October 1967, 533-560 pp.
5. Megget, L.M., "Anchorage of Beam Reinforcement in Seismic Resistant Reinforced Concrete Frames", Master of Engineering Report, University of Canterbury, February 1971, 71p.
6. Renton, G., "The Behaviour of Reinforced Concrete Beam-Column Joints Under Cyclic Loading", Master of Engineering Report, University of Canterbury, February 1972, 162p.
7. Patton, R.N., "Behaviour of Reinforced Concrete Beam-Column Joints with Anchor Blocks", Master of Engineering Report, University of Canterbury, February 1972, 91p.
8. Park, R. and Paulay, T., "Behaviour of Reinforced Concrete Beam-Column Joints Under Cyclic Loading", Proceedings, Fifth World Conference on Earthquake Engineering, Paper 88, Vol.1, Session 2D, Rome, June 1973, 772-781 pp.

9. Yeoh, S.K., "Prestressed Concrete Beam-column Joints", Master of Engineering Report, University of Canterbury, February 1978, 71p.
10. Paulay, T., Park, R. and Priestley, M.J.N., "Reinforced Concrete Beam-Column Joints Under Seismic Actions", Journal of the American Concrete Institute, Proceedings, Vol.75, No. 11, November 1978, 585-593 pp.
11. Beckingsale, C.W., "Post-Elastic Behaviour of Reinforced Concrete Beam-Column Joints", Ph.D. Thesis, Department of Civil Engineering, University of Canterbury, April 1980, 359p.
12. NZS 3101: Part 1, "Code of Practice for the Design of Concrete Structures" and Part 2, "Commentary on Code of Practice for the Design of Concrete Structures", Standards Association of New Zealand, Wellington, 1982.
13. Birss, G.R., "The Elastic Behaviour of Earthquake Resistant Reinforced Concrete Interior Beam-Column joints", Research Report 78-13, Department of Civil Engineering, University of Canterbury, February 1978, 96p.
14. Miburn, J.R. and Park, R., "Behaviour of Reinforced Concrete Beam-Column Joints Designed to NZS 3101" Research Report 82-7, Department of Civil Engineering, University of Canterbury, February 1982, 105p.
15. Stevenson, E.C., "Fibre-Reinforced Concrete in Seismic Design", Research Report 80-7, Department of Civil Engineering, University of Canterbury, June 1980, 95p.
16. Fenwick, R.C. and Nguyen, H.T., "Reinforced Concrete Interior Beam-Column Joints for Seismic Loading", Report No. 220, Department of Civil Engineering, University of Auckland, January 1981, 58p.

17. Wong, P.K.C. Priestly, M.J.N. and Park, R., "Seismic Behaviour of Reinforced Concrete Frames Incorporating Beams With Distributed Reinforcement", Research Report 87-4, Department of Civil Engineering, University of Canterbury, 1987, 65p.
18. ACI-ASCE Committee 352, "Recommendations for Design of Beam-Column Joints in Monolithic Reinforced Concrete Structures" Draft 352R, October, 1989.
19. Dai, R. and Park, R., "A Comparison of the Behaviour of Reinforced Concrete Beam-Column joints Designed for Ductility and Limited Ductility", Research Report 87-4, Department of Civil Engineering, University of Canterbury, 1987, 65p.
20. Park, R. and Dai, R., "A Comparison of the Behaviour of Reinforced Concrete Beam-Column Joints Designed for Ductility and Limited Ductility", Bulletin of the New Zealand National Society for Earthquake Engineering, Vol. 21, No. 4, December 1988, 255-278.
21. Kazuhiro Kitayama, Shunsuke Otani and Hiroyuki Aoyama, "Earthquake Resistant Design Criteria for Reinforced Concrete Interior Beam-Column Joints", Pacific Conference on Earthquake Engineering, New Zealand, 5-8 August 1987, 315-326pp..
22. Cheung, P.C., Paulay, T. and Park, R., "Seismic Design of Reinforced Concrete Beam-Column Joints With Floor Slab", Research Report 91-4, Department of Civil Engineering, University of Canterbury, October 1991, 328p.
23. Cheung, P.C., Paulay, T. and Park, R., "Some Possible Revisions to the Seismic Provisions of the New Zealand Concrete Design Code Moment Resisting Frames" Pacific Conference on Earthquake Engineering, Auckland, New Zealand, 20-23 November, 1991, Volume 2, 79-90 pp.

24. 2/DZ 4203, "Second Draft for Comment, General Structural Design and Design Loadings for Buildings", Standards Association of New Zealand, Wellington, 1989.
25. NZS 4203:1984, "Code of Practice for General Structural Design and Design Loadings for Buildings", Standards Association of New Zealand, Wellington, 1984, 100p.
26. Leon, R.T., "Shear Strength and Hysteretic Behaviour of Interior Beam-Column Joints", Structural Journal, American Concrete Institute, Vol.87, No.1, January-February 1990, pp. 3-11.
27. Shunsuke Sugano, Toshio Nagashima, Hideki Kimura and Atushi Ichikawa "Behaviour of Beam-Column Joints using High-Strength Materials", ACI Special Report, 29 August, 1990.
28. Shunsuke Sugano, Toshio Nagashima, Hideki Kimura, Akio Tamura and Atushi Ichikawa, "Experimental Studies on Seismic Behaviour of Reinforced Concrete Members of High Strength Concrete", Second International Symposium On Utilization of High Strength Concrete, U.C. Berkeley, 20-23 May, 1990.
29. "Code of Practice for General Structural Design and Design Loadings for Buildings, NZS 4203:1984", Standards Association of New Zealand, Wellington, 1984.
30. Soleimani, D., Popov, E.P., and Bertero, V.V., "Hysteretic Behaviour of Reinforced Concrete Beam-Column Subassemblages", ACI Journal, Vol. 76, No. 11, November 1979, pp 1179-1195.
31. Paulay, T., and Priestley, M.J.N., "Seismic Design of Reinforced Concrete and Masonry Buildings", John Wiley and Sons, Inc., New York, 1992, pp 744.

CHAPTER 1

BEAM-COLUMN JOINT

1.1 INTRODUCTION

The ductile design method of earthquake resistant structures indicates that both strength and ductility are the criteria in designing a building to withstand severe earthquake loading. To absorb and dissipate an input earthquake energy, and to avoid collapse of tall reinforced concrete multistorey frames, a structural system with strong columns-weak beams must be required [1]. The joints connecting the columns and beams should not be weak link during seismic attack. A series of examples of beam-column joint failures, especially 1980 El Asnam earthquake [2], have made that is known that beam-column joints can be critical regions in reinforced concrete ductile moment resisting frames under severe earthquake action. To investigate the behaviour of beam-column joints in reinforced concrete ductile moment resisting frames, a great deal of experimental and analytical researches have been conducted in University of Canterbury since the early 1970's, which led to the current New Zealand design approach for the seismic design of reinforced concrete beam-column joints.

Beam-column joint cores are subjected to large shear forces due to lateral earthquake force and also need to provide sufficient anchorage length for longitudinal beam and column bars. Fig. 1.1 shows internal forces transmitted from adjacent members to the joint. It is obvious that the state of stress is quite complex in the joint. The design of a beam-column joint is a complicated problem. Some suggestions of design criteria for joints proposed by Paulay and Park[3] as follows:

- (1) The strength of a joint should not be less than the maximum strength of the weakest member it connects. This requirement is to ensure that failure will not occur in the joint core, and hence is to eliminate the need for repair of a relatively inaccessible region, and to prevent significant energy dissipation by shear and bond mechanisms in the joint core which undergo strength and stiffness degradation when subjected to cyclic loading in the inelastic range.

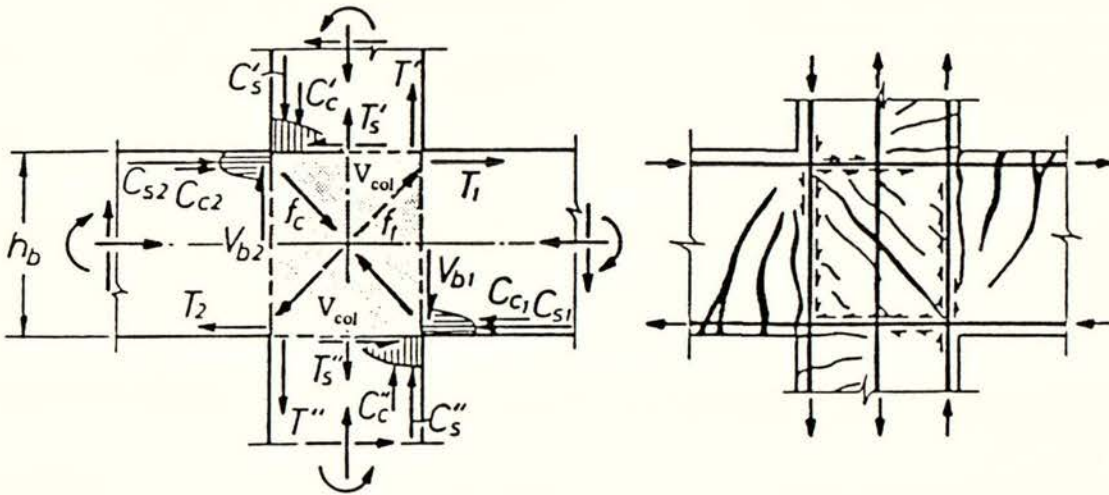


Fig.1.1 Internal forces on an interior beam-column joint core

- (2) The capacity of a column should not be jeopardised by possible strength degradation within the joint core due to cyclic inelastic displacements. The joint is an integral part of the column.
- (3) During moderate seismic disturbances, a joint should preferably respond within the elastic range. Joint core deformation should not significantly affect the frame stiffness and storey drift.
- (4) The reinforcement in the joint core necessary to ensure satisfactory performance should not cause undue construction difficulties.

1.2 LITERATURE REVIEW

A wide variety of studies on beam-column joints have been undertaken in many seismic prone countries, since the results of seven beam-column joints tested by Hanson and Conner [4] were first reported in 1967. The above research report indicated that the beam-column joints could be critical regions in reinforced concrete frames under seismic

actions. Either bond failure or shear failure in the joint was observed in almost all beam-column joints tested. The mechanisms of joint shear resistance were not clearly determined in the early studies.

Assessment of the results of the tests on beam-column joints conducted by several researchers [5,6,7] in the early 1970's resulted in the proposal of a model for joint core shear resistance proposed by Park and Paulay [8] in 1973. It was postulated that the shear resistance of the joint core was provided by a concrete diagonal compression strut mechanism and a truss mechanism requiring both horizontal and vertical shear reinforcement. Vertical shear reinforcement is necessary to form a truss mechanism in the joint, a finding which had been overlooked by all previous researchers. This was demonstrated by Yeoh and Park [9] who tested three beam-column joints in 1978. It was also suggested that no joint shear force could be carried by the concrete diagonal compression strut mechanism (See section 2.2.1), unless a significant column axial load was present, in reinforced concrete ductile moment resisting frames.

Paulay et al [10] in 1978 improved the previous model by demonstrating how the degree of participation of each of the mechanisms (concrete diagonal compression strut and truss) depended on the loading history and condition of the concrete in the joint core region in 1978. This paper clarified the mechanisms of joint core shear resistance. The need for vertical shear reinforcing in the joint core was emphasized again.

In the meantime, the results of tests on three interior beam-column joints by Beckingsale [11] showed close agreement with the predictions of the postulated model, which became widely accepted in New Zealand and formed the basis of the chapter on the design of beam-column joints in the NZS 3101:1982 [12]. Beckingsale also pointed out that some slippage of the longitudinal beam bars in post-elastic range had to be accepted.

To investigate the behaviour of beam-column joints with reduced contents of joint shear reinforcement, in 1978 Briss [13] tested two interior joints with less joint shear reinforcement than Beckingsale's joints, and with the same joint design shear force.

Even though the behaviour of joints was satisfactory when the test units were loaded in the elastic range, the performance of joints was unsatisfactory when loaded in the inelastic range.

In 1982, Milburn's [14] tests, conducted on two interior joints and two exterior joints, confirmed that the joint core shear reinforcing requirements in the NZS 3101:1982 were safe and pointed out that forcing the beam plastic hinges to form away from the column faces was advantageous for interior joints.

Over the last ten years, some test programmes [15, 16,17] (See Fig.1.2 and 1.3) have been conducted in New Zealand, which attempted to look for new effective construction techniques to reduce the content of joint core shear reinforcement, and to improve the bond condition in the joint region, have been conducted in New Zealand.

With the use of high strength materials, smaller member sections, and larger reinforcing bar diameter, special attention to the design and detailing of the joint has become more important [18].

In 1987, Dai and Park [19,20] reported the results of seismic load tests on four beam-column joints with gravity loading on the beams. Three of these joints did not satisfy the requirements for ductile detailing of NZS 3101:1982 for joint shear reinforcement and anchorage length. Although some pinching was observed in the lateral load versus displacement hysteresis loops, the performance was considered to be acceptable. It was concluded that the present NZS 3101:1982 provisions for beam bar diameters could be relaxed.

At the same time, the experimental work of four beam column joints had been completed by Kitayama et al [21]. They noted that bond deterioration and shear resistance in the joint were closely related and indicated that some pinching of the hysteresis loops should be permitted, since it made little difference to the dynamic response of the frame. The design joint shear force should be limited to prevent shear compression failure after the bond deterioration along the beam reinforcement in the joint core.

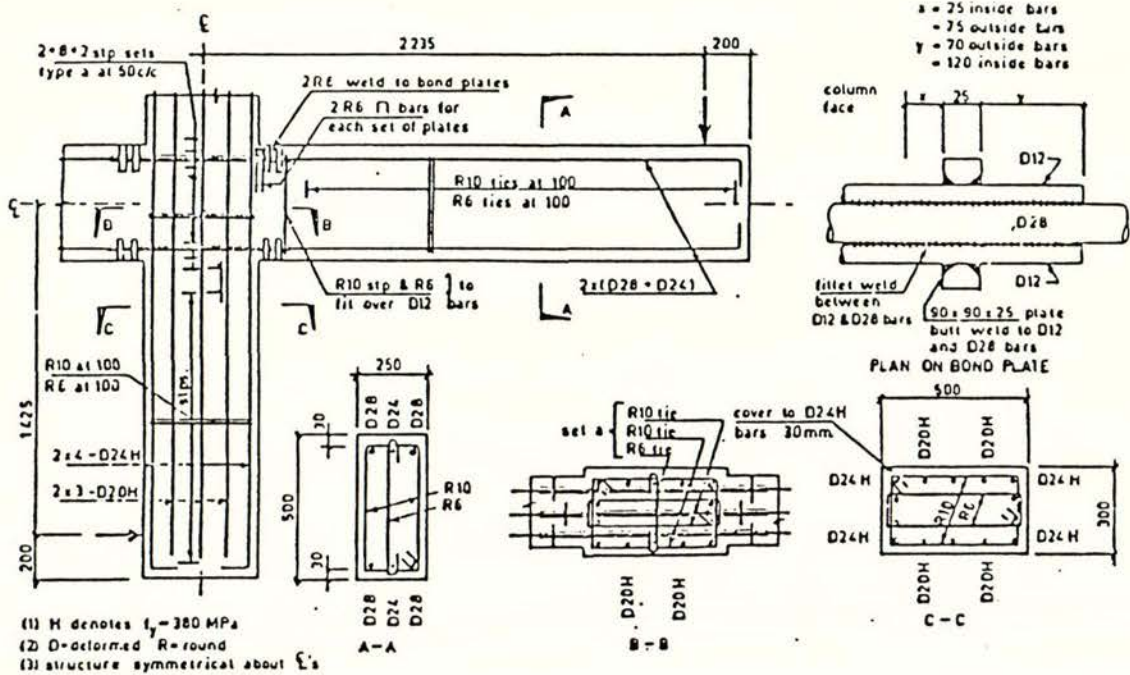


Fig.1.2 Joint with steel bond plates [16]

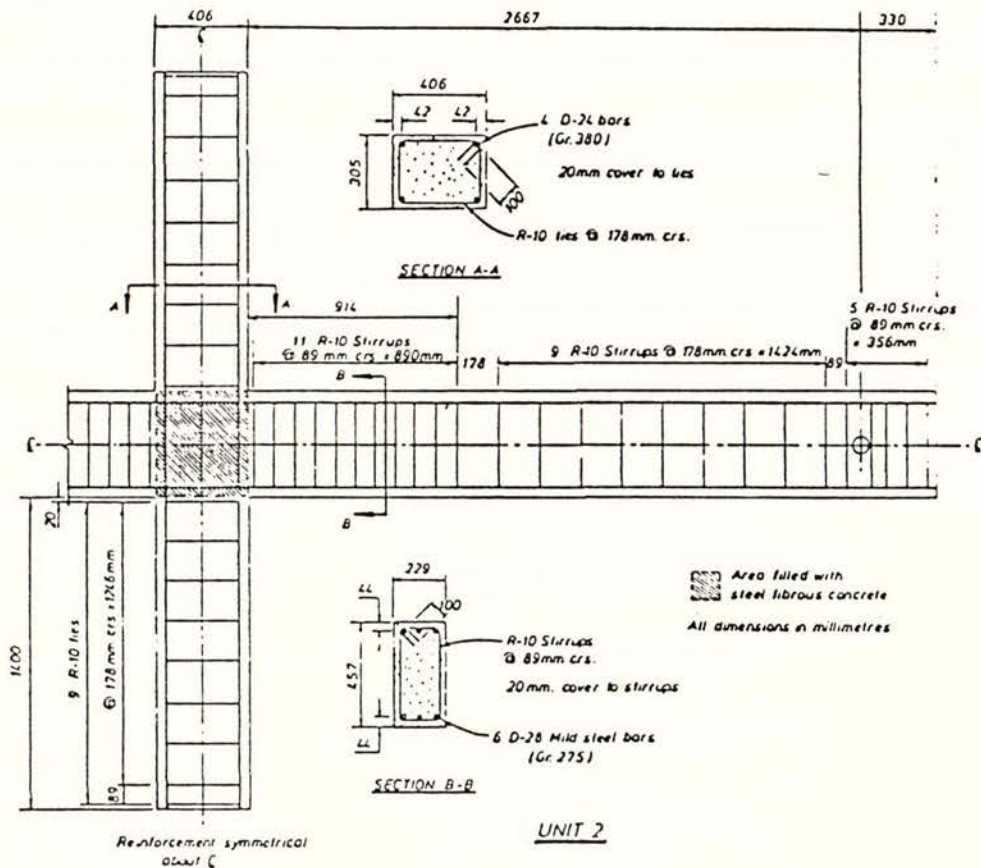


Fig.1.3 Joint with steel fibrous concrete in joint core [15]

Cheung, Paulay and Park [22,23], after testing and analyzing three full scale beam-column joints assemblies incorporating floor slabs, which were designed according to the New Zealand concrete design code provisions for ductile moment resisting frames, considered that current New Zealand design procedures could be relaxed a little in terms of both bond and shear strength requirements, and more refined models for bond strength and shear strength of joint cores were postulated.

1.3 THE AIMS OF THIS PROJECT

Most of the previous tests on reinforced concrete beam-column joints conducted at the University of Canterbury, have been on test specimens were with Grade 275 or 300 steel bar used as beam flexural reinforcement and conventional concrete compressive strengths. With the current availability of higher strength steel and concrete, it is evident that the anchorage lengths requirements of the longitudinal reinforcement passing through beam-column joint cores needs to be reassessed. The main purpose of this research project is to investigate the behaviour of beam-column joints in reinforced ductile moment resisting frames with a range of concrete compressive strengths and reinforced with Grade 430 steel.

Six interior beam-column joints were built and tested under simulated earthquake loading. Only the beam bar diameter of one specimen was designed according to the requirement for ductile detailing of NZS 3101:1982. The beam bar diameter of the others were based on the formula recommended by Park and Dai [20], which is a relaxation of the code requirement.

CHAPTER 2

MODEL OF THE BEHAVIOUR INTERIOR BEAM-COLUMN JOINTS2.1 ACTIONS ON INTERIOR PLANE FRAME JOINTS

The deflected shape of a moment resisting plane frame subjected to lateral seismic loading is shown in Fig. 2.1. For the sake of simplicity, all points of contraflexure are assumed at the mid-point of the members. The effects of gravity loads on the beams and higher modes of vibration and stiffness variation between storeys on the columns may often move the point of contraflexure well away from the mid-point positions.

A subassemblage of the frame with loading shown in Fig. 2.2 is same as that used for the the units in this project, except that no axial column load was applied, since that is the most critical case for the joint core shear strength and the bond strength of longitudinal beam bars within the joint core region.

In order to study the behaviour of the beam-column joint, it is necessary firstly to define moments and shears acting on the joint core region under seismic loading as shown in Fig. 2.3. By considering the equilibrium of moments about the centre of the joint core, and assuming $V_{col} = V'_{col}$, it is evident that

$$(M_1 + 0.5h_c V_{b1}) + (M_2 + 0.5h_c V_{b2}) - 0.5L_c V_{col} - 0.5L_c V'_{col} = 0 \quad (2.1)$$

The principle of strong column-weak beam is followed in the design of tall reinforced concrete ductile moment resisting frames. It implies that plastic hinges will occur at the column face in the beams. Due to larger inelastic storey displacements, some strain hardening of the tensile steel at a plastic hinge section in a beam may commence before the full ductile capacity of the section is reached, which leads an overstrength flexural reinforcing strengths being developed at the beam plastic hinges. Then the actions M and V are substituted for the overstrength values of M° and V° in

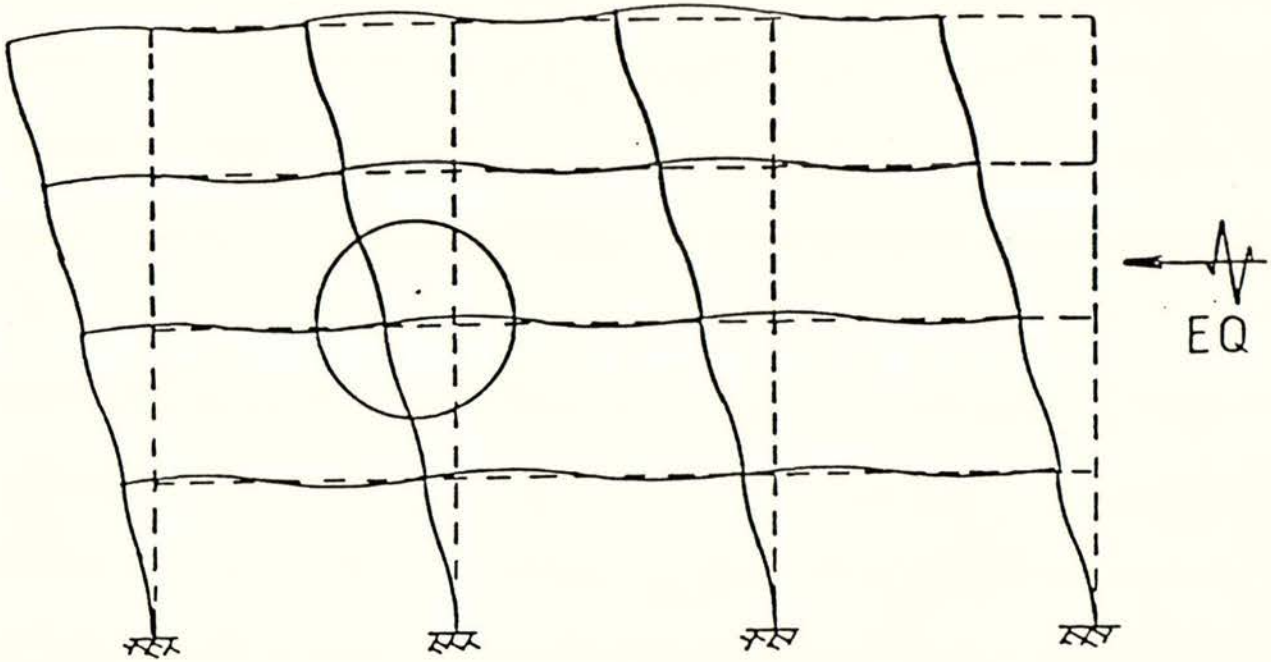


Fig. 2.1 Deflected shape of moment resisting framed structure subjected to lateral load

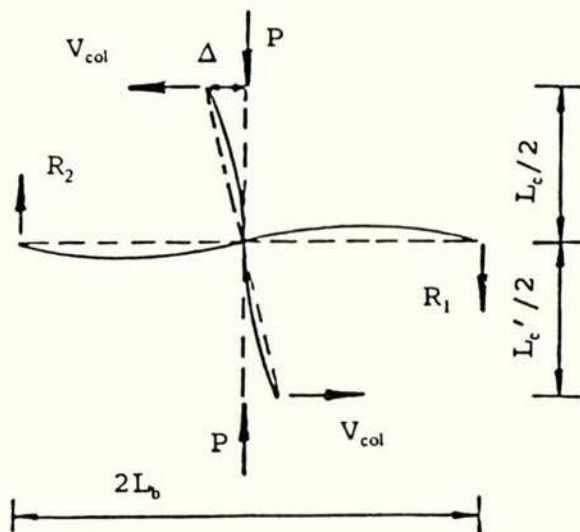


Fig. 2.2 The isolated beam-column joint subassembly

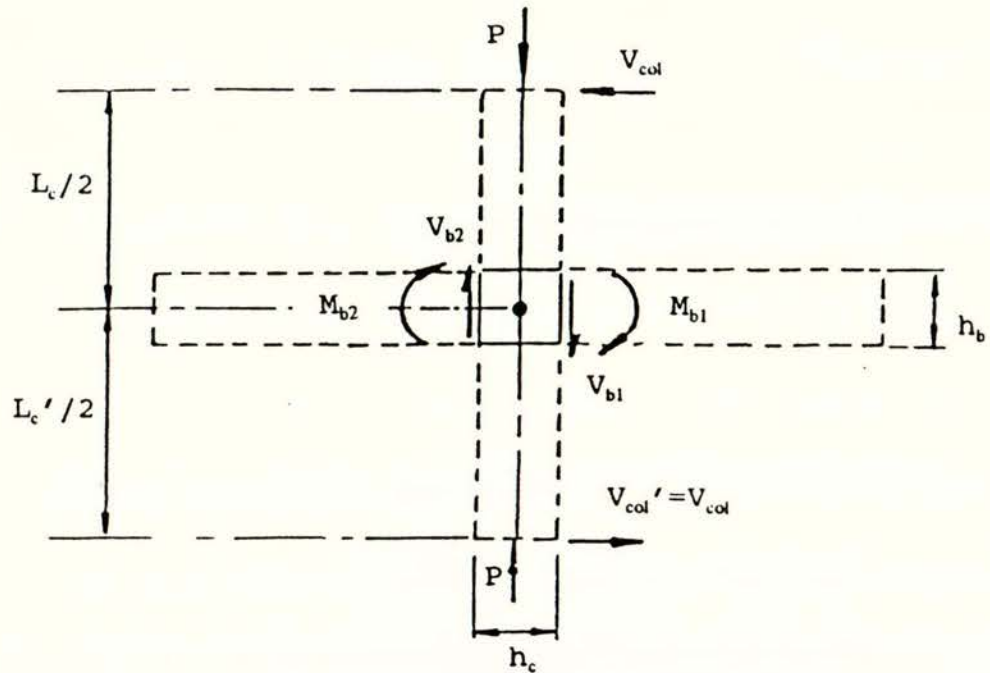


Fig. 2.3 Actions on an interior beam-column joint

the Eq. (2.1). Therefore

$$V_{col} = \frac{M_{b1}^{\circ} + M_{b2}^{\circ} + 0.5h_c(V_{b1}^{\circ} + V_{b2}^{\circ})}{0.5(L_c + L_c')} \quad (2.2)$$

The external and internal actions on an interior joint has been drawn in Fig.1.1. When adjacent beams develop their maximum possible flexural strength, the design horizontal shear force V_{jh} across the mid-depth of the joint core is

$$V_{jh} = T_1 + C_{c2} + C_{s2} - V_{col} \quad (2.3a)$$

$$V_{jh} = T_2 + C_{c1} + C_{s1} - V_{col} \quad (2.3b)$$

It can be noted that equilibrium of forces in the beam requires

$$T_1 = C_{c1} + C_{s1} \quad (2.4a)$$

$$T_2 = C_{c2} + C_{s2} \quad (2.4b)$$

Also an overstrength factor α is included when the tension forces T_1 and T_2 in the

reinforcement are calculated. In New Zealand α is commonly assume to be 1.25 for Grade 300 and 430 steel. Hence Eq.(2.3) can be rewritten as

$$V_{jh} = T_1 + T_2 - V_{col} \quad (2.5)$$

Correspondingly, the design vertical joint shear force V_{jv} is written as

$$V_{jv} = T' + C_c' + C_s' - V_{b1} \quad (2.6a)$$

$$V_{jv} = T'' + C_c'' + C_s'' - V_{b2} \quad (2.6b)$$

The ductile design approach implies that the columns are expected to remain elastic under seismic actions. Therefore, the overstrength factor is not applied to the tension forces T' and T'' in the column reinforcement. When the top and bottom beam bars are unsymmetrical, V_{b1} is not equal to V_{b2} .

By taking into account the distances between the stress resultants and member dimensions, the following expression is generally sufficiently accurate for design purposes to estimate the design vertical joint shear force,

$$V_{jv} = V_{jh} \frac{h_b}{h_c} \quad (2.7)$$

2.2 SHEAR RESISTING MECHANISMS FOR INTERIOR JOINTS

The current provisions of the New Zealand concrete design code [12] for the design of joints for shear resistance is based on strut and truss mechanisms (See Fig. 2.4) proposed by Park and Paulay. The strut mechanism has a diagonal compression strut acting along the diagonal of the joint panel as the resultant of concrete compression and shear forces around the joint (See Fig. 2.4(c)). The truss mechanism is made up by the bond force of the vertical and horizontal reinforcement and forces in the corner regions of the joint (See Fig. 2.5(d)).

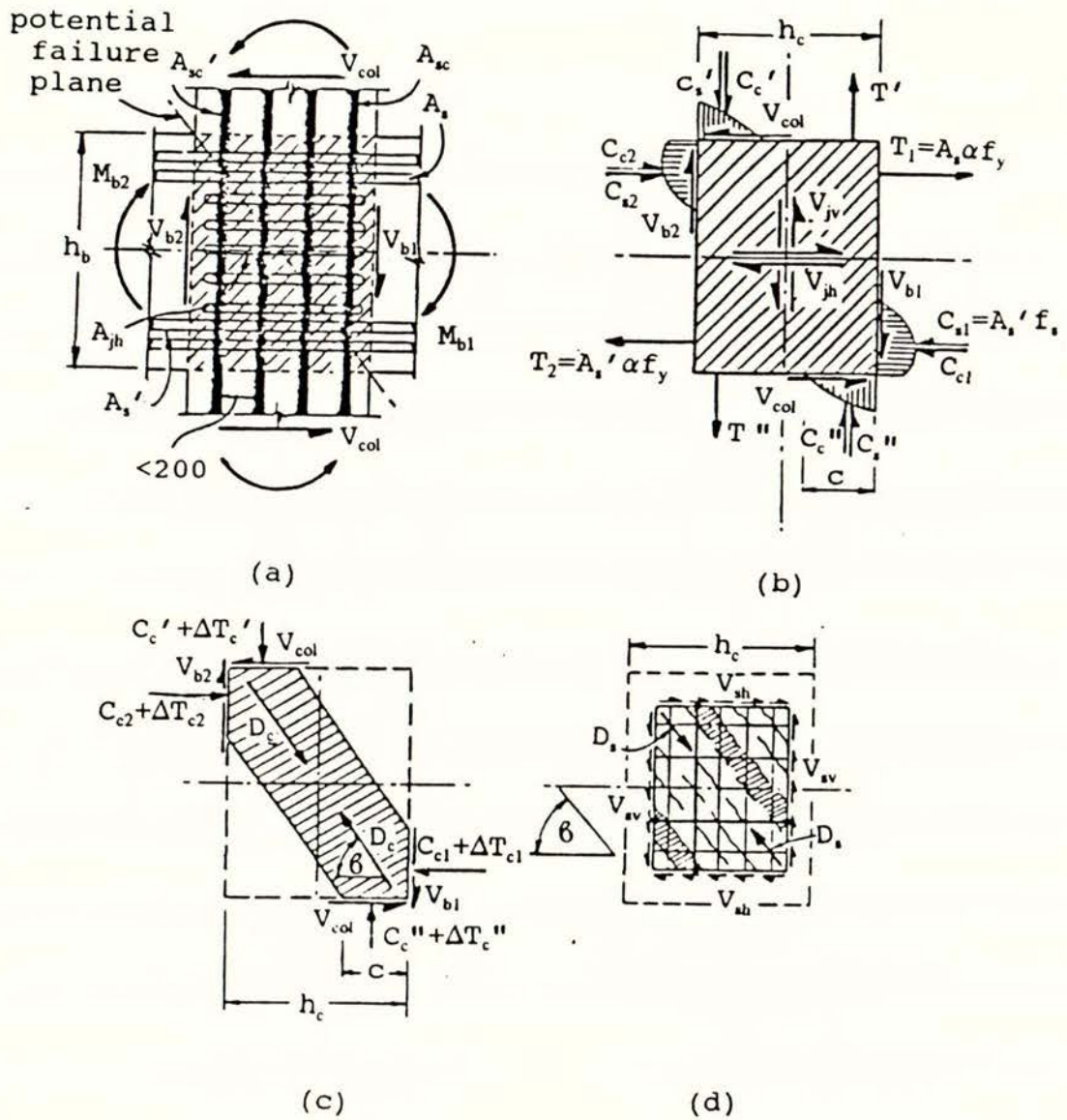


Fig. 2.4 Principal mechanisms of shear resistance of an inelastic interior joint core [3]

2.2.1 Diagonal Compression Concrete Strut Mechanism

Fig. 2.4(c) shows that if the horizontal and vertical forces in the corner regions of the joint can be transferred across the joint core by a diagonal concrete strut, which carries a compressive force, D_c at an angle θ to the horizontal. This mechanism does not need any joint reinforcement except confining reinforcement to ensure that the concrete strut can sustain the compressive stresses. It is apparent that a system of forces in equilibrium may exist, consisting of the concrete compression forces, column and beam shear forces and the bond forces, ΔT_c , existing within the compression zone. The horizontal component of the diagonal compression force is given by

$$V_{ch} = C_{c1} + \Delta T_{c1} - V_{col} = D_c \cos \beta \quad (2.8)$$

where ΔT_{c1} is the bond force transmitted from the beam longitudinal reinforcing to the concrete within the strut. Similarly, the vertical component is

$$V_{cv} = C_c' + \Delta T_c' - V_{b1} = D_c \sin \beta \quad (2.9)$$

In the elastic range, that is before the occurrence of significant yielding in the beam reinforcement, the concrete compression forces in the beams C_{c1} (C_{c2}) and the bond forces ΔT_{c1} (ΔT_{c2}), will be a large fraction of total horizontal force to be transferred across the joint. Thus in this situation the diagonal strut mechanism may resist a main proportion of the total applied horizontal joint shear, V_{jh} . However, as cyclic inelastic loading progresses under severe earthquake actions, flexural cracking of the beams at the column faces become more severe. These flexural cracks may not close again upon moment reversals unless the beam bars, situated in the compression zone, slip or yield extensively. The concrete compression forces in the beam, C_{c1} , and C_{c2} , are likely to be small. Meanwhile, the penetration of strains in excess of yield strain in the beam bars into the joint core means bond deterioration along the beam bars, and the total horizontal force available to combine with the vertical forces to allow a diagonal strut to act will therefore be small. Eventually the horizontal joint core shear resistance may be transferred from the strut (D_c) mechanism to the truss (D_s) mechanism.

2.2.2 Truss Mechanism

A second mechanism by which joint shear may be resisted is shown in Fig. 2.4(d). This mechanism consists of joint core horizontal reinforcement (normally in the form of joint hoops), joint core vertical reinforcement (normally in the form of column intermediate bars) and diagonal concrete struts. As is shown in Fig. 2.4(d), the horizontal shear force resisted by this truss mechanism is given by

$$V_{sh} = V_{jh} - V_{ch} = D_s \cos\beta \quad (2.10)$$

Where D_s is the total resultant force resisted by the diagonal compression field at an angle of β to the horizontal.

It should be noted that inclusion of horizontal joint reinforcing alone is insufficient to ensure the satisfactory performance of this mechanism. Vertical compression components must be supplied by vertical reinforcement across the joint core. This is particularly important in the design of joints for which the column axial load is small. As before, the vertical component of shear force may be also defined as

$$V_{sv} = V_{jv} - V_{cv} = D_s \sin\beta \quad (2.11)$$

2.2.3 Additional Sources of Shear Resistance

Generally, aggregate interlock and dowel action are the two other suggested potential mechanisms of shear resistance. However, both aggregate interlock and dowel action of longitudinal bars passing through the joint core can be only classified as secondary sources of joint shear resistance. They can not be considered as reliable mechanisms of shear resistance in design.

2.3 THE RELATIONSHIP OF BOND AND SHEAR RESISTING MECHANISMS IN THE JOINT

The total design horizontal joint shear force V_{jh} is carried by the diagonal

concrete strut mechanism V_{ch} and the truss mechanism V_{sh} . That is

$$V_{jh} = V_{ch} + V_{sh} \quad (2.12a)$$

similarly,

$$V_{jv} + V_{cv} + V_{sv} \quad (2.12b)$$

To motivate these two shear resisting mechanisms, it is necessary that there exists bond between longitudinal bars and the joint core concrete. The behaviour of the joint depends on the bond performance of the longitudinal bars.

Generally, near perfect bond between a beam bar and the joint core concrete is assumed in the approach taken by the current New Zealand concrete design code [12] provisions for joint design. In other words, the stresses and strains in the beam bars near the centre of the joint core should be almost zero. The magnitudes and variations of bond stress within the joint core will be discussed in the following paragraphs.

(a) The Joint Core in the Elastic Range

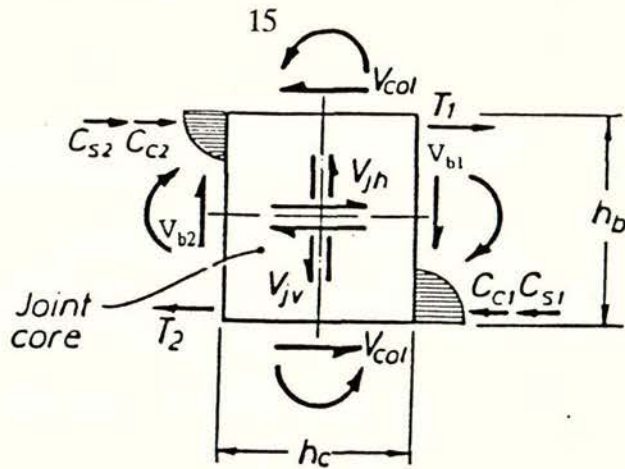
For convenience of discussion, no column axial load is considered to be acting on the interior joint. Fig. 2.5 illustrates variations of bond stresses of the top beam bar of the interior joint at various stages of the loading. The external actions on and shear forces across the joint core are shown in Fig. 2.5(a). To balance input force T_1 and C_{s2} which are the tensile and compressive forces of the bar as shown in Fig. 2.5(b), bond force, $u_1 h_c$ assuming a uniform distribution of bond forces across the joint core, of the top beam bar is required. That is

$$u_1 h_c = T_1 + C_{s2} \quad (2.13)$$

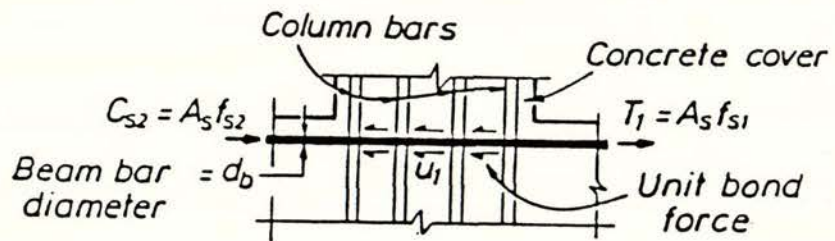
where h_c is the depth of joint (column) and u_1 is unit bond force given by

$$u_1 = \pi d_b u_b \quad (2.14)$$

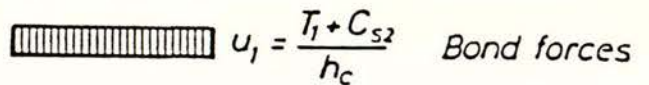
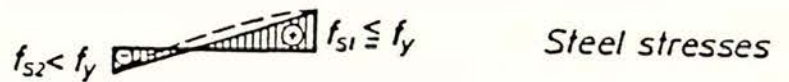
substituting Eq. (2.14) into Eq. (2.13) gives



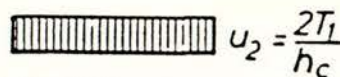
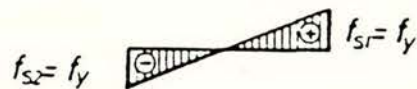
(a) Forces at Interior Joint Core



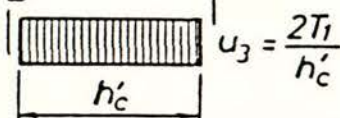
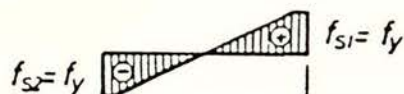
(b) Top Beam Bars with Area A_s



(c) When $|C_{c2}| > 0$, $|C_{s2}| < |T_2|$



(d) When $|C_{s2}| = |T_1|$, C_{c2} May Be Zero



(e) After Some Yield Penetration

Fig. 2.5 Behaviour of a top beam bar with perfect bond across joint core during formation of plastic hinges [22]

$$u_b = \frac{T_1 + C_{s2}}{\pi d_b h_c} \quad (2.15)$$

where u_b is the average bond stress and d_b is the bar diameter.

If the conditions in the joint core when yielding of the top beam bar first occurs are considered, a vector diagram of forces may be constructed as illustrated in Fig. 2.6(c). At this stage it is assumed that stress distribution in the top beam bars as they pass through the joint core, is linear and thus the bond stress, given by the rate of change of the steel stress, is constant as shown in Fig. 2.5(c). It is evident in Fig. 2.6 that the diagonal compression strut is maintained by that portion of the bond force previously defined as ΔT_c together with the concrete compression forces and column shear force in the horizontal direction and similar column internal forces in the vertical direction. Evidently the truss mechanism V_{sh} does not resist the entire joint shear force V_{jh} . Only the parts of the beam and column bar bond forces not utilised here will need to be maintained by the truss mechanism (See Fig. 2.4(d)).

Fig. 2.5(d) shows a critical case. When the flexural steel compression force C_{s2} is increased the diagonal strut mechanism is reduced gradually.

(b) The Joint Core in the Inelastic Range

When some yield penetration takes place in the top beam bar as shown in Fig. 2.5(e), the joint core commences inelastic range. It may be seen that the bond resistance of the cover concrete at both sides of the column is degraded due to the yield penetration. The average unit bond force is assumed to be distributed over a reduced core depth h'_c as shown. At this stage, the function of the truss mechanism V_{sh} becomes more significant.

Fig. 2.7(a and b) illustrate the steel and bond stresses and bond after significant yield penetration and strain hardening. The truss mechanism resists nearly the total input horizontal shear force. In other words, the horizontal shear resistance of the concrete

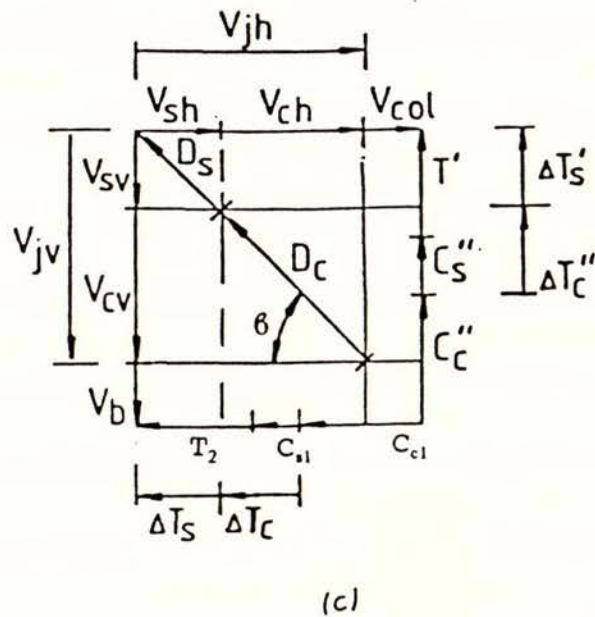
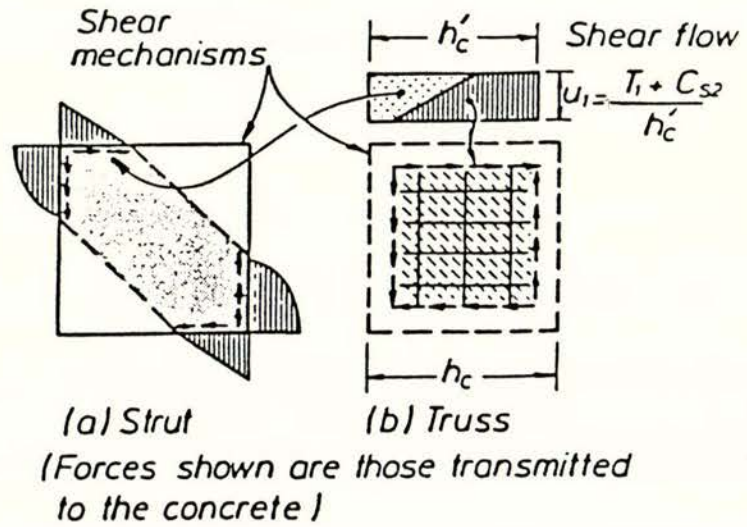


Fig. 2.6 Bond and shear mechanisms in a joint core in the elastic range [14,22]

strut mechanism tends to zero. However when the axial compression force on a column is large, the concrete strut mechanism resists more shear. A larger portion of the bond forces from the beam bars can be assumed to be transferred to the diagonal strut (See Fig. 2.8), since the neutral axis depth in the column section increases with axial compression. Thus, in this case a small contribution is required from the truss mechanism. Hence less horizontal shear reinforcement in the joint core is necessary when the axial compression load on the column is increased.

It is noted in the above discussion that no slip of beam bar within the joint core is assumed. However, the actual situation is that local bond-slip may occur since the bond between a beam bar and the core concrete not perfect. Fig. 2.9 shows the distributions of steel stress and bond over the joint core under this circumstance. The concrete compression force C_{c2} will not vanish due to local slip of beam bar. Thereby, the diagonal concrete strut mechanism is enhanced. Correspondingly, the steel compression force C_{s2} will be reduced. In the extreme case, when the bond breaks down in the joint core, the beam bars will be anchored in the adjacent beams. The concrete flexural compression force C_c becomes very large when the slip beam bars through the joint core, thus further mobilising the strut mechanism (See Fig. 2.10). Both the shear input by bond and the resistance by truss mechanism then diminish. A break-down of bond within interior joints does not necessarily result in a loss of strength. However, the bond-slip may seriously affect the hysteretic response of ductile frames, reaching in remarkable pinching in the load-displacement loops, and a very flexible frame.

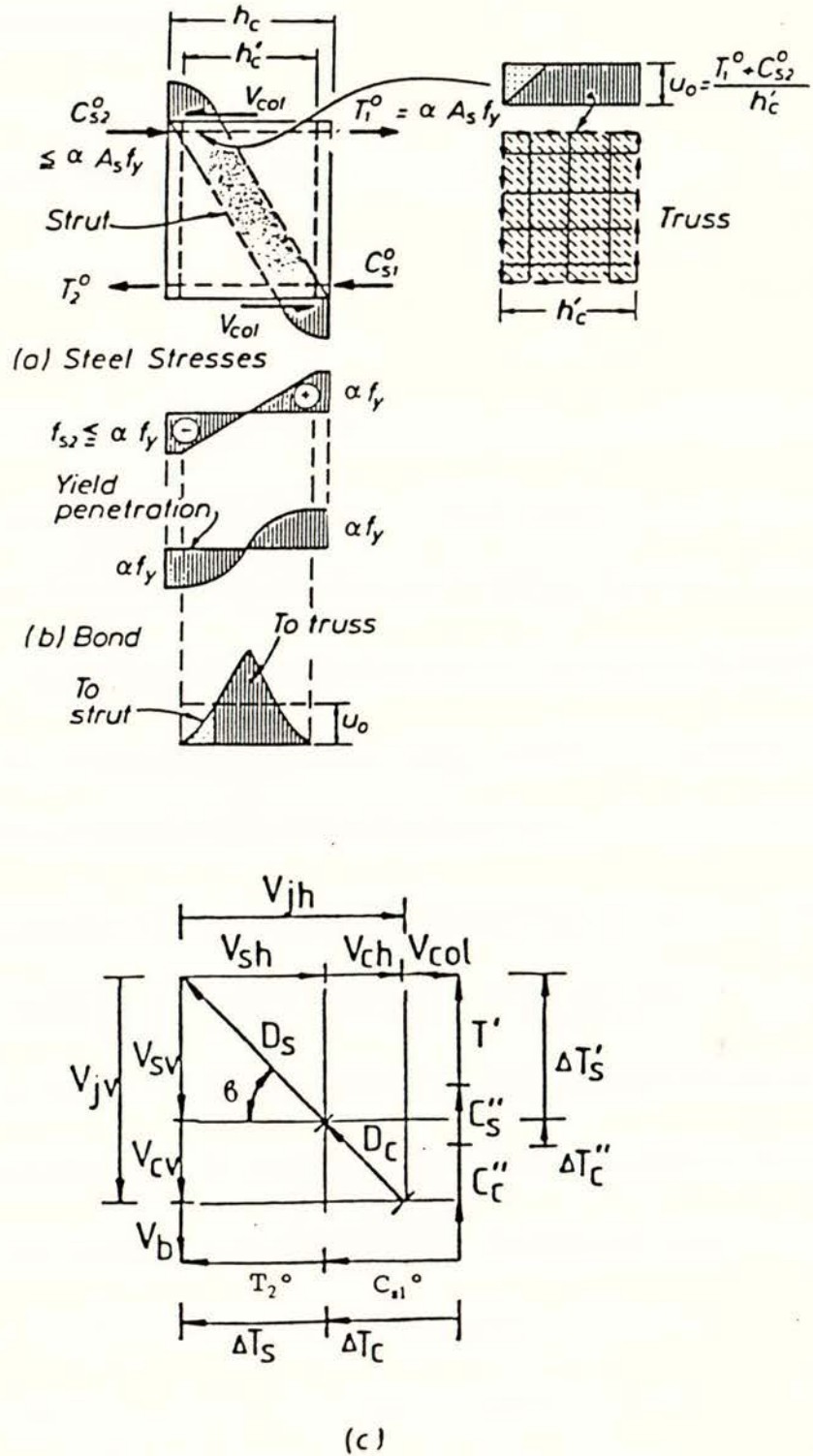


Fig. 2.7 Bond and shear mechanisms in a joint core in the inelastic range assuming perfect bond and strain hardening of beam bars [14,22]

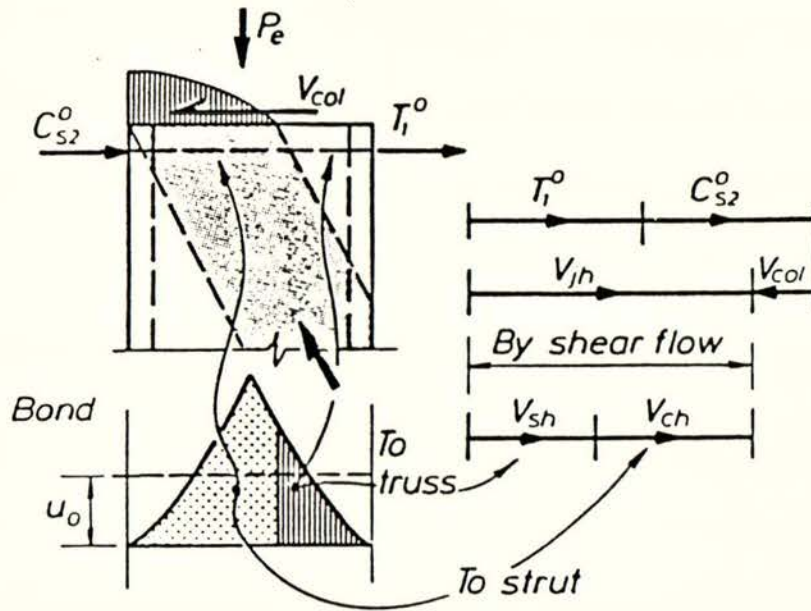


Fig.2.8 Joint core in inelastic range with large axial compression load on column [22]

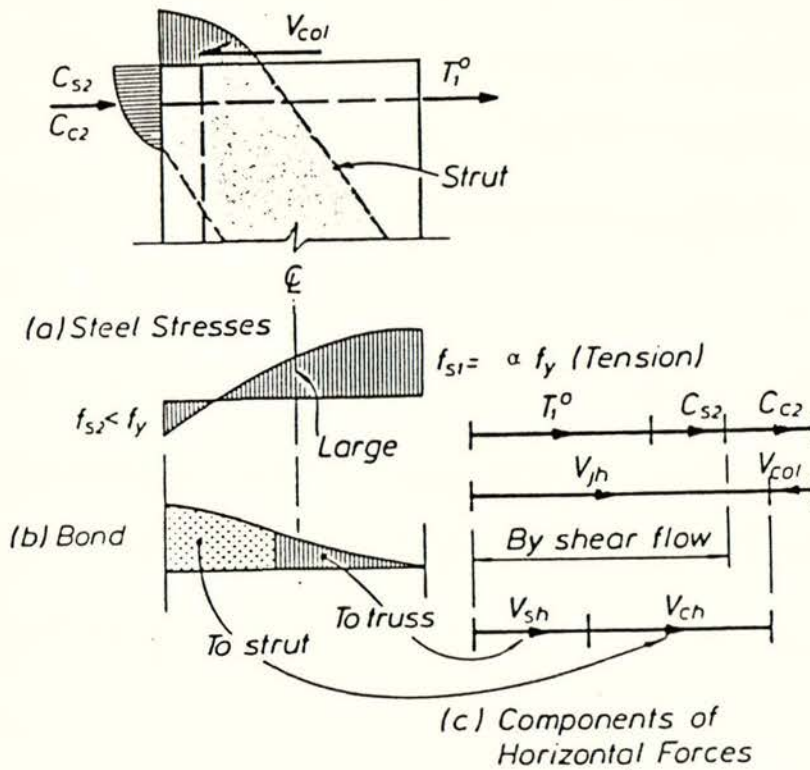


Fig.2.9 Joint core in elastic range with imperfect bond along beam bars [22]

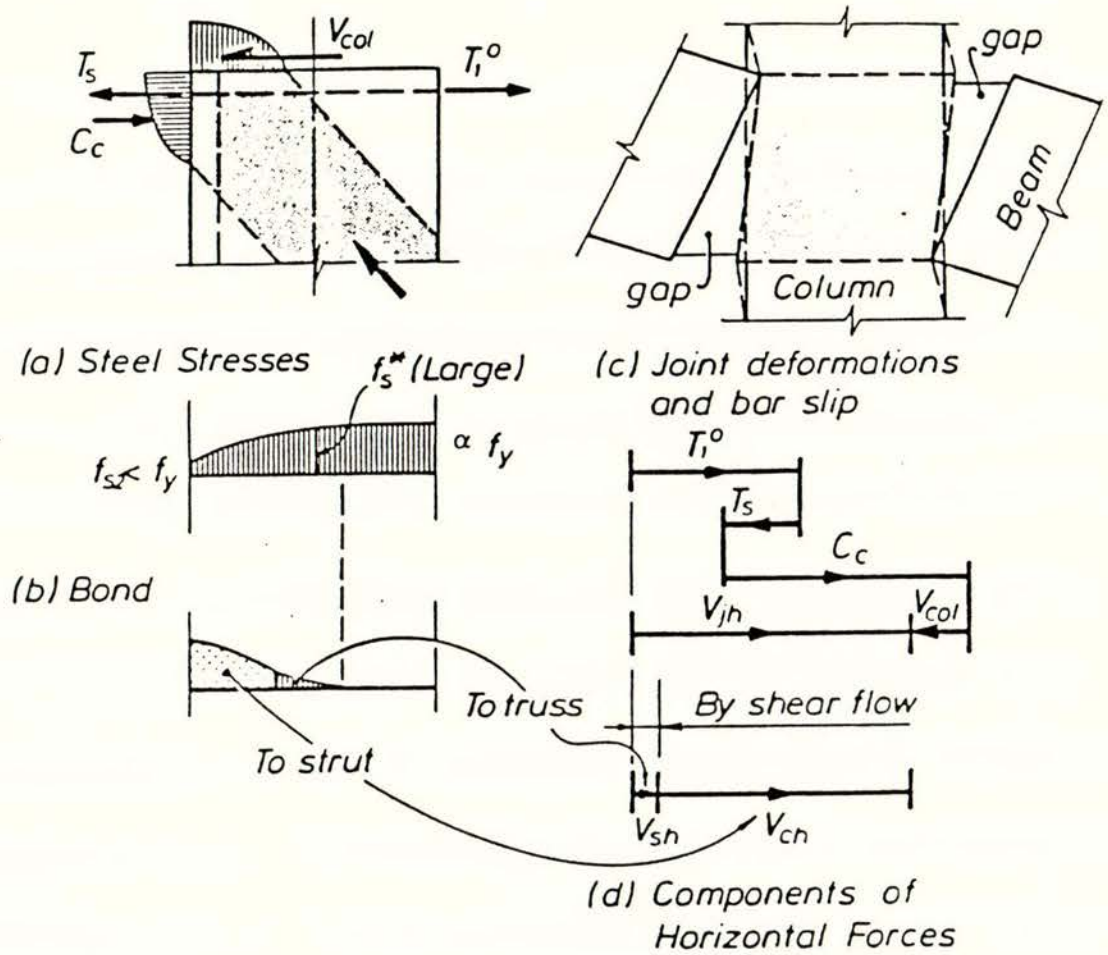


Fig. 2.10 Joint core in inelastic range with bond failure of beam bars [22]

CHAPTER 3

CODE REQUIREMENTS FOR CONVENTIONAL BEAM-COLUMN JOINTS3.1 GENERAL

The provisions of the New Zealand concrete design code NZS 3101:1982 [12] given in this section apply to design of beam-column joints subject to shear induced by gravity or earthquake loads or both. According to NZS 3101:1982, beam-column joints shall satisfy the following criteria:

- (a) A joint shall perform under service loads at least as well as the members that it joins.
- (b) A joint shall have a dependable strength sufficient to resist the most adverse load combinations sustained by the adjoining members, as specified by the appropriate loading code, several times where necessary.

3.2 DESIGN ASSUMPTIONS

The requirements of NZS 3101:1982 [12] are intended to ensure that a joint core has sufficient strength to cause energy dissipation to occur in the potential plastic hinge regions of the adjoining members and not in the joint core. Accordingly, the joint core should be designed to withstand the forces arising when the overstrength of the framing members is developed, considering actions in both principal directions separately where necessary. The design actions are obtained by assuming that the stresses in the flexural steel at the plastic hinges are 1.25 times the lower character yield strength in the case of both Grade 300 and 430 steel.

3.3 HORIZONTAL JOINT SHEAR

In order to prevent the diagonal concrete strut from crushing, the nominal horizontal joint core shear stress in either direction is limited to:

$$v_{jh} = \frac{V_{jh}}{b_j h_c} \leq 1.5 \sqrt{f'_c} \text{ (MPa)} \quad (3.1)$$

The effective joint width, b_j , is defined thus:

- (a) when $b_c > b_w$, either $b_j = b_c$ or $b_j = b_w + 0.5h_c$, whichever is the smaller.
- (b) when $b_c < b_w$ either $b_j = b_w$ or $b_j = b_c + 0.5h_c$, whichever is the smaller.

Transverse joint reinforcement is required to resist the shear in excess of that taken by the concrete strut mechanism. The reinforcement should be designed to resist

$$V_{sh} = V_{jh} - V_{ch} \quad (3.2)$$

The magnitude of the concrete contribution is dependent on several parameters and allowable values vary as follows:

V_{ch} should be taken as zero unless one of the following situations applies:

- (1) When the minimum average compressive stress on the gross concrete area of the column above the joint exceeds $0.1f'_c/C_j$

$$V_{ch} = \frac{2}{3} \sqrt{\frac{C_j P_e}{A_g} - \frac{f'_c}{10}} (b_j h_c) \quad (3.3)$$

where $C_j = V_{jh}/(V_{jx} + V_{jy})$ where V_{jx} and V_{jy} are horizontal design shear forces in the joint core in the two principal directions ($C_j = 1$ for one-way frame), P_e is minimum axial compressive column load, and A_g is gross area of column cross section.

- (2) When the design is such that plastic hinge occurs at a distance away from the column face not less than the beam depth nor 500 mm (See Fig. 3.1), or for

external joints where the flexural steel is anchored outside the column core in a beam stub,

$$V_{ch} = 0.5 \frac{A_s'}{A_s} V_{jh} \left(1 + \frac{C_j P_e}{0.4 A_g f_c'} \right) \quad (3.4)$$

where A_s and A_s' are area of tension and compression longitudinal reinforcement of beam, respectively. A_s'/A_s shall not be taken larger than 1.0. Even for such an elastic joint, however, when the column axial load results in tensile stresses over the gross concrete area exceeding $0.2 f_c'$ then $V_{ch} = 0$. For axial tension between these limits V_{ch} may be obtained by linear interpolation between zero and the value given by Eq. (3.4) when P_e is taken as zero.

- (3) For external joints without beam stubs, Eq. (2.4) may be used when multiplied by the factor

$$\frac{3h_c (A_{jv} \text{ provided})}{4h_b (A_{jv} \text{ required})} \quad (3.5)$$

which shall not be taken as greater than 1.0. Use of this factor requires that the beam bars be anchored using a 90° standard hook in the joint core (See Fig. 3.3).

- (4) When the ratio h_c/h_b is greater than or equal to 2.0, V_{ch} need not be taken as less than

$$V_{ch} = 0.2 b_j h_c \sqrt{f_c'} \quad (3.6)$$

This arises because of the improved bond conditions and correspondingly better concrete shear capacity expected from joint cores with this aspect ratio.

3.4 VERTICAL JOINT SHEAR

The total area of vertical shear reinforcement, normally in the form of intermediate column bars on the side faces of the column, should not be less than

$$A_{jv} = \frac{V_{sv}}{f_{yv}} \quad (3.7)$$

where the vertical design shear force to be resisted by this shear reinforcement is

$$V_{sv} = V_{jv} - V_{cv} \quad (3.8)$$

When a plastic hinge is not expected to occur in the column above or below the joint core, V_{cv} is given by

$$V_{cv} = \frac{A'_{sc}}{A_{sc}} V_{jv} \left(0.6 + \frac{C_j P_e}{A_g f'_c} \right) \quad (3.9)$$

except where axial load results in tensile stresses over the column section. Where A_{sc} and A'_{sc} are area of tension and compression reinforcement in one face of column, respectively. When P_e is tensile, the value of V_{cv} is interpolated linearly between the value given by Eq. (3.9) when P_e is taken as zero and zero when the axial tensile stress over the gross concrete area is $0.2f'_c$.

However, if plastic hinges are expected to form in the column above or below the joint core, V_{cv} should be taken as zero for any axial load on the column.

The spacing of vertical shear reinforcement in each plane of any beam framing into the joint should not exceed 200 mm and in no case should there be less than one intermediate bar in each side of the column in that plane.

3.5 CONFINEMENT

The confinement of the concrete in the joint core is, as for the potential plastic hinge regions in columns. When rectangular hoops are used, the transverse steel

area within spacing s_h is to be not less than the greater of

$$A_{sh} = 0.3s_h h' \left[\frac{A_g}{A_c} - 1 \right] \frac{f_c'}{f_{yh}} [0.5 + 1.25 P_e \phi f_c' A_g] \quad (3.10)$$

or

$$A_{sh} = 0.12s_h h' \frac{f_c'}{f_{yh}} \left[0.5 + 1.25 \frac{P_e}{\phi f_c' A_g} \right] \quad (3.11)$$

The spacing vertical of horizontal hoops is limited to the lesser of 200 mm or 10 times longitudinal bar diameters.

When a capacity design procedure precludes the development of column plastic hinges, the above values A_{sh} may be reduced by one half.

3.6 BAR ANCHORAGE IN INTERIOR JOINTS

To keep bond stresses to an acceptable level, the diameters of deformed longitudinal bar d_b passing through a joint core are limited as follows for both Grade 300 and 430 steel reinforcement ($f_y = 300 - 430$ MPa):

(a) Beam bar:

When plastic hinge can occur adjacent to the column face:

$$d_b \leq 12 \frac{h_c}{f_y} \quad (3.12)$$

When plastic hinge is located at a distance from the column face of at least the beam depth or 500 mm, whichever is less:

$$d_b \leq 15 \frac{h_c}{f_y} \quad (3.13)$$

where h_c = column depth.

(b) Column bar:

When columns are intended to develop plastic hinges:

$$d_b \leq 15 \frac{h_b}{f_y} \quad (3.14)$$

When columns are not intended to develop plastic hinges:

$$d_b \leq 20 \frac{h_b}{f_y} \quad (3.15)$$

where h_b = beam depth.

3.7 BAR ANCHORAGE AT EXTERIOR JOINTS

The basic development length of a deformed bar in tension terminating with a standard 90° hook (See Fig. 3.3) is

$$l_{dh} = \frac{66d_b}{\sqrt{f'_c}} \frac{f_y}{300} \quad (3.16)$$

Where the bar diameter is 32 mm or smaller with side cover not less than 60 mm and cover on tail extension not less than 40 mm, the value may be reduced to $0.7l_{dh}$, and where the concrete is suitably confined the value may be reduced to $0.8l_{dh}$.

The basic development length for a deformed bar in compression is

$$l_{db} = 0.20d_b \frac{f_y}{\sqrt{f'_c}} \quad (3.17)$$

but not less than $0.40d_b$. Where the concrete is suitably confined the value may be reduced to $0.75l_{db}$.

The anchorage is considered to commence within the column at distance $0.5h_c$ or $10d_b$ from the column face, whichever is less, except that when the plastic hinge is located away from the column face, the anchorage may be considered to commence at the column face (See Fig. 3.4).

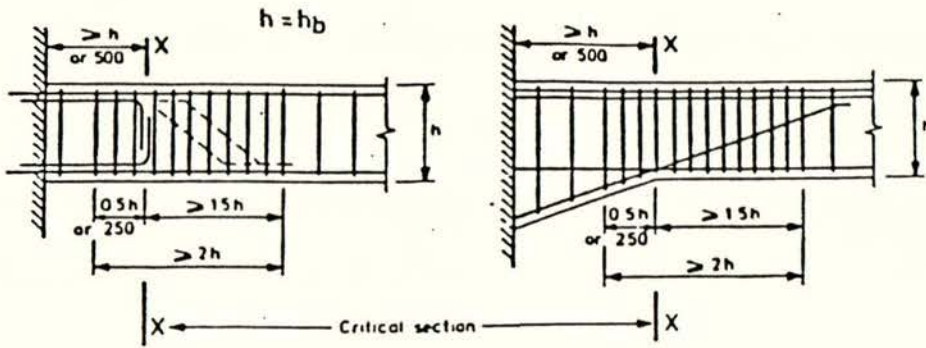


Fig. 3.1 Plastic hinges located in beams away from column faces [12]

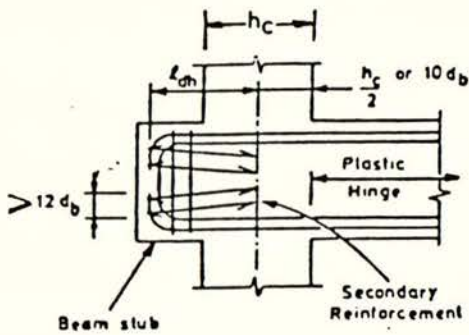


Fig. 3.2 Anchorage of bars in beam stub [12]

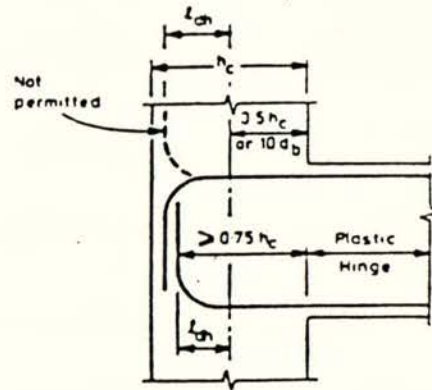


Fig. 3.3 Anchorage of beam bars when critical section of plastic hinge forms at column face [12]

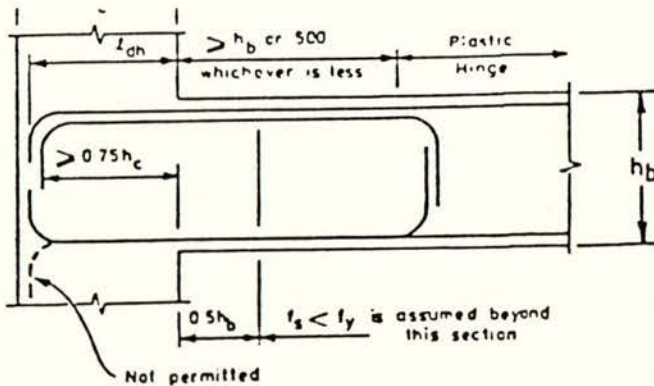


Fig. 3.4 Anchorage of beam bars when critical section of plastic hinge is located at sufficient distance from column face [12]

CHAPTER 4

TEST PROGRAMME

4.1 INTRODUCTION

Six specimens of reinforced concrete beam-column joints were tested under simulated earthquake loading in this project. The units may be considered to be approximately three-quarter scale models. The beam dimensions were 500 x 250 mm and column dimensions were 450 x 300 mm. The overall dimensions of the units are shown in Fig. 4.1.

The six units were divided into three groups according to the specified compression strength of concrete in the design of test units. Both symmetrical and unsymmetrical reinforced section were designed in each group. The amount of joint core shear reinforcement in all units did not to meet the requirements of NZS 3101:1982 [12]. In the joint core, the horizontal shear reinforcement provided by the hoops was 60% of that required by NZS 3101:1982 and the vertical shear requirement provided by intermediate column bars was 75% of that required. The longitudinal bar diameter of all units did not satisfy the requirement for ductile detailing of NZS 3101:1982 except for the longitudinal beam bars of Unit 1.

4.2 DESIGN OF UNITS

In the all six units, the plastic hinges were designed to occur in the beams adjacent to the column faces and the columns were kept in the elastic range during the tests. To achieve this, the columns were designed to have an ideal flexural strength of at least 1.8 times the ideal flexural strength of the beams. Transverse reinforcement in the beams and columns complied full with the requirements of NZS 3101:1982.

In the all six units, the longitudinal reinforcement in the beams and columns was from Grade 430 deformed steel bar and transverse steel in the beam, column and joint was from Grade 300 plain round steel. The reinforcement is described below.

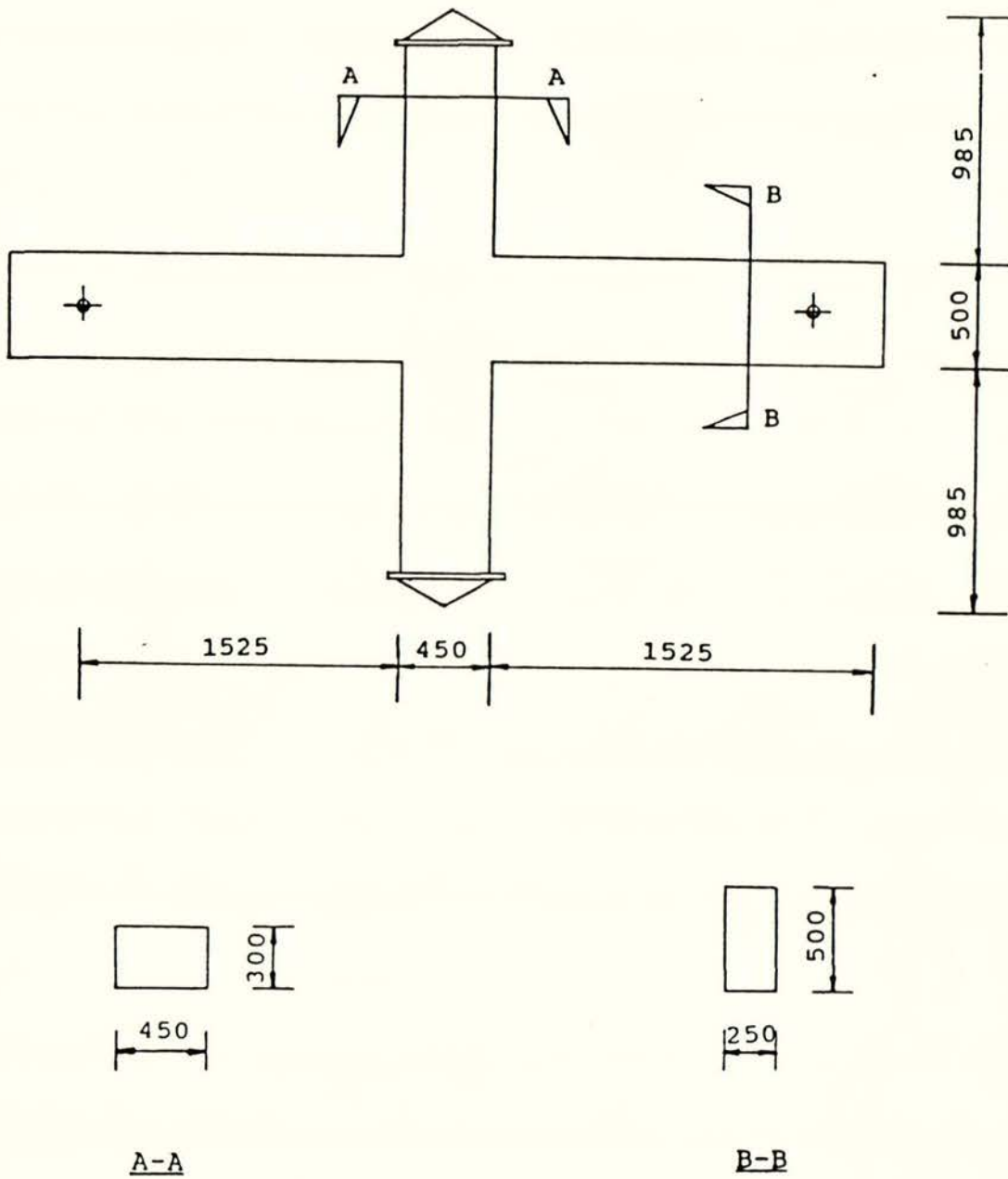


Fig. 4.1 Dimensions of the test units

UNIT 1: The detail of the reinforcement for Unit 1 is shown in Fig. 4.2. HD12 steel bars, seven in the top and seven in the bottom, were used as flexural reinforcement in

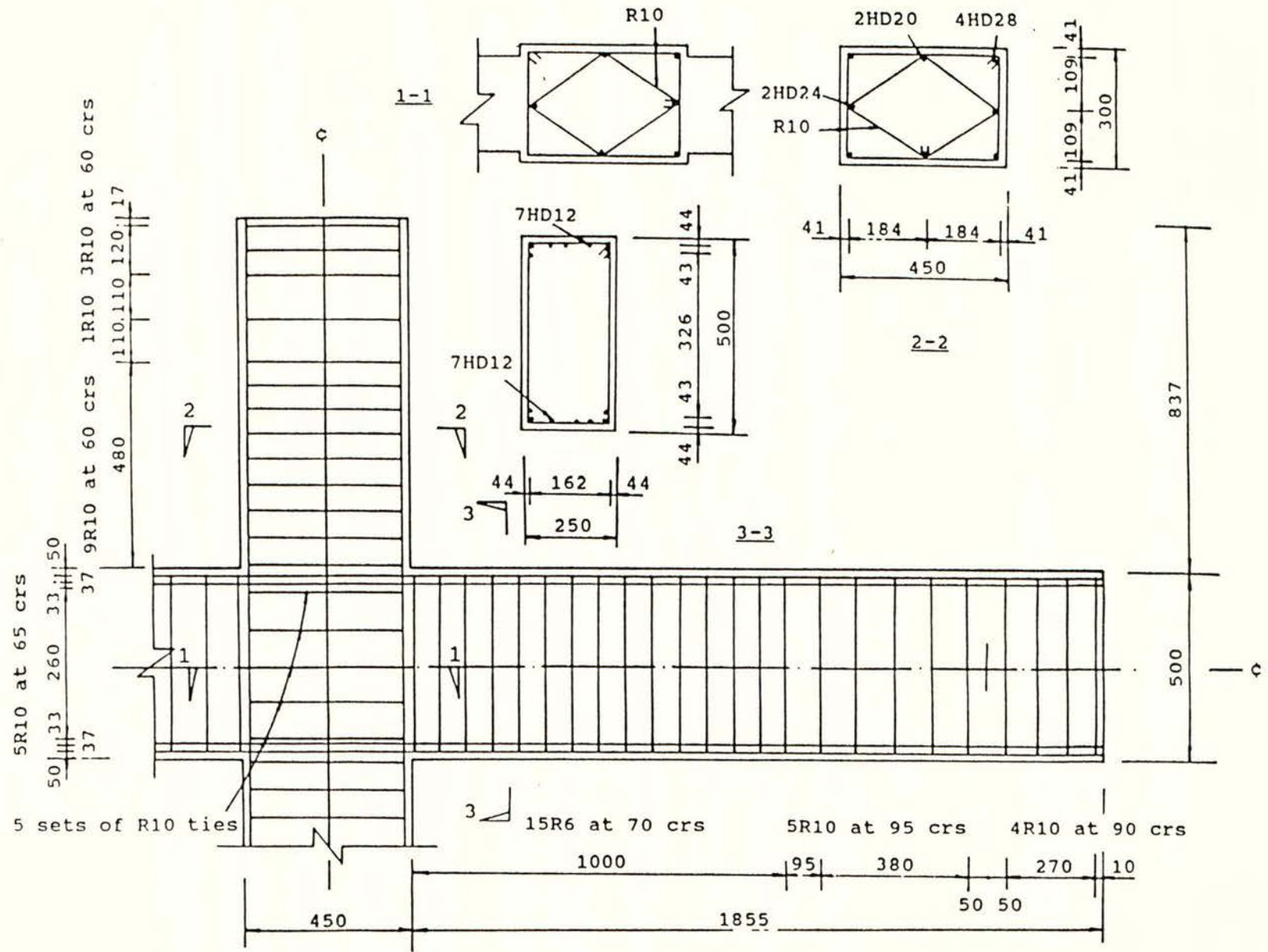


Fig.4.2 Detail of reinforcement of Unit 1

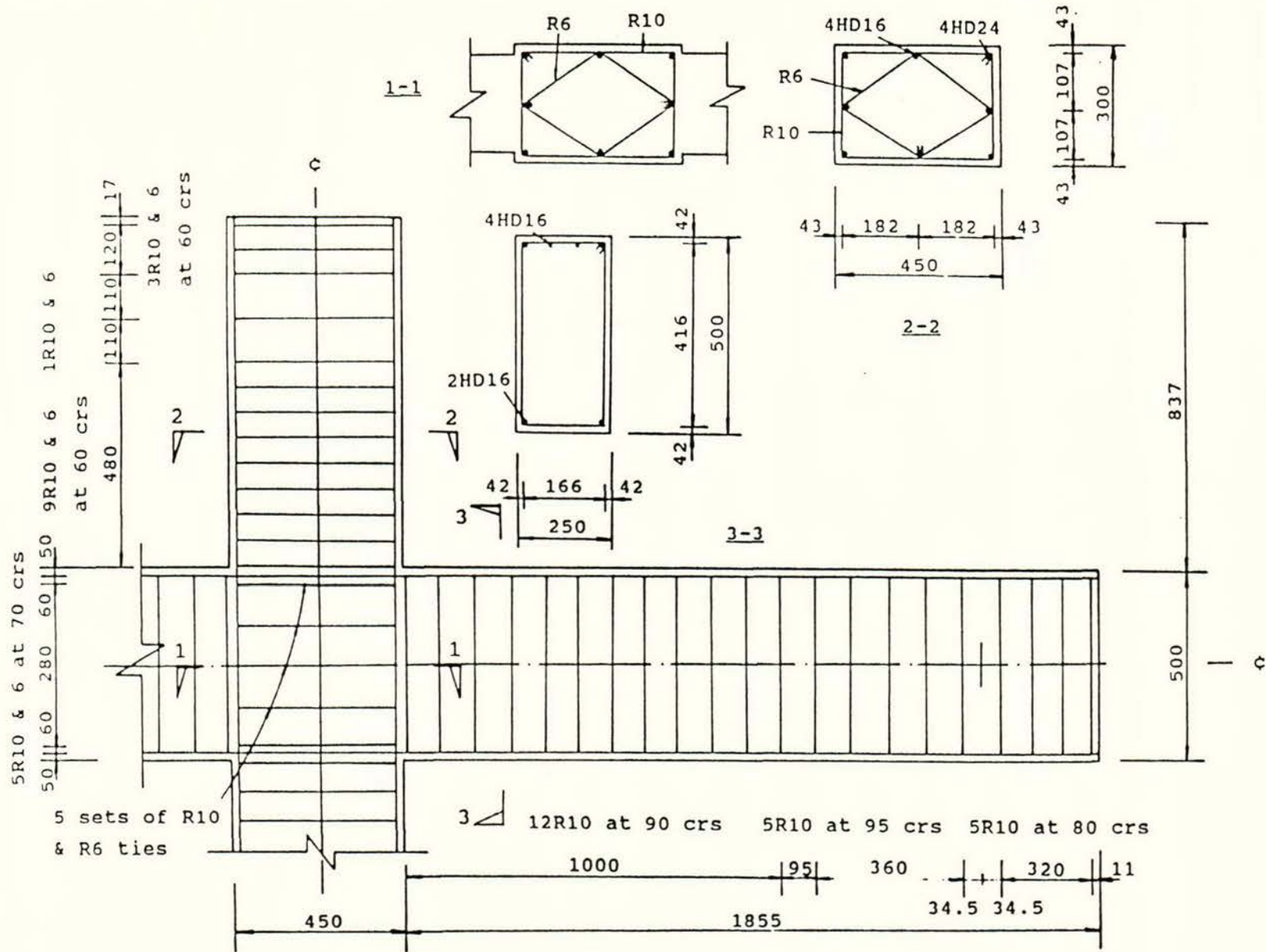


Fig.4.3 detail of reinforcement of Unit 2

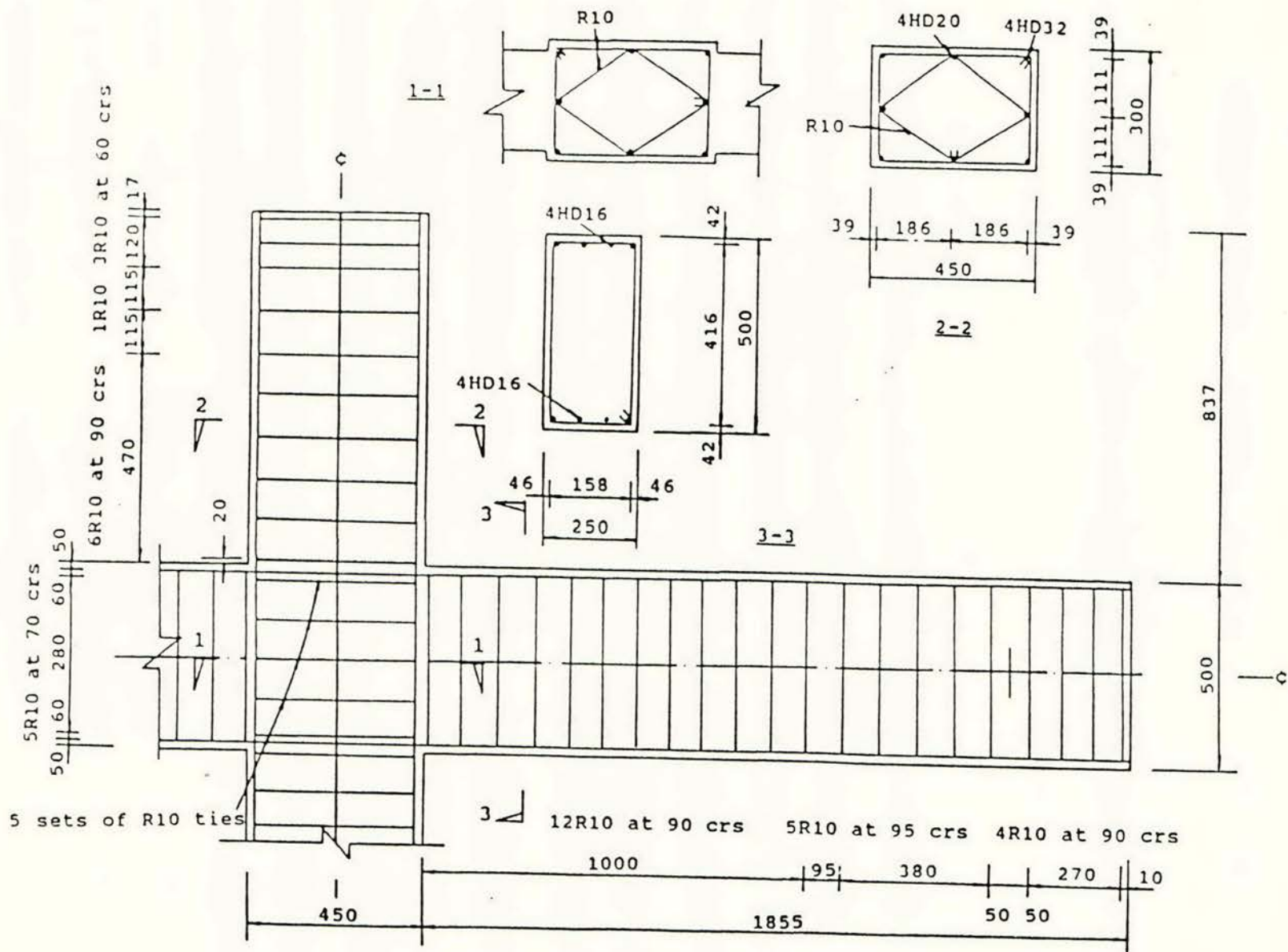


Fig.4.4 Detail of reinforcement of Unit 3

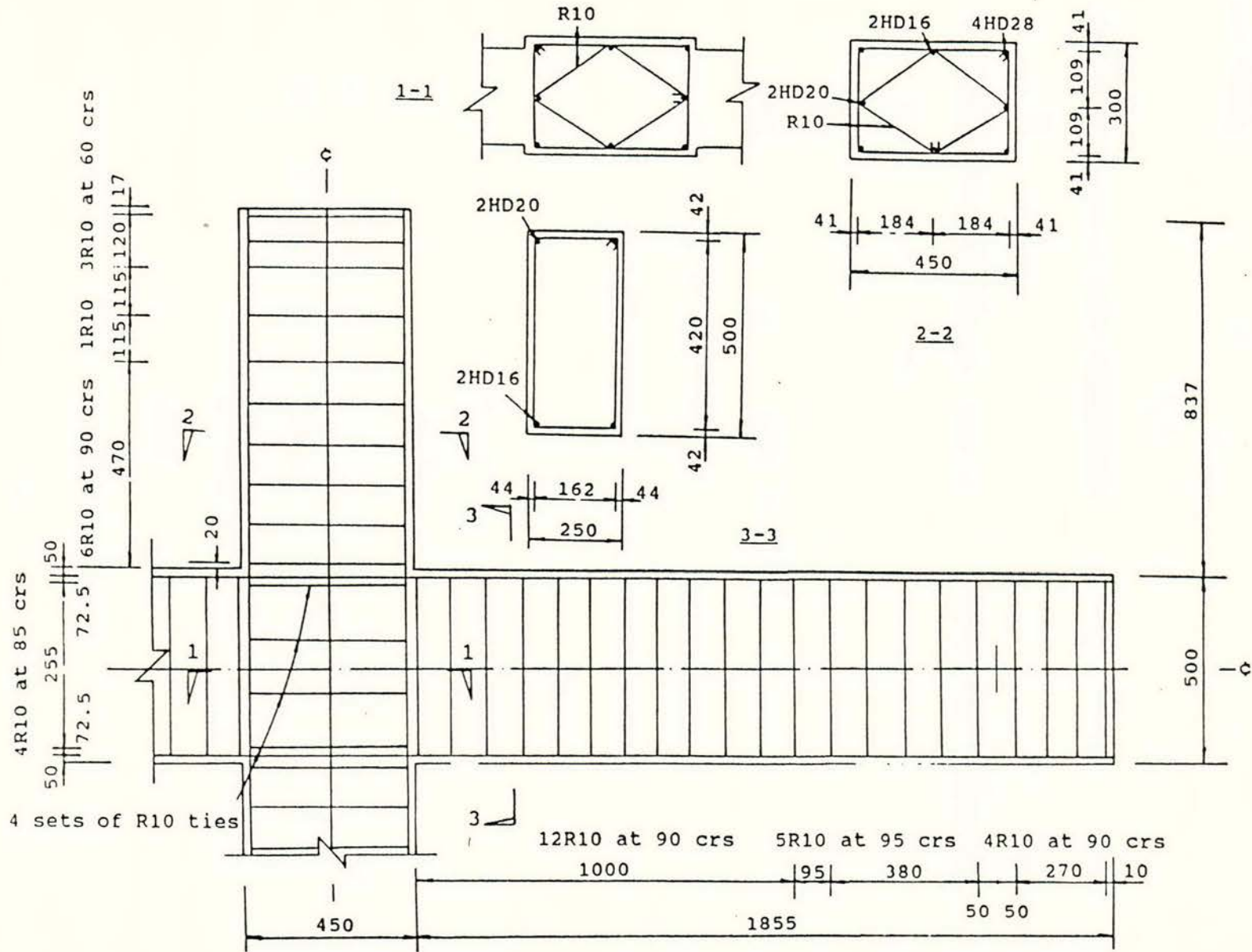


Fig.4.5 Detail of reinforcement of Unit 4

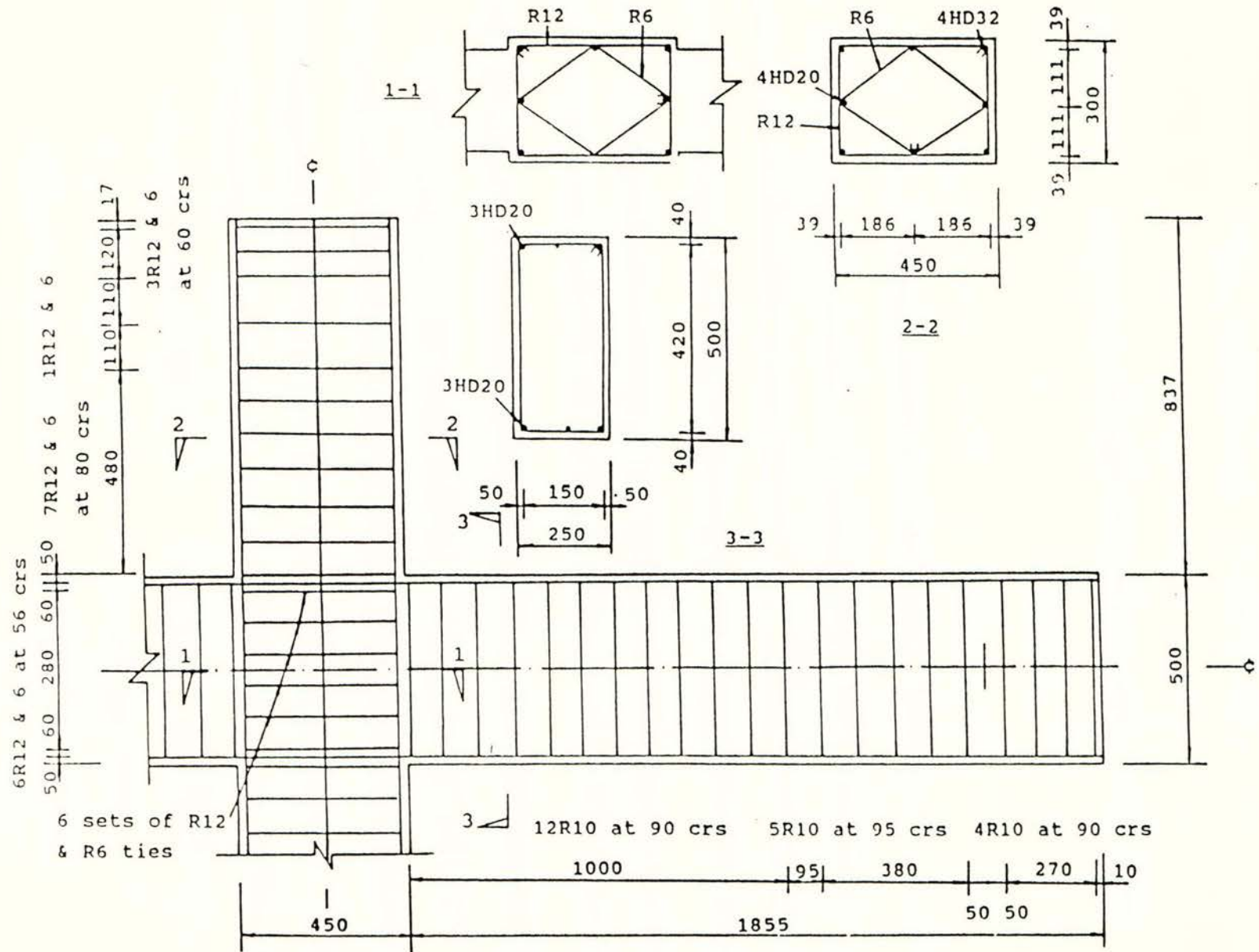


Fig.4.6 Detail of reinforcement of Unit 5

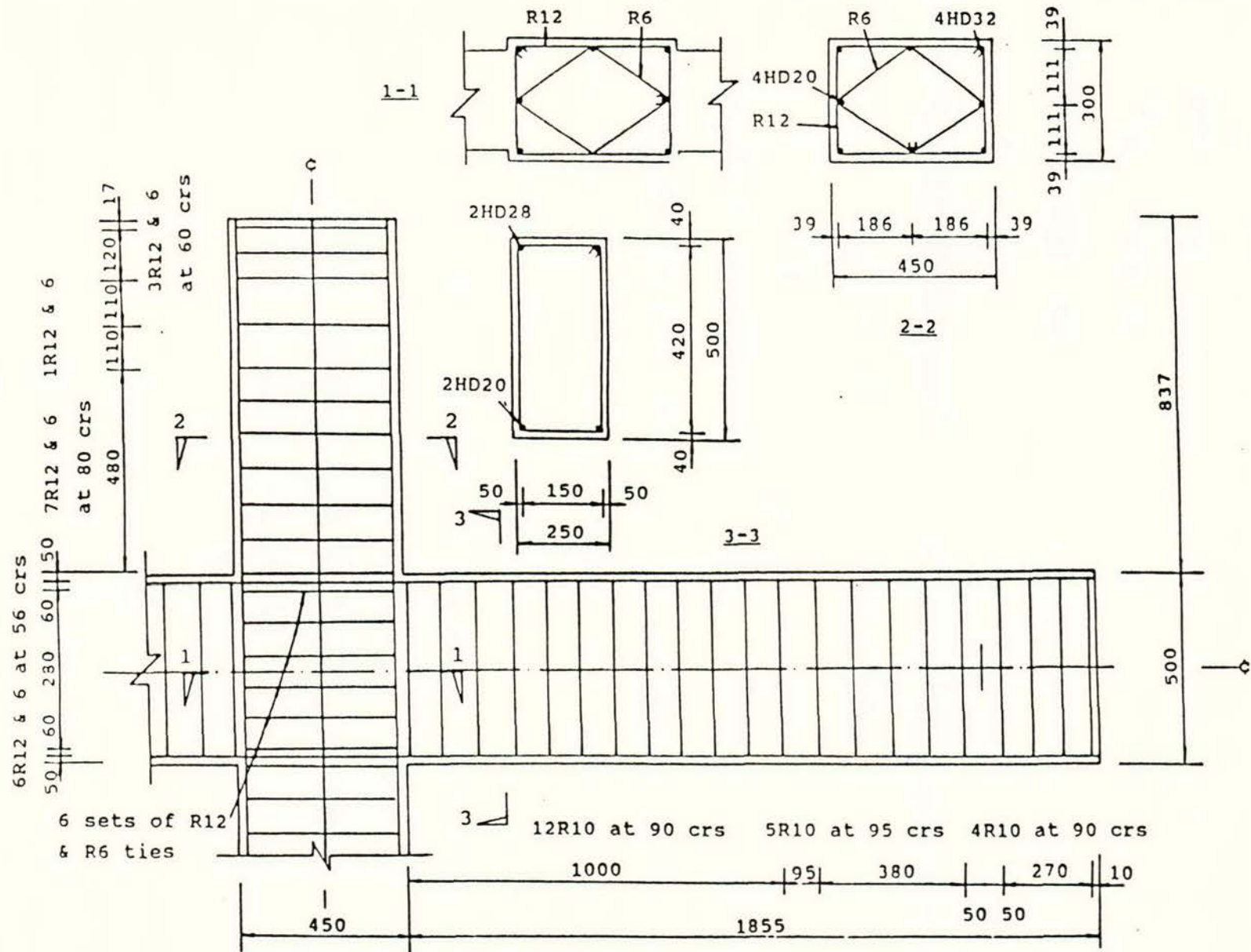


Fig.4.7 Detail of reinforcement of Unit 6

the beam. The longitudinal reinforcement ratio in the top and bottom of the beam steel beam ratio was 0.73%.

Four HD28 and two HD24 bars were used as column longitudinal reinforcement, providing sufficient flexural capacity to ensure that plastic hinging occurred in the beam. The longitudinal column reinforcement ratio ρ_t was 1.40%.

Five sets of R10 hoops (rectangular plus shaped) were used as horizontal joint shear reinforcement, and the two HD24 intermediate column bars were there for vertical joint shear reinforcement.

UNIT 2: The detail of the reinforcement for Unit 2 is shown in Fig. 4.3. HD16 steel bars, four in the top two in the bottom, were used as beam flexural reinforcement. The longitudinal reinforcement ratio in the top and bottom of the beam was 0.71% and 0.36%, respectively.

Four HD24 and two HD16 bars were used as column longitudinal reinforcement, providing sufficient flexural capacity to ensure that plastic hinging occurred in the beam. The longitudinal column reinforcement ratio ρ_t was 0.92%.

Five sets of R10 (rectangular) and R6 (shaped) hoops were used as horizontal joint shear reinforcement, and the two HD16 intermediate column bars were there for vertical joint shear reinforcement.

UNIT 3: The detail of the reinforcement for Unit 3 is shown in Fig. 4.4. HD16 steel bars, four in the top and four in the bottom, were used as flexural reinforcement in the beam. The reinforced ratio in the top and bottom was 0.71%.

Four HD32 and two HD20 bars were used as column flexural reinforcement, providing sufficient flexural capacity to ensure that plastic hinging occurred in the beam. The longitudinal column reinforcement ratio ρ_t was 1.60%.

Five sets of R10 hoops (rectangular and shaped) were as horizontal joint shear

reinforcement and the two HD20 intermediate column bars were used there for vertical joint shear reinforcement.

UNIT 4: The detail of the reinforcement for Unit 4 is shown in Fig. 4.5. Two HD20 steel bars were used as top flexural reinforcement, and two HD16 were used as bottom reinforcement, in the beam. The longitudinal reinforcement ratio in the top and bottom of the beam was 0.56% and 0.36%, respectively.

Four HD28 and two HD20 bars were used as column flexural reinforcement, providing sufficient flexural capacity to ensure plastic hinging occurred in the beam. The longitudinal column reinforcement ratio ρ_t was 1.29%.

Four sets of R10 hoops (rectangular and shaped) were used as horizontal joint shear reinforcement and the two HD16 intermediate column bars were there for vertical joint shear reinforcement.

UNIT 5: The detail of the reinforcement for Unit 5 is shown in Fig. 4.6. HD20 steel bars, three in the top and three in the bottom, were used as beam flexural reinforcement. The longitudinal reinforcement ratio in the beam in the top and bottom was 0.84%.

Four HD32 and two HD20 bars were used as column flexural reinforcement, providing sufficient flexural capacity to ensure that plastic hinging occurred in the beam. The longitudinal column reinforcement ratio ρ_t was 1.60%.

Six sets of R12 (rectangular) and R6 (shaped) hoops were used as horizontal joint shear reinforcement and the two HD20 intermediate column bars were there for as vertical joint shear reinforcement.

UNIT 6: The detail of the reinforcement for Unit 6 is shown in Fig. 4.7. Two HD28 and two HD20 steel bars were used as top and bottom beam flexural reinforcement, respectively. The longitudinal reinforcement ratio in the top and bottom of the beam was 1.09% and 0.56%, respectively.

Four HD32 and two HD20 bars were used as column flexural reinforcement, providing sufficient flexural capacity to ensure plastic hinging occurred in the beam. The longitudinal column reinforcement ratio ρ_t was 1.60%.

Six sets of R12 (rectangular) and R6 (shaped) hoops were used as horizontal joint shear reinforcement and the two HD20 intermediate column bars were there for vertical joint shear reinforcement.

4.3 PROPERTIES OF MATERIALS

4.3.1 Concrete

All of the concrete used was prepared by a commercial ready-mix plant. The maximum aggregate size was 15 mm. The specified compressive cylinder strength of concrete at 28 days for Units 1, 2, 3, 4, 5 and 6 was 20, 20, 40, 40, 60 and 60 MPa with 100 mm slump, respectively.

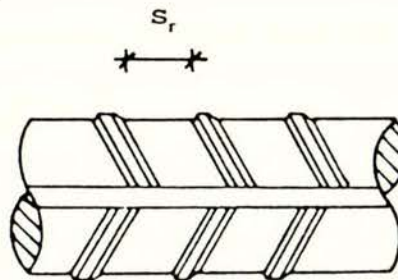


Fig. 4.8 Span of ribs in a steel bar

Twelve 100 mm diameter by 200 mm height test cylinders were cast with each unit. Six cylinders were cured in a fog room, while the rest were cured under the same conditions as the unit. Compression tests on these cylinders were conducted on seventh and twenty-eighth days as well as at the beginning of each unit's test. Table 4.1 summarises the properties.

Table 4.1 Properties of Concrete

Unit	1	2	3	4	5	6
Slump (mm)	130	50	160	80	60	75
f'_c at 7 Days (MPa)		20.5	23.7	28.9	42.7	37.1
f'_c at 28 Days (MPa)	28.2	30.3	32.0	36.9	60.7	59.3
Age at Test (days)	94	92	81	58	29	29
f'_c at Test	30.9	40.8	42.5	47.2	60.7	59.3

Table 4.2 Properties of Steel

Steel	Grade 430 (MPa)						Grade 300 (MPa)		
	HD12	HD16	HD20	HD24	HD28	HD32	R6	R10	R12
f_y (MPa)	453	445	492	461	463	447	356	348	327
ϵ_y $\times 10^{-3}$	2.23	2.23	2.63	2.48	2.33	2.31	2.6	1.9	1.63
ϵ_{sh} $\times 10^{-3}$	17.6	16.6	14.5	13.0	16.3	16.3			
f_{su} (MPa)	617	605	665		618	616	440	480	451
s_r mm	4.8	6	9.5	10.2	13				

Note: s_r is defined as shown in Fig. 4.8

4.3.2 Steel

In order to minimize experimental scatter, the majority of the steel reinforcement was obtained in one delivery so that the properties were expected to be consistent. The tensile properties of the steel bars were obtained by testing under progressively increasing monotonic tensile loading in an Avery Universal Testing Machine of 100 or 1000 kN capacity with the strain being measured by a Baly mechanical extensometer of 50.8 mm gauge length. Typical stress-strain curves are shown in Fig. 4.9 while Table 4.2 summarizes the steel properties.

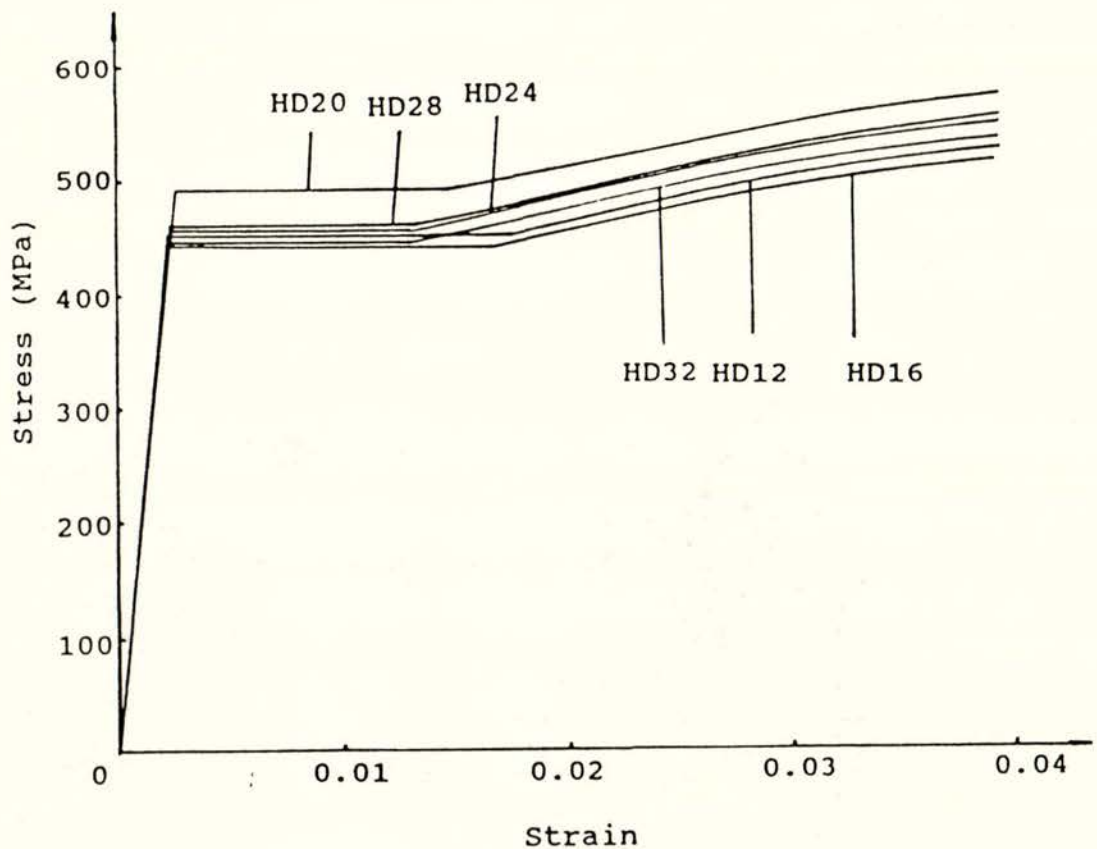


Fig. 4.9 Stress-strain curves for Grade 430 steel bars

4.4 FABRICATION OF THE UNITS

The longitudinal flexural reinforcement was gas cut to the required length. All transverse hoops were cut and bent in a plant before delivery. The bend diameters and hooks were as specified in NZS 3101. All strain gauges were put on at the required positions, before the reinforcement cages were completed outside the mould, taking considerable care to achieve the desired spacings. Lifting hooks were built into the beams, positioned away from the critical sections.

The mould was made from a plywood base and steel sides and was oiled before each unit was cast to facilitate stripping. Two plastic (PVC) tubes were placed at each end of the beam, and eight 25 mm diameter x 400 mm length Grade 430 steel bars were placed at each end of the column for the transmission of loading during the tests, after the reinforcement cage was correctly position in the mould (See Fig. 4.10).

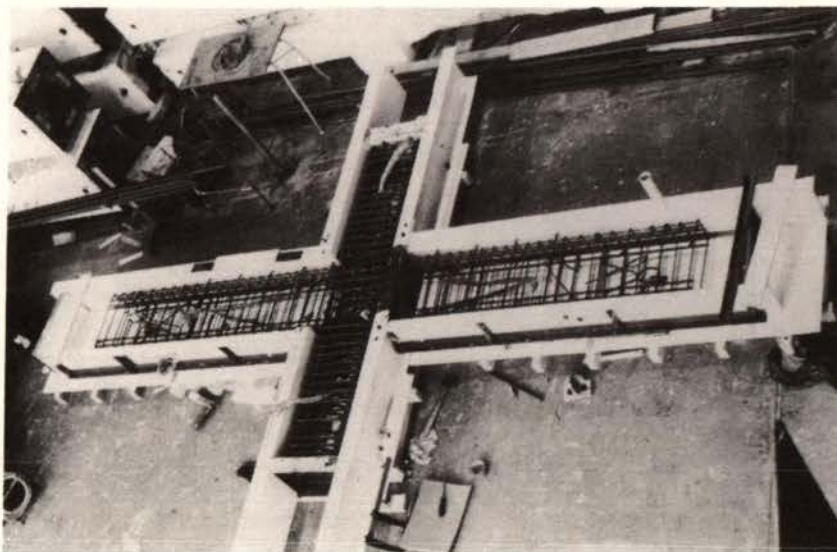


Fig. 4.10 Steel cage of Unit 1 in the mould

The test units were all cast in the horizontal in one pour. Concrete was placed in the mould, vibrated using an internal vibrator, and screened off. After the top surface of the unit had been floated off to a smooth finish it was cured under damp sacking and polythene for one or two weeks depending on the seven days compression strength of concrete. Then the unit was lifted out of the mould and stood upright.

In order to improve the visibility of cracking during the tests, the units were painted with flat white paint.

4.5 TEST RIG

The test rig used is shown in Fig. 4.11 and 4.12. The in-plane horizontal load was applied to the top hinge of the column by a double acting 300 kN capacity MTS hydraulic jack. A steel beam was bolted to the column of the reaction frame at one end and connected to the jack using a gimbel at the other end. Free rotation of the jack was allowed in the vertical plane, thus accommodating the expected vertical movement of the unit. A strain-gauged load cell was placed between the jack and a link block connected to the top hinge. The link block effectively extended the ram of the jack.

Each end of the beam was held against vertical displacement by vertical steel members on each side of the beam and a 50.8 mm diameter steel pin passing through the beam, which provided the vertical reaction forces to the beam. The vertical steel members consisted of two short of 152 x 76 channels in the end and a 102 x 51 box in the middle. This connection allowed free horizontal movement of the beam but not vertical displacement.

After plastic hinges appear in the beam, out-of-plane displacement of the unit may occur. In order to prevent this deformation, the vertical steel members on each end of the beam were braced and a device was set up on the top of the column to provide lateral stability to the system.

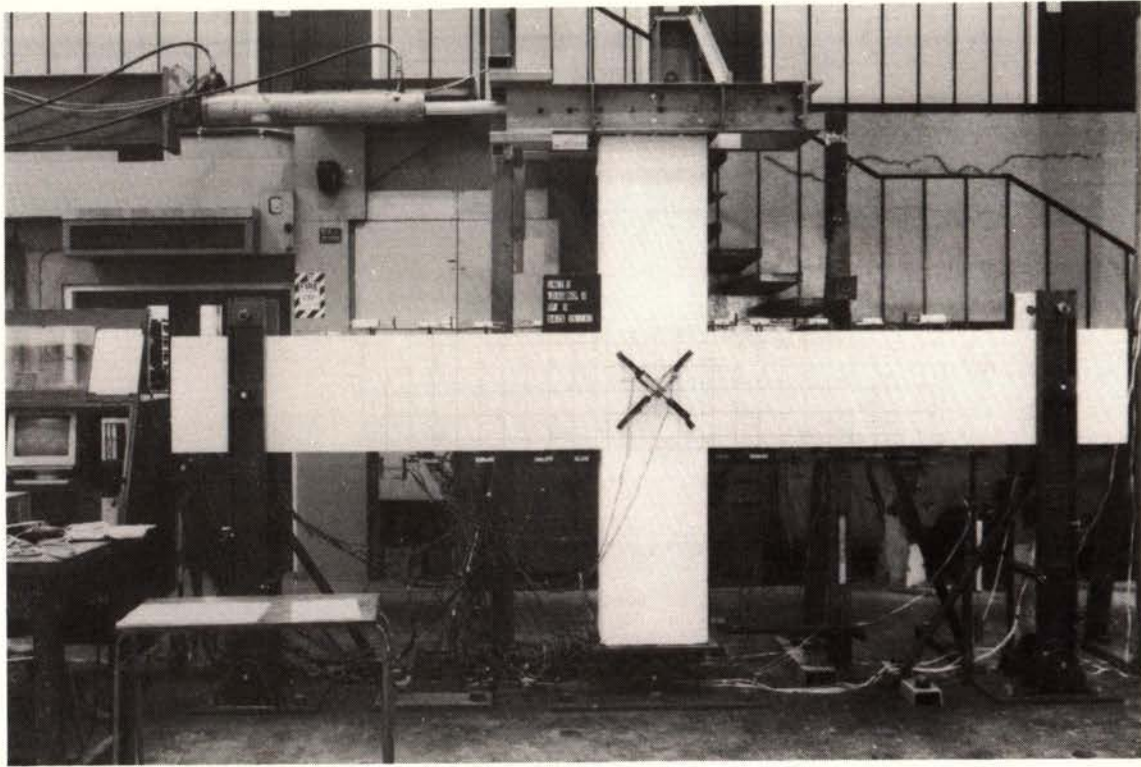


Fig. 4.12 A unit in the test rig

4.6 INSTRUMENTATION

4.6.1 General

All electrical resistance strain gauges, linear potentiometer and clip gauges were connected to a Metrabyte 128 Channel Data Logger.

4.6.2 Load

The magnitude of the horizontal load applied to the column was measured by a 300 kN load cell. Load cell was calibrated using a Budd Strain Indicator and a 1100 kN Avery Universal Testing Machine prior to testing. The calibration equation was used to determine the magnitude of the column load. The 300 kN capacity load cell was equipped with two separate circuits to give two outputs. The first circuit was read directly from a Budd Strain Indicator. The second circuit was used to drive the Y-axis of a Howlett-Packard Pen Recorder. A 300 mm travel linear potentiometer, which measured

the horizontal displacement of the column was used to drive the X-axis, so that an instantaneous plot of load- displacement relationship for the column.

Four electrical resistance strain gauges with full-bridge connection were attached to the beam support-legs to measure the reaction force of the end of the beam, which was calibrated using a load cell.

4.6.3 Displacements

Fig. 4.11 and 4.12 show the arrangement of linear potentiometers. Small aluminium plates were glued to all bearing faces to provide a smooth bearing surface for the potentiometer tips.

A 300 mm travel linear potentiometer was placed near the top point of the column to measure the horizontal displacement. Two 200 mm and one 50 mm travel linear potentiometers were used to measure the column deflection up the height. A 50 mm travel dial gauge was used to check the movement of the base plate that connected the strong floor and the bottom of the column.

Seven 50 mm and two 30 mm travel linear potentiometers, and one clip gauge, were used to determine the curvatures of each beam within 1000 mm from the column face.

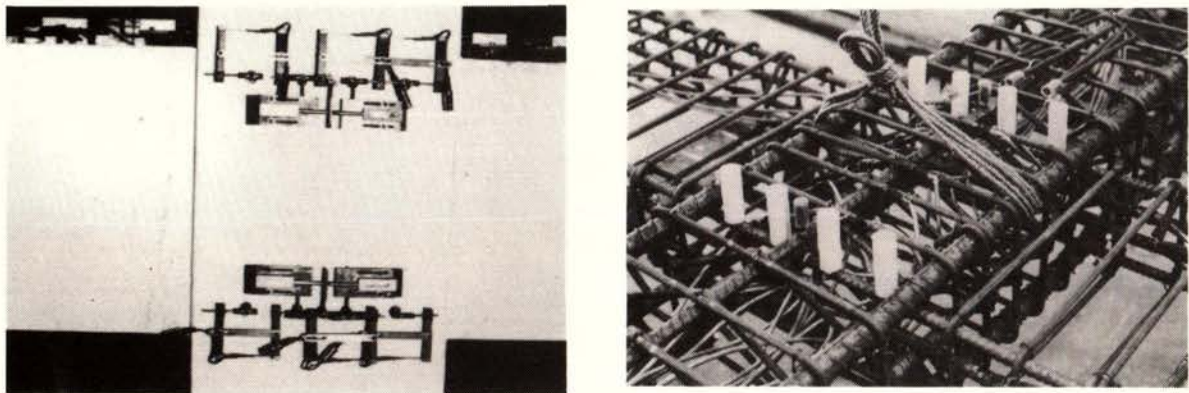
Two 50 mm travel linear potentiometers were used to monitor the vertical displacement of each beam end. A 200 mm travel linear potentiometer was placed at west end of the beam to monitor horizontal movement of the beam.

4.6.4 Joint Shear Distortion

A pair of 30 mm travel linear potentiometers were placed along the diagonals of the joint core to measure the shear distortion of the joint core (See Fig. 4.11 and 4.12).

4.6.5 Beam Bar Slip

The slips of the beam bars in the centre of the joint were measured using four 30 mm travel linear potentiometers placed on the top and bottom beam bars. To set up these linear potentiometers, 10 mm diameter short steel stubs had been welded to the beam bars. A 20 mm diameter hole was prepared for each stub so that the beam bar could move freely (See Fig. 4.11 and 4.13).



(a) After setting up

(b) Before setting up

Fig. 4.13 Location of instrumentation to measure a slippage of beam bars in a beam-column joint

4.6.6 Strains

Electrical resistance strain gauges (SHOWA TYPE N11-FA-5-120-11) were used to measure the strain variations along the longitudinal reinforcing bars in the beam, intermediate column bars and horizontal hoops in the joint, as shown in Fig. 4.14. To eliminate as far as possible the effect of bending strains due to bending of the bar, the strain gauges were placed at the mid-depth of the longitudinal bars. The strain gauges on the joint core hoops were attached in pairs above and below the rectangular hoop bar and at the mid-depth of the diamond hoop bar in the direction of shear transfer. Six clip gauges were used to measure the strains in the beam bar in the joint region (See Fig. 4.11).

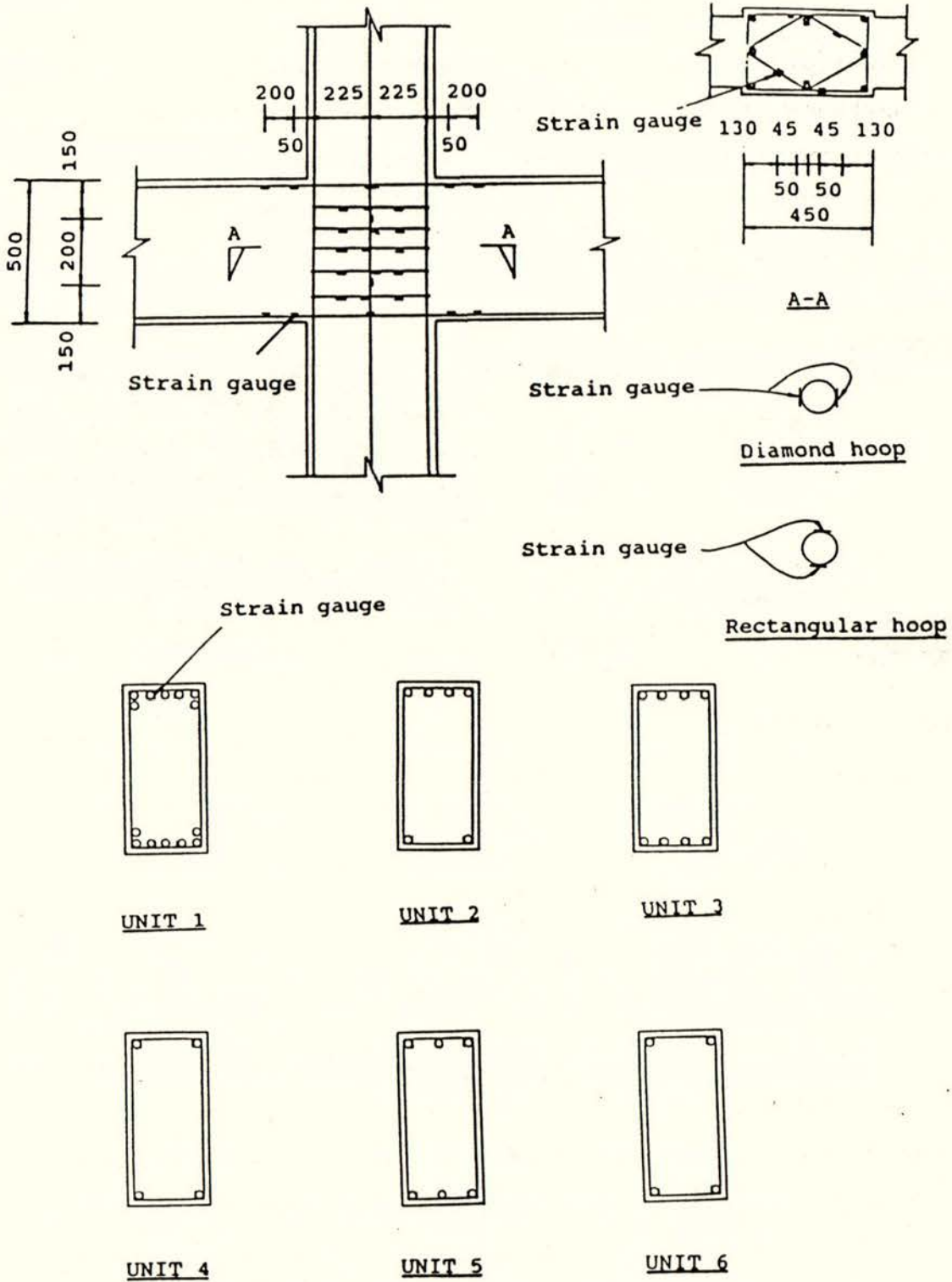


Fig. 4.14 Position of electrical resistance strain gauges on reinforcing steel of units

4.6.7 Observation of Cracking

Cracks on one face of each unit were marked on the white painted surface with felt-tip pens as they were observed, using a different colour for each direction of loading. Crack widths were measured at the peak of each loading run, with particular attention being paid to the cracks in the joint core and the column surface on the beam. Also, photographs were taken.

4.7 LOADING SEQUENCE

The loading sequence used for the tests is shown in Fig. 4.15. First, a load controlled elastic cycle to three quarters of the theoretical horizontal column ultimate load V_i for each unit was applied. V_i was calculated using the actual material strengths but ignoring strain hardening of steel, and assuming an extreme fibre concrete compressive strain of 0.003, a rectangular concrete compressive stress block with a mean stress of $0.85 f'_c$ and a strength reduction factor $\phi = 1.0$. Appendix A shows the theoretical V_i values calculated for the units. At the lateral V_i , the lateral displacements of the top of the column in two direction, Δ_{y1} and Δ_{y2} , were measured. The first yield displacement for the beam-column joint was then taken as

$$\Delta_y = \frac{4}{3} \left[\frac{1}{2} (\Delta_{y1} + \Delta_{y2}) \right] \quad (4.1)$$

All displacement ductility factors defined as

$$\mu = \frac{\Delta}{\Delta_y} \quad (4.2)$$

where Δ is maximum lateral displacement. The above method has become a standard procedure for obtaining Δ_y at the University of Canterbury.

The applied loading in the inelastic range was displacement controlled to the imposed displacement ductility factors μ shown in Fig. 4.15.

The New Zealand Loading Code, NZS 4203 [29], specifies that for the

performance of a ductile structural element to be considered satisfactory, it should retain at least 80% of its initial strength after withstanding four complete cycles of loading to a displacement ductility factor of four in each direction. The cycle loading pattern used was meant to be in compliance with this code requirement, and also to allow comparison with previous University of Canterbury tests.

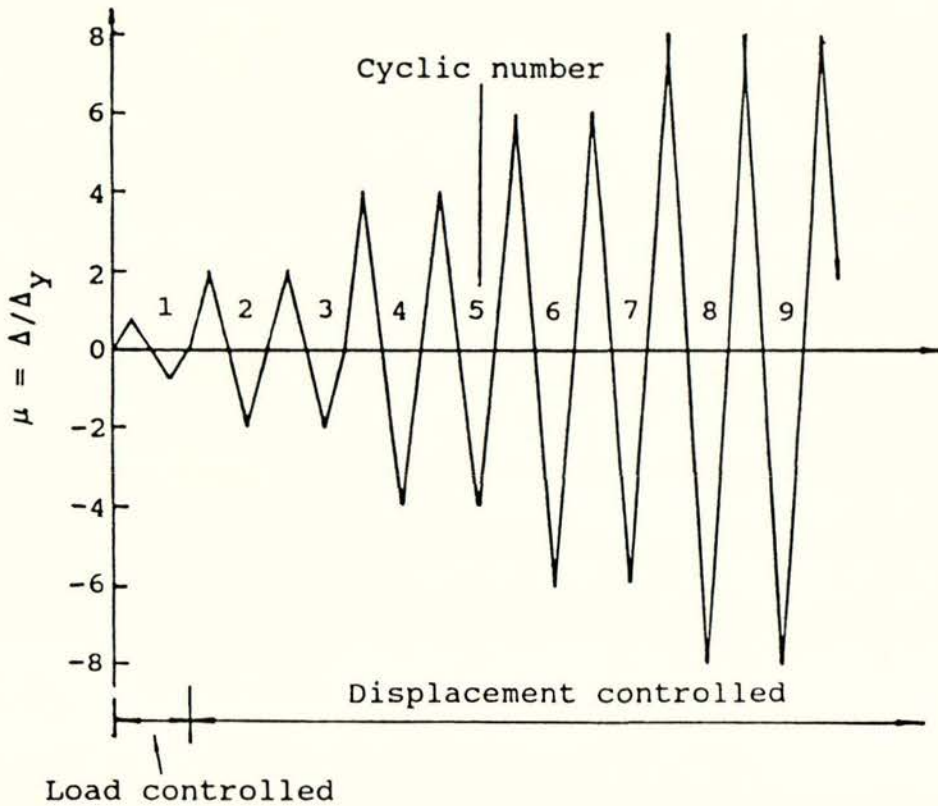


Fig. 4.15 Cyclic loading sequence used in the tests

CHAPTER 5

TEST RESULTS OF UNITS

Test results of all six units are described in this chapter. The theoretical displacement ductility factor μ is quoted when the progress of the test is described. However, the measured displacement ductility factor is easily found in the figures showing the hysteresis loops of the storey shear versus displacement.

5.1 GENERAL OBSERVATIONS

5.1.1 General

For all six units tested, the cracking in the column was far less severe than in the beam as the column was in the elastic range. The design strength of the column was nearly 1.8 times that of the beam. The following discussion refers mainly to the behaviour of the joint core and the beam.

5.1.2 Unit 1

The development of cracking is illustrated by a series of photographs taken at the various peaks of the displacement level, as shown in Fig. 5.1. A few flexural cracks appeared in the beam and column, before several diagonal cracks appeared in the joint, when the storey shear was about 60% of the theoretical strength based on measured properties in the initial stage of loading [See Fig. 5.1 (a and b)]. At the peaks of first cycle to $\mu = \pm 0.75$, the beam was still in the elastic range. At this stage, the cracks were very fine in both the joint core and the beam. According to the conventional method for defining to the yield displacement at this university, the measured yield displacement Δ_y was 20.7 mm after the movement of the rigid body of the unit was deducted. The yield storey drift Δ_y/L_c was 0.84%.

In the subsequent cycles in the inelastic range, yield strain in the beam bars at the column face was reached at $\mu = 2$. The plastic hinges developed in the beams at both

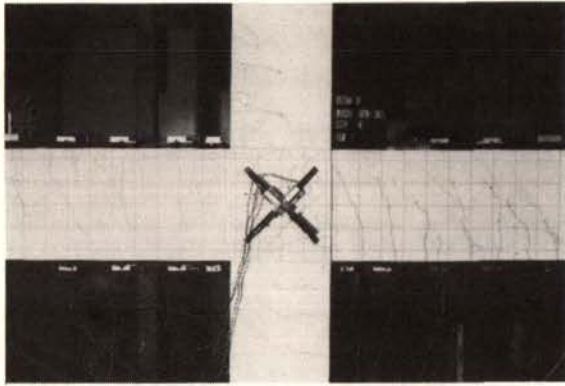
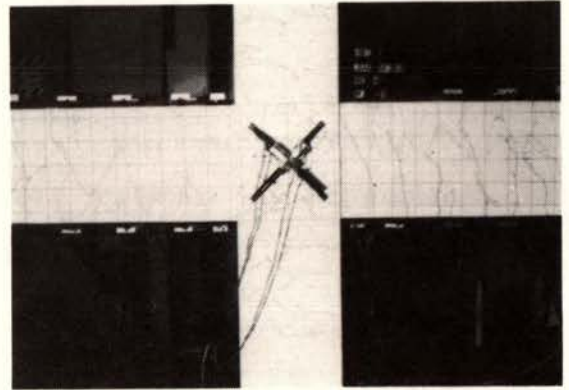
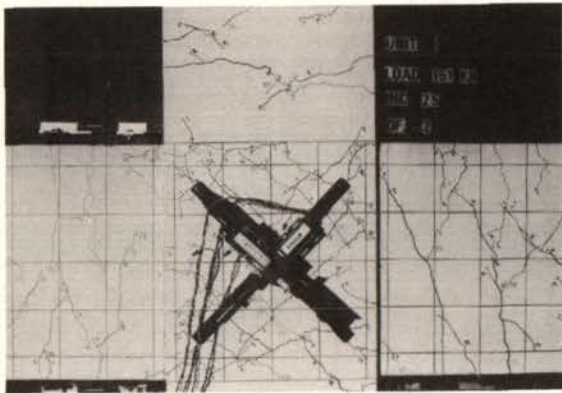
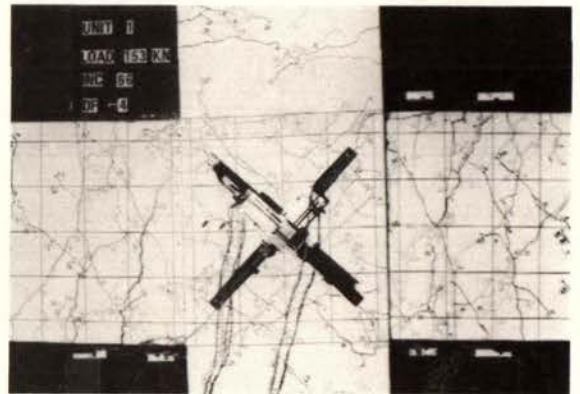
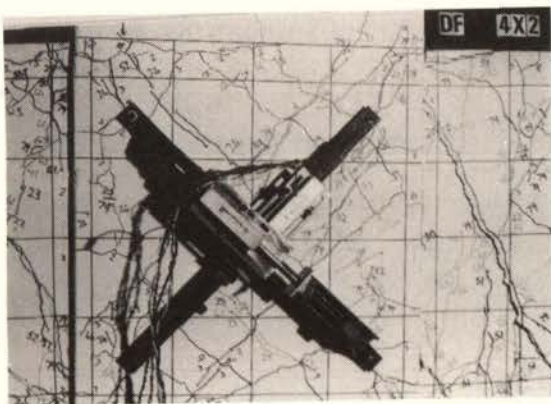
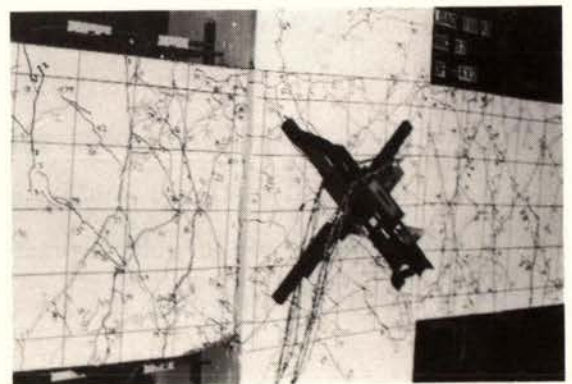
(a) $\mu = 0.75$, cycle 1(b) $\mu = -0.75$, cycle 1(c) $\mu = -2$, cycle 2(d) $\mu = -4$, cycle 4(e) $\mu = 4x2$, cycle 5(f) $\mu = -4x2$, cycle 5

Fig. 5.1 Progressive crack development for Unit 1

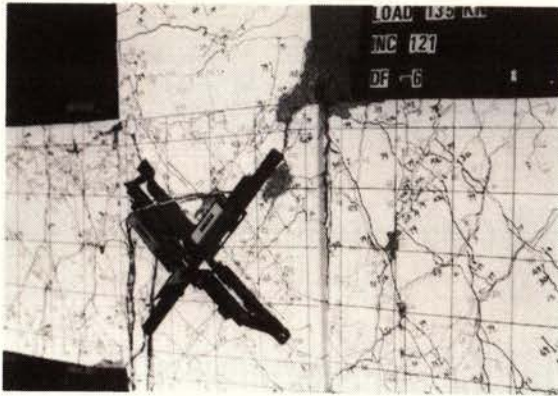
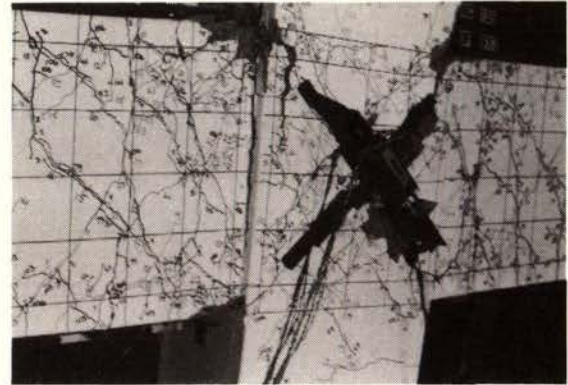
(g) $\mu = -6$, cycle 6(h) $\mu = 6 \times 2$, cycle 7

Fig. 5.1 Continued (Unit 1)

of the column face. More cracks formed in the joint core as shown in Fig. 5.1(c). No more new cracks appeared at the second cycle with same ductility factor, but the maximum surface crack width became wider in the joint core. The maximum crack width was 0.33 mm in the joint core and 2.0 mm in the beam close to the column face. The crack in the beam at column face closed under load reversal.

At the peak of first cycle to $\mu=4$, concrete crushing were observed first in the compression zone of the beam as shown in Fig. 5.1(d). More cracks developed and the width of cracks in the beam and the joint core became wider. The maximum crack width was 1.0 mm in the joint core. The joint core tended to expand. It was observed that the top beam bars moved slightly in the joint region. Crushing of concrete occurred in the joint core and slip of both the top and bottom beam bars occurred after the second cycle of loading to $\mu=-4$. However the pinching of hysteresis loops was not serious. The yield strain was reached in all rectangular joint hoops and in the diamond joint hoops positioned in the top parts of the joint.

In the first cycle to $\mu = \pm 6$, the joint core expanded significantly. At the same time, the plastic hinges in the beam developed further. There was considerable pinching in the hysteresis loops after the first cycle to $\mu = +6$. The test was stopped when the

measured storey shear was below 80% of the theoretical strength based on the measured properties. No beam bar buckling was found throughout the test. The beam depth was about 505 mm measured at 125 mm far away the column face after the test.

5.1.3 Unit 2

The development of cracking is illustrated by a series of photographs taken at the various peaks of the displacement level, as shown in Fig. 5.2. A few flexural cracks appeared in the beam and column when the storey shear was between 50% and 60% of the theoretical strength based on measured properties in the initial stage of loading (See Fig. 5.2(a and b)). At the peaks of the first load cycle to $\mu = \pm 0.75$, no cracks appeared in the joint core and the beam was still in the elastic range. The measured yield displacement Δ_y was 14.4 mm after the movement of the rigid body of the unit was deducted. The yield storey drift Δ_y/L_c was 0.58%.

In the subsequent cycles in the inelastic, plastic hinges developed in the beam at the column faces. In the first cycle to $\mu = +2$, several diagonal cracks appeared in the joint core when the storey shear was about 81% of the theoretical strength. The yield strain of the beam bar at the column face was reached at the peaks of the first cycle to $\mu = \pm 2$. The maximum measured crack width was 0.5 mm in the joint core and 4.0 mm at the column face in the beam. Almost all cracks in the joint core took place during loading cycles to $\mu = \pm 2$.

It was first observed that the movement of the bottom beam bars exceeded the half of s_r in the joint region after $\mu = -4$. Significant pinching was seen in the hysteresis loops of the storey shear and displacement after the second cycle to $\mu = +4$. No new cracks appeared in the joint core. The maximum crack width of the joint core was 0.7 mm. In the plastic hinges in the beams the maximum crack width was 8.5 mm at the column face in the bottom of the beam. At the peak of second cycle to $\mu = -4$, some concrete crushing was seen first in the compression zone of the beam.

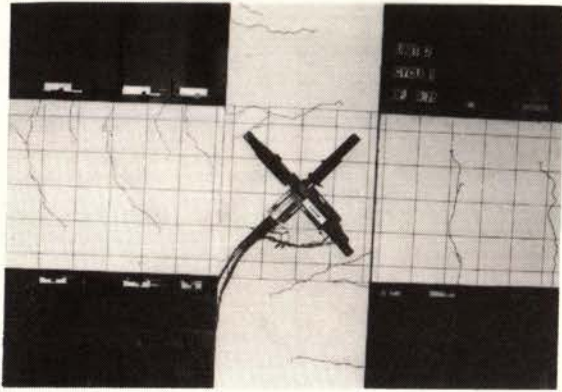
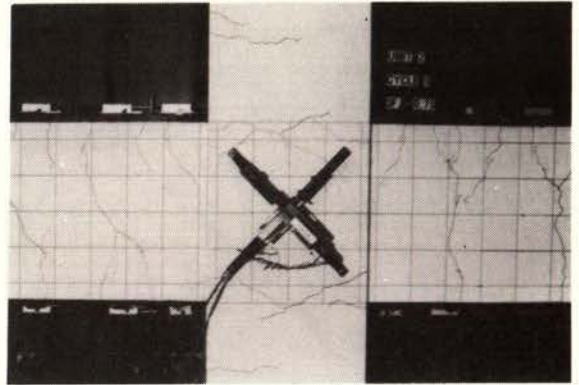
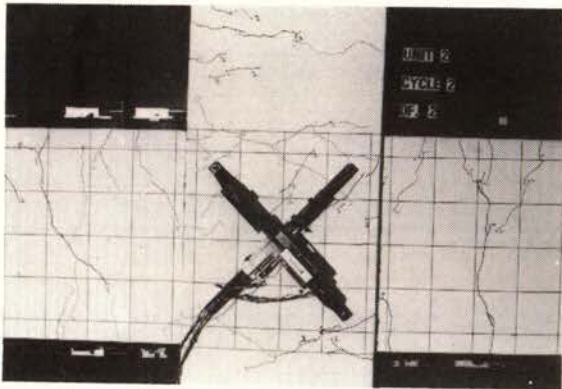
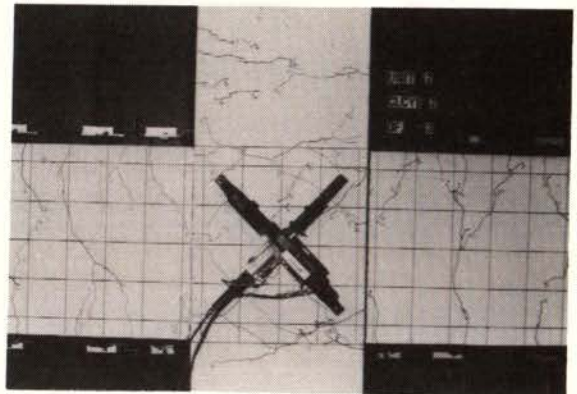
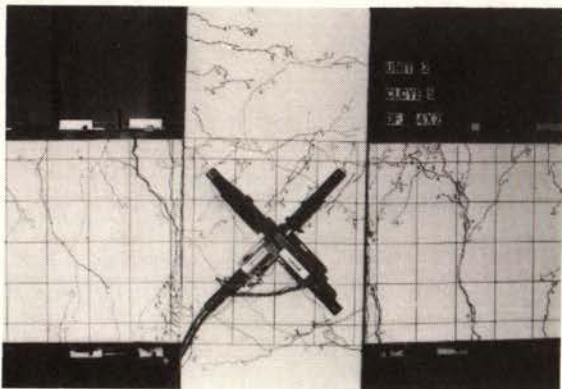
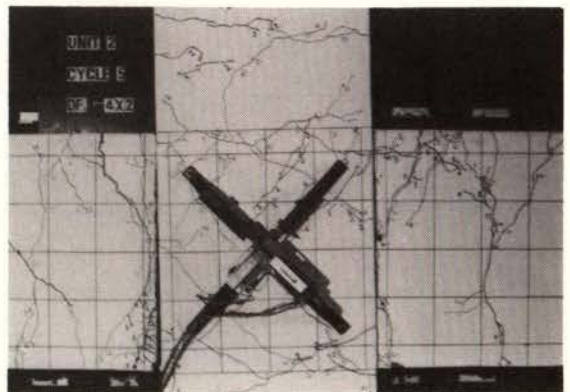
(a) $\mu = 0.75$, cycle 1(b) $\mu = -0.75$, cycle 1(c) $\mu = 2$, cycle 2(d) $\mu = -2$, cycle 2(e) $\mu = 4 \times 2$, cycle 5(f) $\mu = -4 \times 2$, cycle 5

Fig. 5.2 Progressive crack development for Unit 2

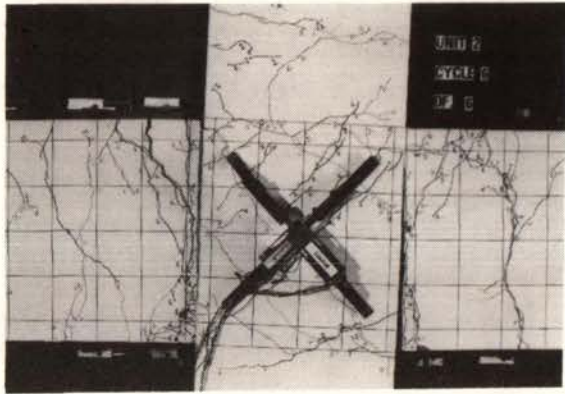
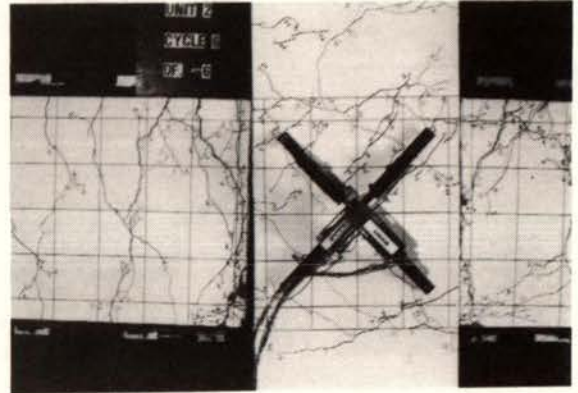
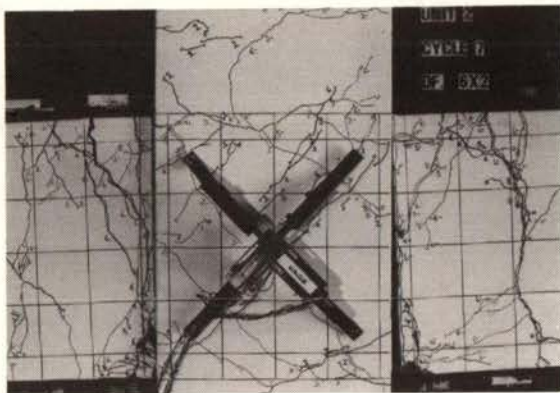
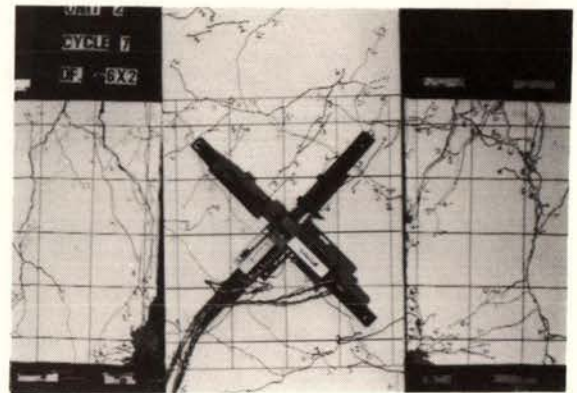
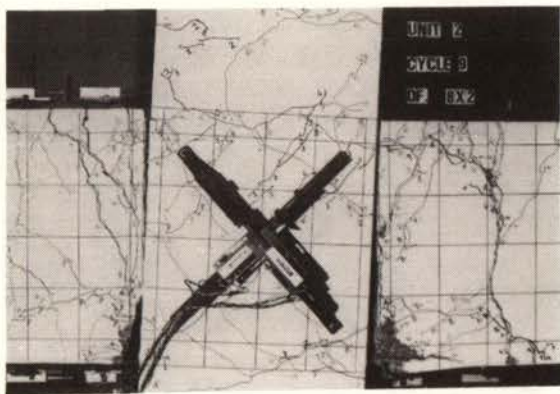
(g) $\mu = 6$, cycle 6(h) $\mu = -6$, cycle 6(i) $\mu = 6x2$, cycle 7(j) $\mu = -6x2$, cycle 7(k) $\mu = 8x2$, cycle 9(l) $\mu = -8x2$, cycle 9

Fig. 5.2 Continued (Unit 2)

After the bottom beam bars slipped slightly, some cracks that were almost horizontal appeared in the beam close to the column face as shown in Fig. 5.2 (g,h,i and j). Even though the slip of the bottom beam bars was significant, the storey shear still kept above the theoretical strength at the peaks of the cycle loading, until the slip of the top beam bars occurred at the second cycle to $\mu = \pm 8$.

The yield strain was not measured in all joint core hoops when the test was terminated. The joint core region was almost integral and the number of cracks was greater on the top than on the bottom of the joint core regions shown in Fig. 5.2(l). Buckling of beam bars was not observed that during the test. The beam depth was almost unchanged after the test. The crack at the column face on the bottom of the beam closed and the two surfaces of the crack at the column face at the top of the beam contacted each other under load reversal throughout the test.

5.1.4 Unit 3

The development of cracking is illustrated by a series of photographs taken at the various peaks of the displacement level as shown in Fig. 5.3. A few flexural cracks were observed in the beam and column, before a diagonal crack in the joint core appeared when the storey shear was about 62% of the theoretical strength based on measured properties in the initial stage of loading [See Fig. 5.1 (a)]. At the peaks of first cycle to $\mu = \pm 0.75$, the beam was still in the elastic range. At this step, the maximum diagonal crack width in the joint core was about 0.2 mm. The measured yield displacement Δ_y was 16.5 mm after the movement of the rigid body of the unit was deducted. The yield storey drift Δ_y/L_c was 0.67%.

In the subsequent cycles, plastic hinges developed in the beam at both of the column faces. The yield strain of the beam bar in the tensile zone at the column face was reached when the displacement was at the level of $\mu = 2$. The plastic hinges developed at both of the column face on the beam. More cracks generated in the joint core as shown in Fig. 5.3(c and d). No more new cracks appeared during the second cycle to the same displacement same ductility factor. The maximum surface crack width

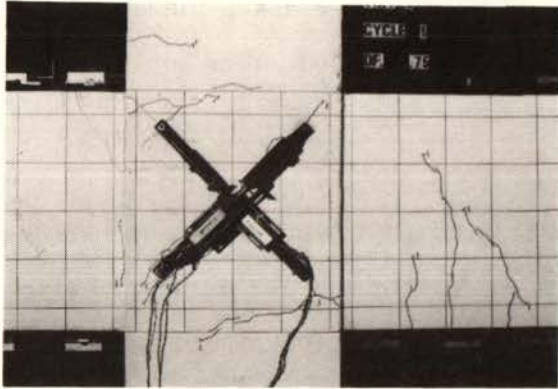
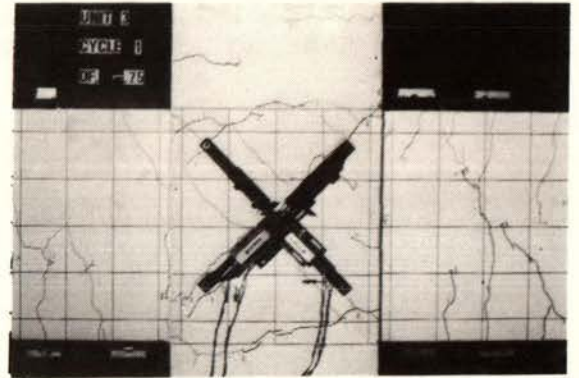
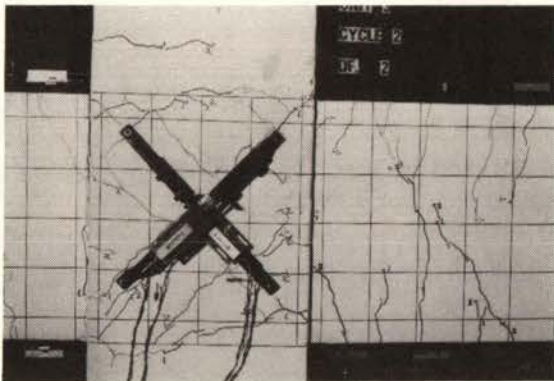
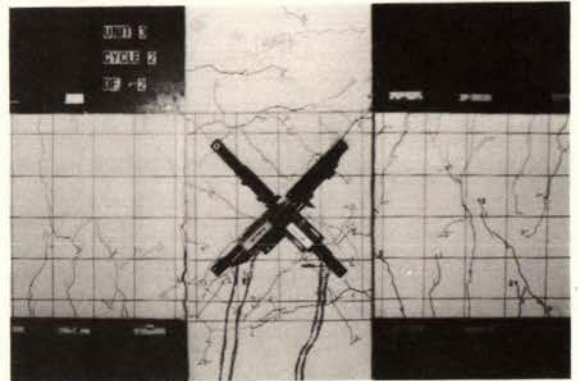
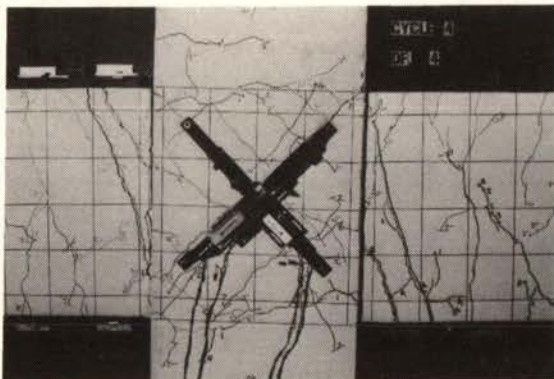
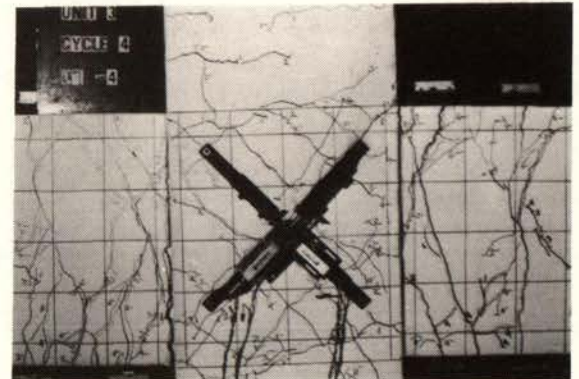
(a) $\mu = 0.75$, cycle 1(b) $\mu = -0.75$, cycle 1(c) $\mu = 2$, cycle 2(d) $\mu = -2$, cycle 2(e) $\mu = 4$, cycle 4(f) $\mu = -4$, cycle 4

Fig. 5.3 Progressive crack development for Unit 3

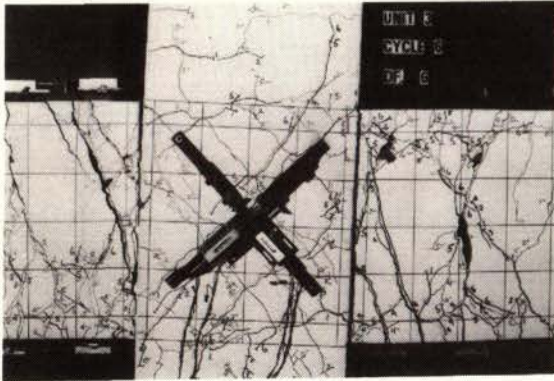
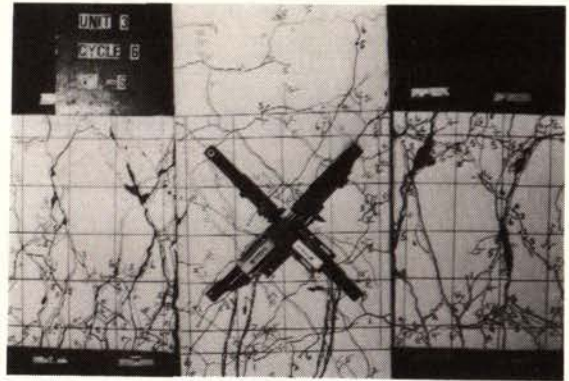
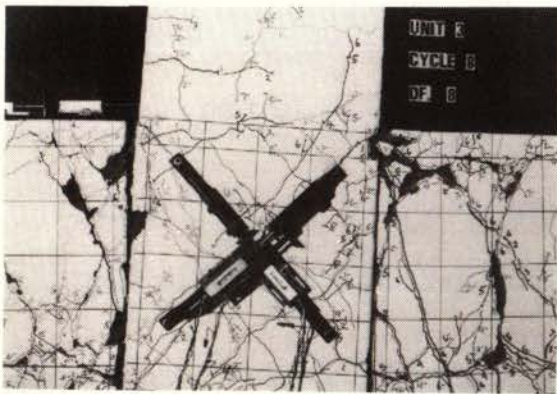
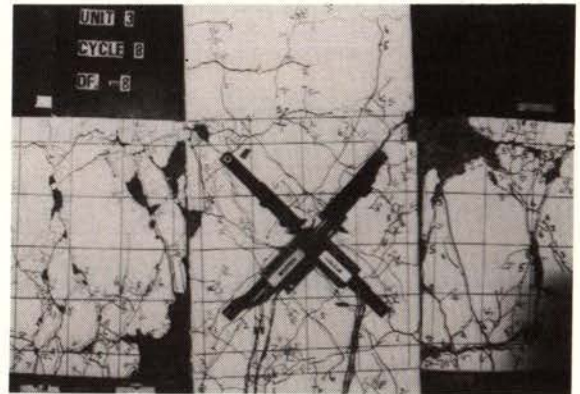
(g) $\mu = 6$, cycle 6(h) $\mu = -6$, cycle 6(i) $\mu = 8$, cycle 8(j) $\mu = -8$, cycle 8

Fig. 5.3 Continued (Unit 3)

became wider in the joint core. The maximum crack width was about 0.60 mm in the joint core and 5.0 mm in the beam close to the column face. The crack in the beam at the column face closed under load reversal.

The response of the tested unit was still satisfactory after two loading cycles were completed at the level of $\mu=4$. The plastic hinges in the beams developed further and more cracks appeared in the joint core and beams. The maximum crack width was 1.0 mm in the joint core and 7.0 mm in the beam close to the column face. Most of the horizontal joint hoops had been yielded.

Concrete crushing occurred first in the compression zone of the beam at the peak of the first cycle to $\mu = +6$ as shown in Fig. 5.3(g). At the same time, the top beam bar in the joint region began to move. The pinching was considerable in the hysteresis loops of storey shear and displacement after a displacement ductility factor of 8 was reached. Even though the plastic hinges in the beam were well developed, no beam bar buckling was observed when the test finished after one loading cycle was completed at the level of displacement ductility factor of 8.

5.1.5 Unit 4

The development of cracking is illustrated by a series of photographs taken at the various peaks of the displacement level as shown in Fig. 5.4. A few flexural cracks appeared in the beam and column, before several diagonal cracks in the joint formed when the storey shear was about 71% of the theoretical strength based on measured properties in the initial stage of loading (See Fig. 5.4 (a and b)). At the peaks of first cycle to $\mu = \pm 0.75$, the beam was still in the elastic range. At this stage, the maximum crack width was about 0.1 mm in the joint core and 0.5 mm in the beam. The measured yield displacement Δ_y was 14.1 mm after the movement of the rigid body of the unit was deducted. The yield storey drift Δ_y/L_c was 0.57%.

The yield strain in the beam bar in the tensile zone at the column face was reached when the displacement was at the level of $\mu = 2$. With the plastic hinges formed in the beam at both of the column faces, more cracks appeared in the joint core, as shown in Fig. 5.1(c and d). The maximum crack width was 0.80 mm in the joint core and 4.5 mm in the beam close to the column face.

Although it was observed that the bottom beam bars moved to have been over one half of s_r in the joint region after the first cycle to $\mu = -4$, the pinch of the hysteresis loops was still not evident. At the peak of the second cycle to $\mu = -4$, concrete crushing took place first in the beam as shown in Fig. 5.1(f). No more cracks appeared. However the cracks lengthened and the width of cracks in the beam and the joint core increased.

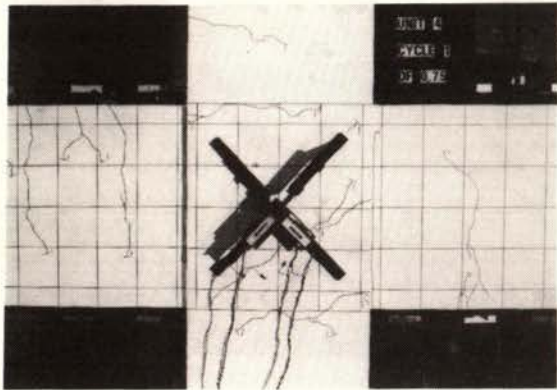
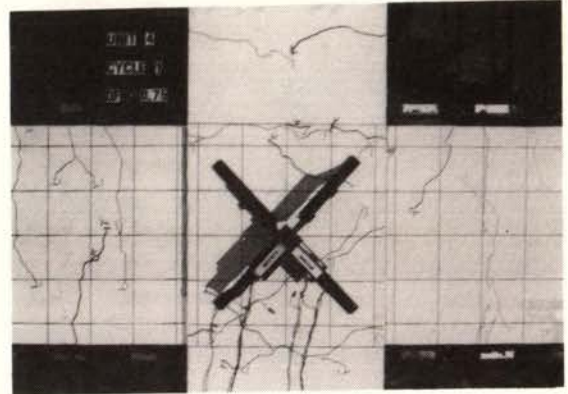
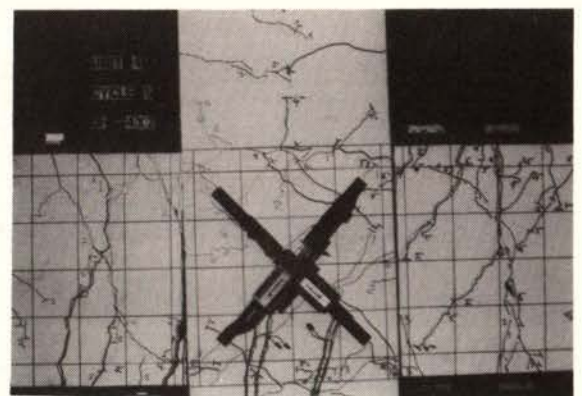
(a) $\mu = 0.75$, cycle 1(b) $\mu = -0.75$, cycle 1(c) $\mu = 2$, cycle 2(d) $\mu = -2x2$, cycle 3(e) $\mu = 4x2$, cycle 5(f) $\mu = -4x2$, cycle 5

Fig. 5.4 Progressive crack development for Unit 4

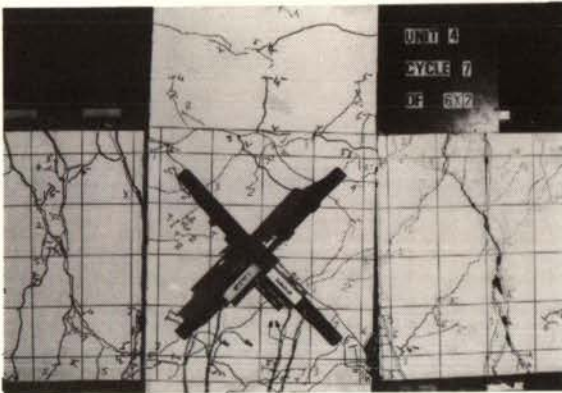
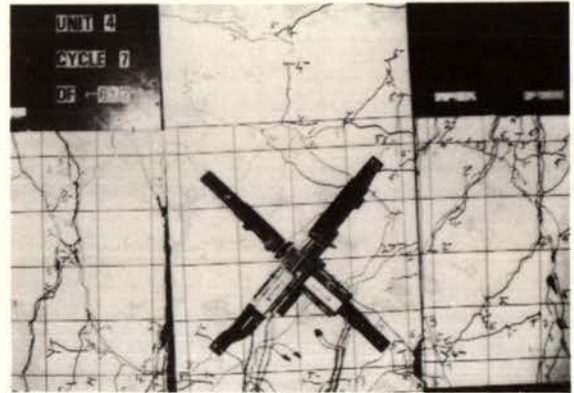
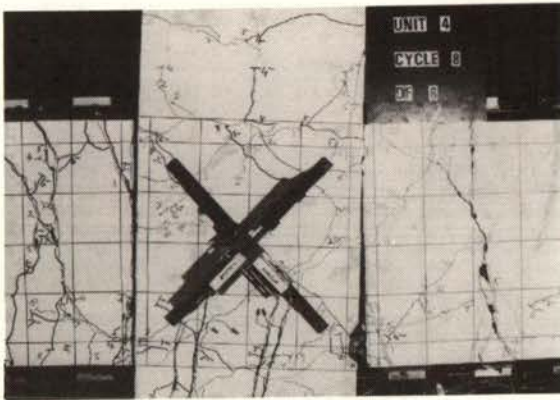
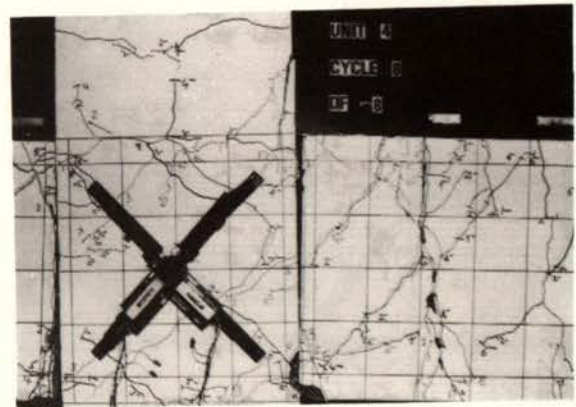
(g) $\mu = 6x2$, cycle 7(h) $\mu = -6x2$, cycle 7(i) $\mu = 8$, cycle 8(j) $\mu = -8$, cycle 8

Fig. 5.4 Continued (Unit 4)

The maximum crack width was about 1.0 mm in the joint core and 6.5 mm in the beam close to the column face. The joint core tended to expand.

After the first cycle to $\mu = +6$, the substantial pinching occurred in the hysteresis loops and some concrete crushing occurred at the bottom of the beam. When the test stopped after one cycle loading to $\mu = 8$, the measured storey shear was still above 80% of the theoretical strength based on the measured properties. No beam bar buckling was observed throughout the test. The beam depth was almost unchanged after the test. The crack at the bottom of the beam at the column face closed, and the two surfaces of the crack at the column face at the top of the beam came into contact after load reversal throughout the test.

5.1.6 Unit 5

The development of cracking is illustrated by a series of photographs taken at the various peaks of the displacement level as shown in Fig. 5.5. After a few flexural cracks appeared in the beam and column, several diagonal cracks formed in the joint core when the storey shear was about 46% of the theoretical strength based on measured properties in the initial stage of loading (See Fig. 5.5 (a and b)). At the peaks of first cycle to $\mu = \pm 0.75$, the beam was still in the elastic range. At this stage, the maximum crack width was 0.3 mm in the joint core and 0.2 mm in the beam. The measured yield displacement Δ_y was 19.6 mm after the movement of the rigid body of the unit was deducted. The yield storey drift Δ_y/L_c was 0.79%.

The yield strain in the beam bar in the tensile zone at the column face was reached, when the displacement was at the level of $\mu = 2$. The plastic hinges developed in the beam at both of the column faces. More cracks appeared in the joint core as shown in Fig. 5.5(c,d,e and f). A few new cracks appeared in the second cycle with same ductility factor, and the maximum crack widths became greater in the joint core. The maximum crack width was 0.90 mm in the joint core and 3.5 mm in the beam close to column face. The crack in the beam at the column face closed during load reversal.

After the second loading cycle to $\mu = +4$, concrete crushing was first seen in the beam as shown in Fig. 5.5(g and h). The maximum crack width was 1.2 mm in the joint and 5.5 mm in the beam close to the column face. It was observed that the top or bottom beam bars did not move in the joint region. Some rectangular joint hoops and all diamond joint hoops had yielded at this stage.

During the loading cycle to $\mu = \pm 6$, the plastic hinges developed further and concrete crushing first occurred in the beam. The top beam bars began to move in the region of the joint core after $\mu = +6$. The joint core tended to expand. Pinching was observed in the hysteresis loops after $\mu = +6$. No beam bar buckling was observed during the test. The beam depth was about 505 mm measured at 125 mm away from the column face after the test.

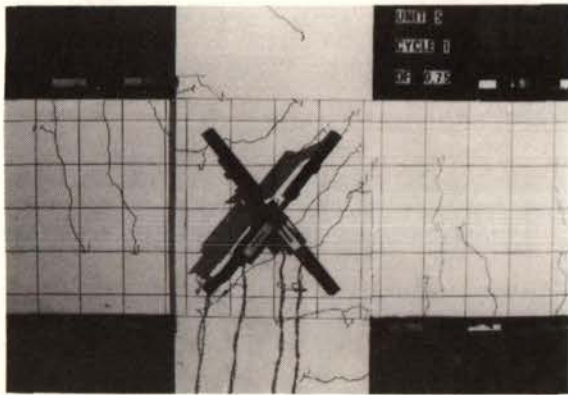
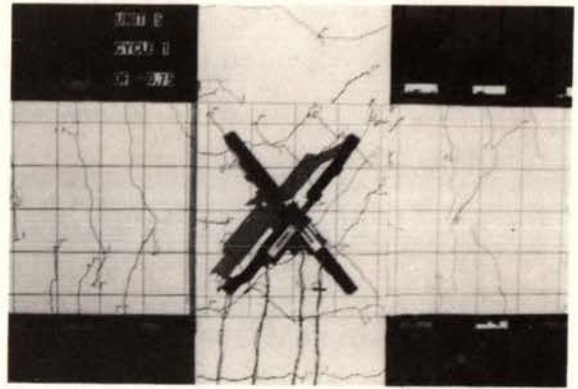
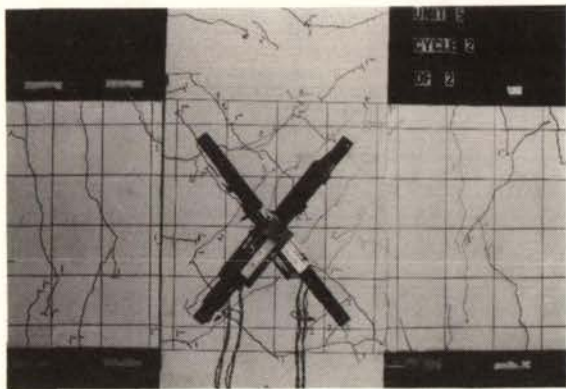
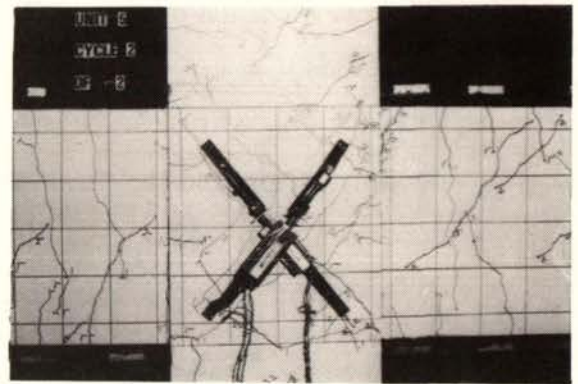
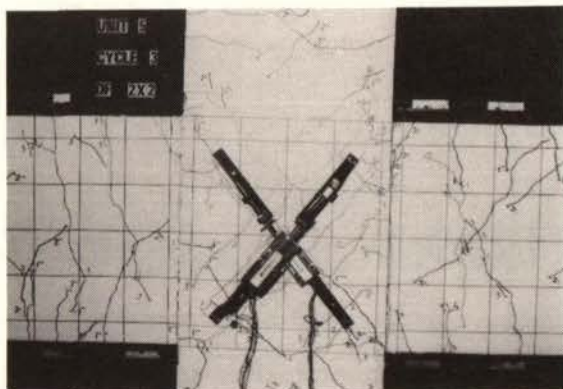
(a) $\mu = 0.75$, cycle 1(b) $\mu = -0.75$, cycle 1(c) $\mu = 2$, cycle 2(d) $\mu = -2$, cycle 2(e) $\mu = 2x2$, cycle 3(f) $\mu = -2x2$, cycle 3

Fig. 5.5 Progressive crack development for Unit 5

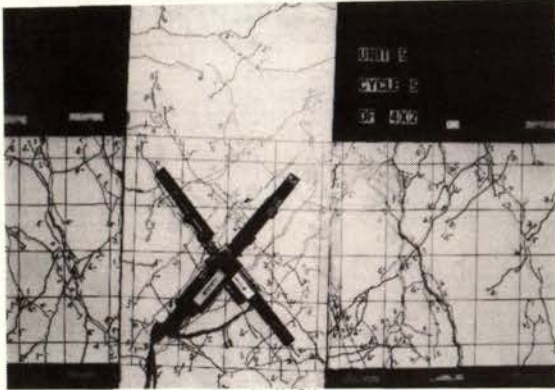
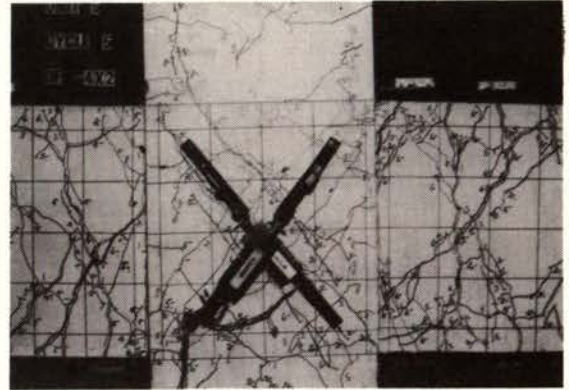
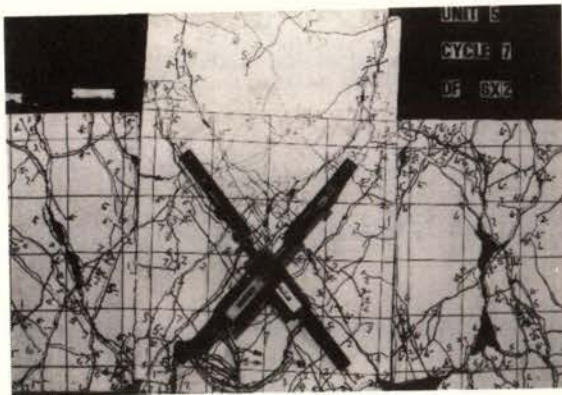
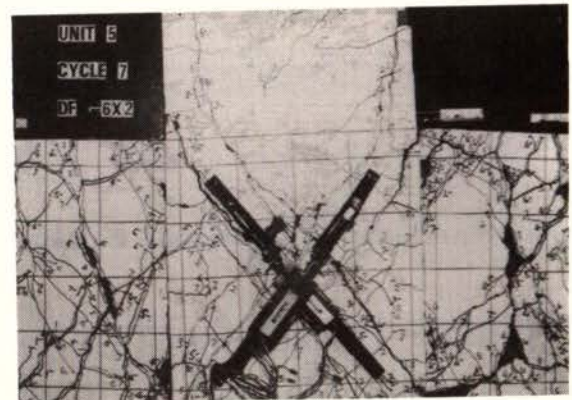
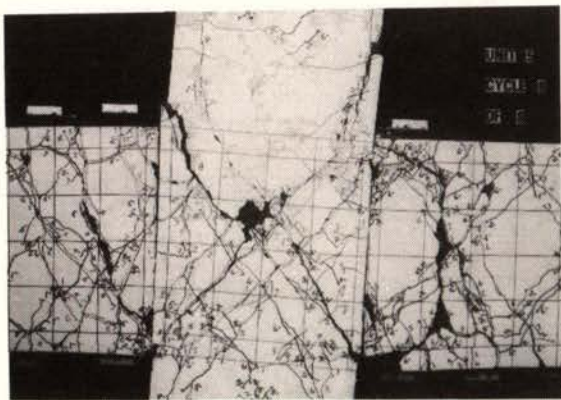
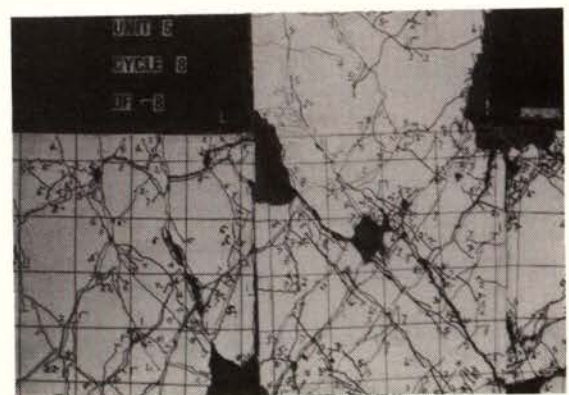
(g) $\mu = 4x2$, cycle 5(h) $\mu = -4x2$, cycle 5(i) $\mu = 6x2$, cycle 7(j) $\mu = -6x2$, cycle 7(k) $\mu = 8$, cycle 8(l) $\mu = -8$, cycle 8

Fig. 5.5 Continued (Unit 5)

5.1.7 Unit 6

The development of cracking is illustrated by a series of photographs taken at the various peaks of the displacement level, as shown in Fig. 5.6. After a few flexural cracks appeared in the beam and column, a diagonal crack formed in the joint when the storey shear was about 61% of the theoretical strength based on measured properties in the initial stage of loading (See Fig. 5.6(a and b)). At the peaks of the first cycle to $\mu = \pm 0.75$, the beam was still in the elastic range. At this stage, the maximum crack width was 0.3 mm in the joint core and 0.3 mm in the beam. The measured yield displacement Δ_y was 16.3 mm after the movement of the rigid body of the unit was deducted. The yield storey drift Δ_y/L_c was 0.66%.

The yield strain in the beam bar in the tensile zone at the column face was reached when the displacement was at the level of $\mu = 2$. Plastic hinges developed in the beam at both of the column faces. More cracks appeared in the joint core as shown in Fig. 5.6(c and d). No new cracks appeared in the second cycle with same ductility factor. The maximum crack width was 0.6 mm in the joint core and 2.6 mm in the beam close to column face.

During the loading cycle to $\mu = \pm 4$, the plastic hinges developed further in the beam, and meanwhile more cracks formed in both the joint core and the beam. The maximum crack width was 0.6 mm in the joint core and 4.5 mm in the beam close to the column face. Only the bottom layer of diamond joint hoops had yielded at this stage.

The bottom beam bars moved in the joint region after the first loading cycle to $\mu = +6$, and the pinching occurred in the measured hysteresis loops. Concrete crushing occurred in the beam and at the corner of the joint. The test was not finished until two loading cycles to $\mu = 8$ were applied. No buckling of beam bar was observed during the test. The beam depth was about 505 mm, measured at 125 mm from the column face after the test. The crack at the column face at the bottom of the beam closed, and the two surfaces of the crack at the column face at the top of the beam contacted each other during load reversals throughout the test.

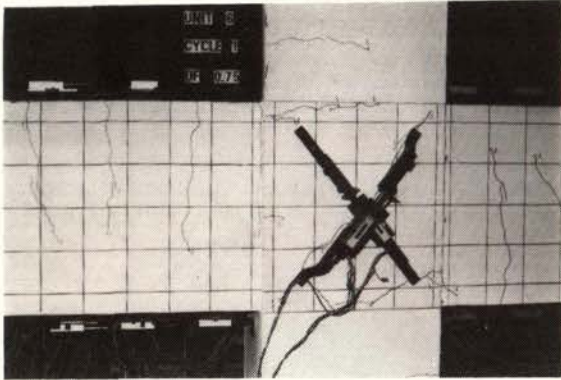
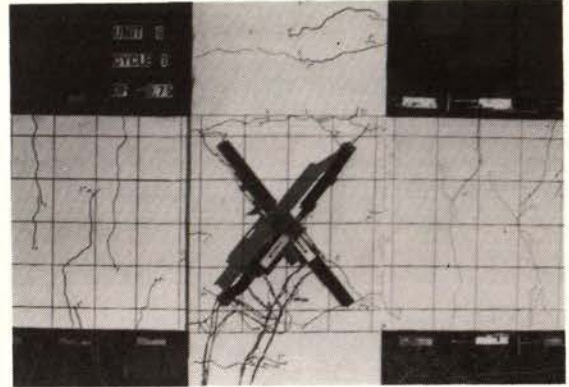
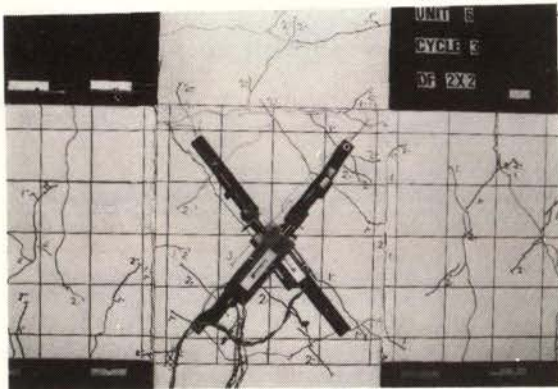
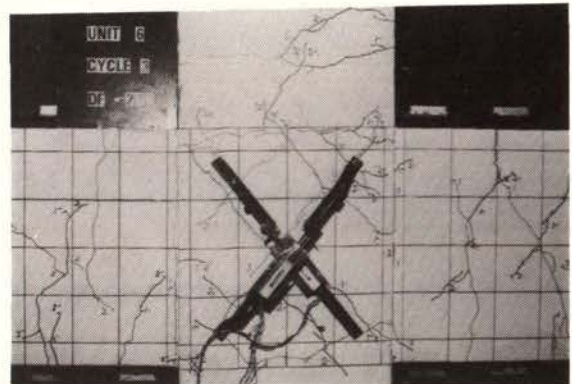
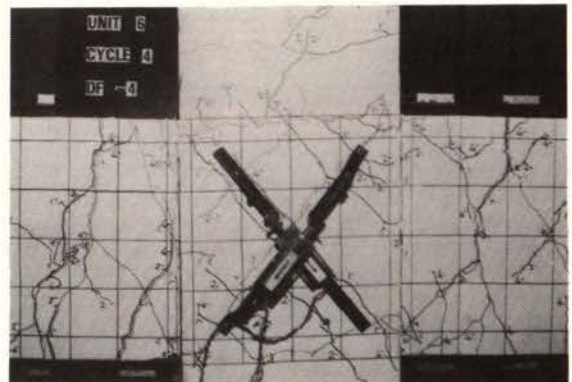
(a) $\mu = -0.75$, cycle 1(b) $\mu = -0.75$, cycle 1(c) $\mu = 2x2$, cycle 3(d) $\mu = -2x2$, cycle 3(e) $\mu = 4$, cycle 4(f) $\mu = -4$, cycle 4

Fig. 5.6 Progressive crack development for Unit 6

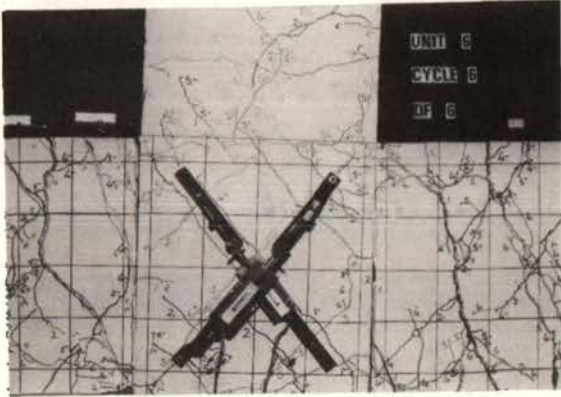
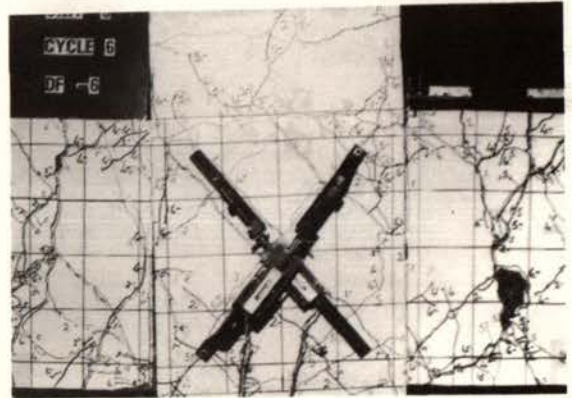
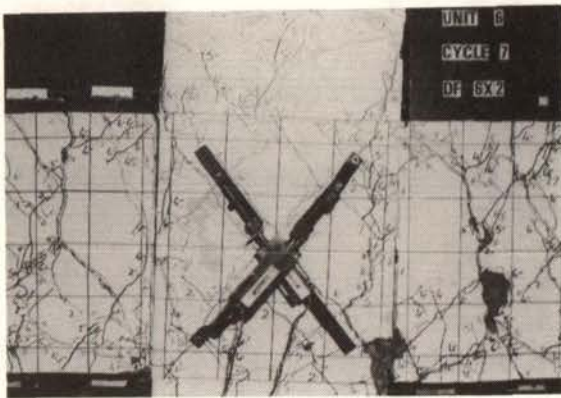
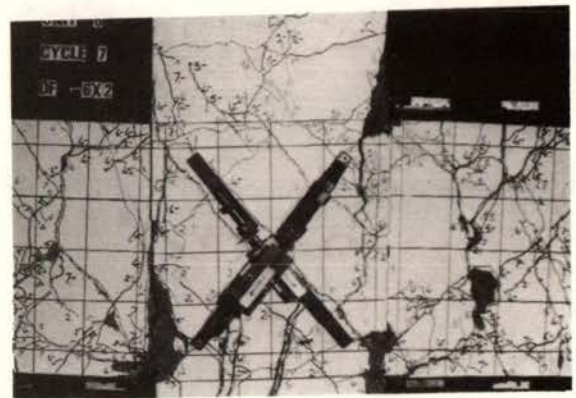
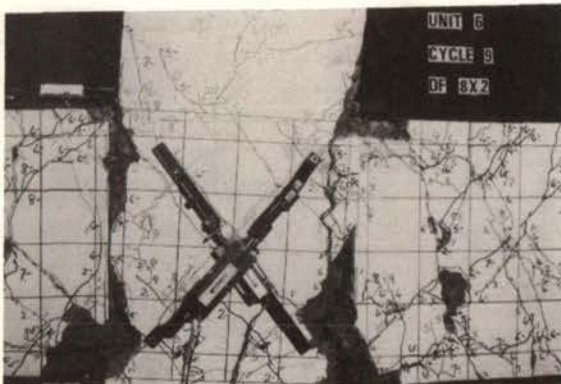
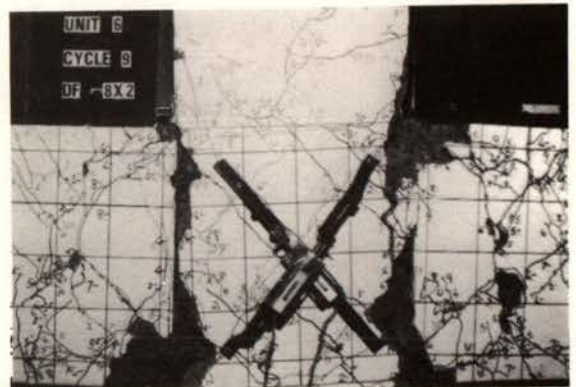
(g) $\mu = 6$, cycle 6(h) $\mu = -6$, cycle 6(i) $\mu = 6x2$, cycle 7(j) $\mu = -6x2$, cycle 7(k) $\mu = 8x2$, cycle 9(l) $\mu = -8x2$, cycle 9

Fig. 5.6 Continued (Unit 6)

5.2 LOAD-DISPLACEMENT RESPONSE

Fig. 5.7 to Fig. 5.12 display the measured storey shear versus displacement hysteresis loops for all six units. It is evident that the pinching of the hysteresis loops of Unit 2 is the most serious of the six units; the next most serious is Unit 4. As mentioned in Section 5.1, the pinching of the hysteresis loops of Unit 2,1,3,4,5 and 6 in the loops started about after the loading cycle was the second cycle to +4, and the first cycle to $\mu = +6$, $\mu = +8$, $\mu = +6$, $\mu = +6$ and $\mu = +6$, respectively. The measured and theoretical first yield displacement of units are listed in Table 5.1.

Table 5.1 Measured $\Delta_{y,m}$ and theoretical $\Delta_{y,t}$

Unit	1	2	3	4	5	6
$\Delta_{y,t}(\text{mm})$	12.6	10.9	11.4	9.1	19.6	14.0
$\Delta_{y,m}(\text{mm})$	20.7	14.4	16.5	14.1	12.7	16.3

5.3 BEAM BAR SLIP

Fig. 5.13 to Fig. 5.18 show the measured hysteresis loops of horizontal column load versus beam bar slip. It can be observed when the significant movement of beam bars commenced due to loss of bond. Table 5.2 lists when slip of beam bars exceeded S_r

Table 5.2 Loss of bond of beam bars

Unit	1	2	3	4	5	6
Top beam after $\mu =$	-4 second cycle	+8 first cycle	+6 first cycle	-6 second cycle	+6 first cycle	-6 second cycle
Bottom beam after $\mu =$	-4 second cycle	-4 first cycle	-6 first cycle	-4 first cycle	-6 second cycle	+6 first cycle

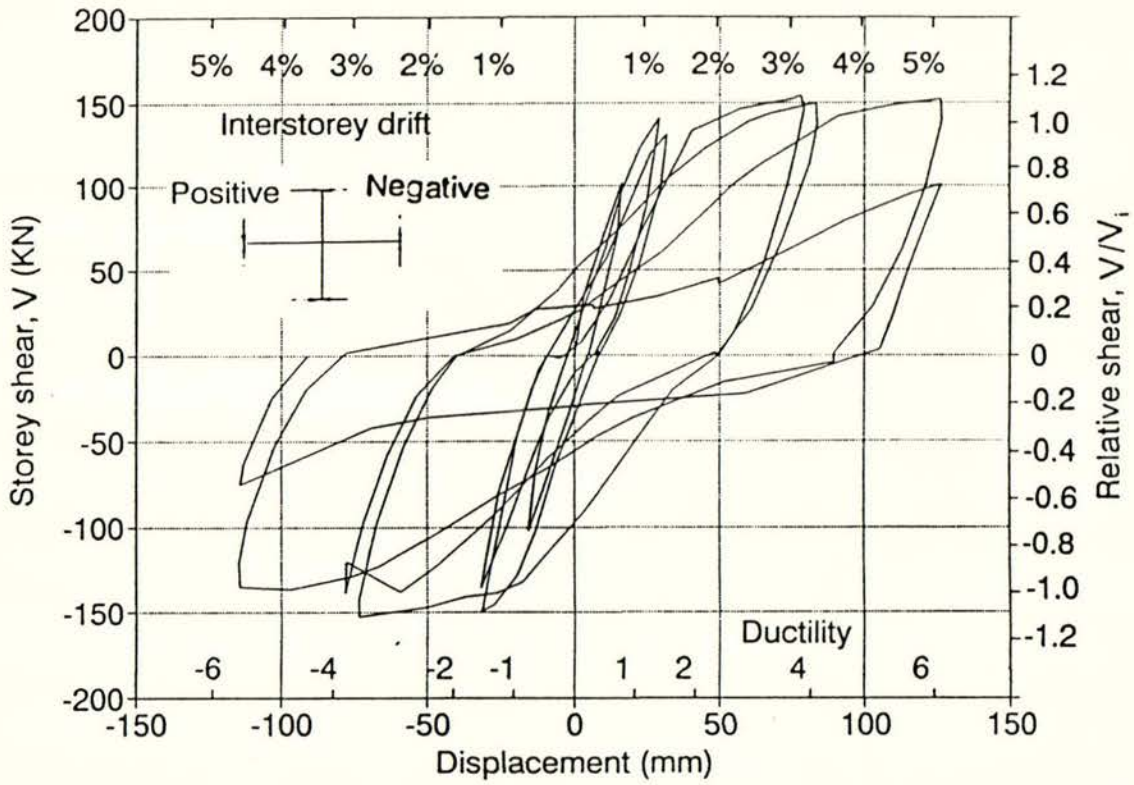


Fig. 5.7 Storey shear versus displacement loops, Unit 1

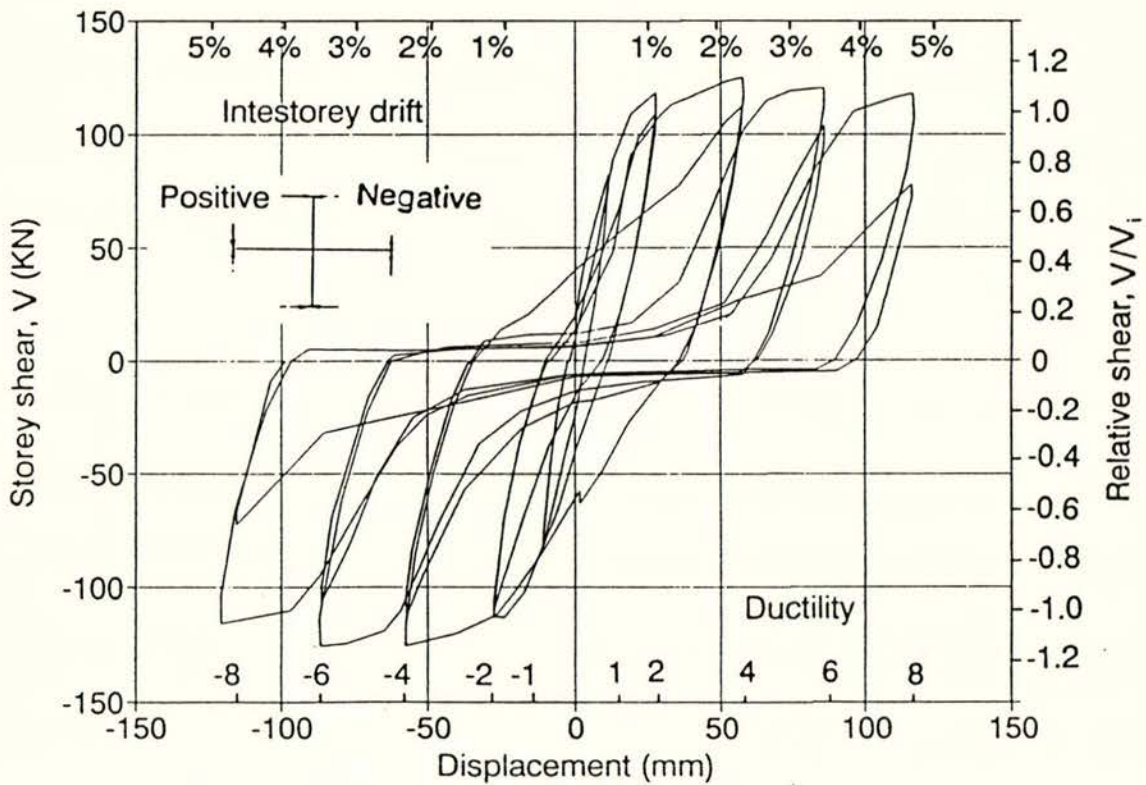


Fig. 5.8 Storey shear versus displacement loops, Unit 2

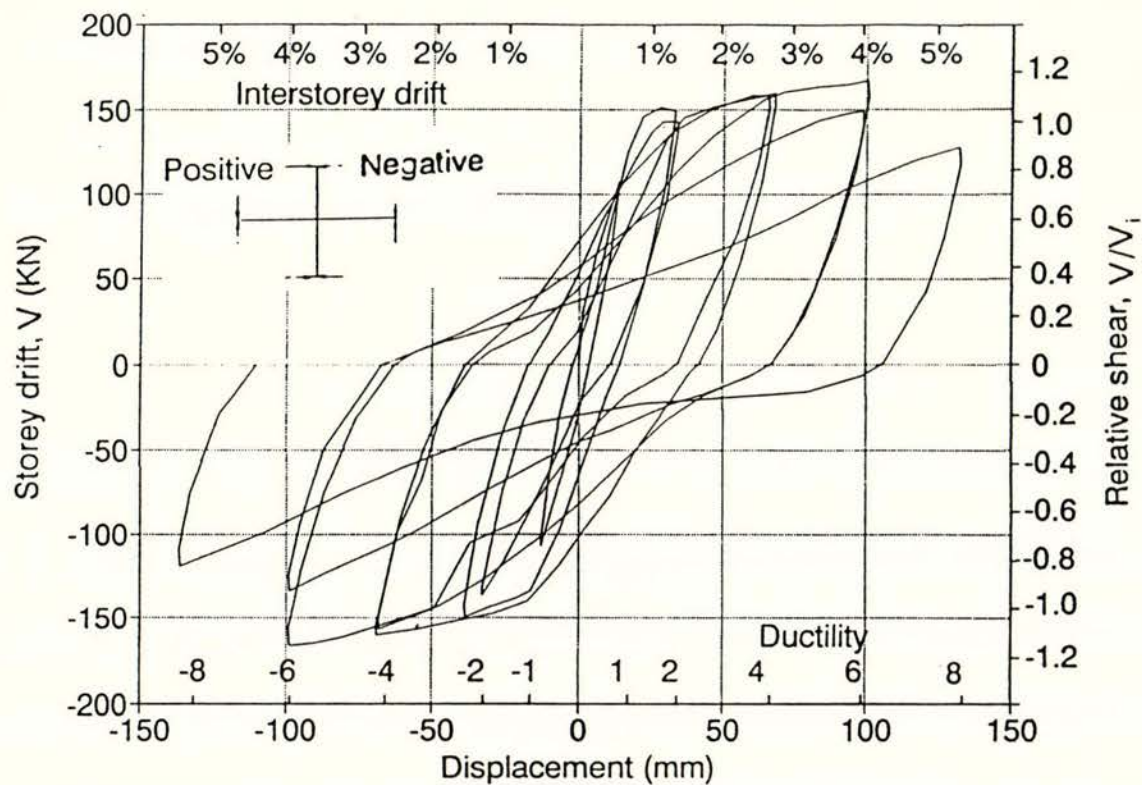


Fig. 5.9 Storey shear versus displacement loops, Unit 3

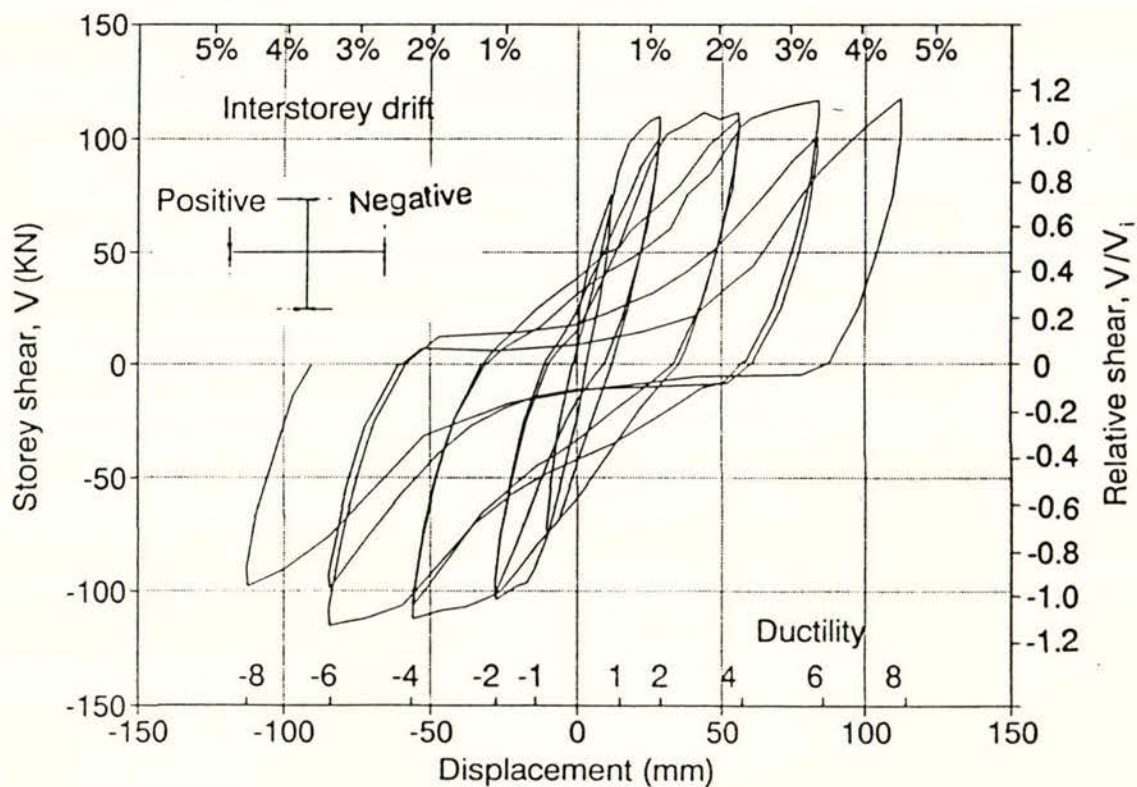


Fig. 5.10 Storey shear versus displacement loops, Unit 4

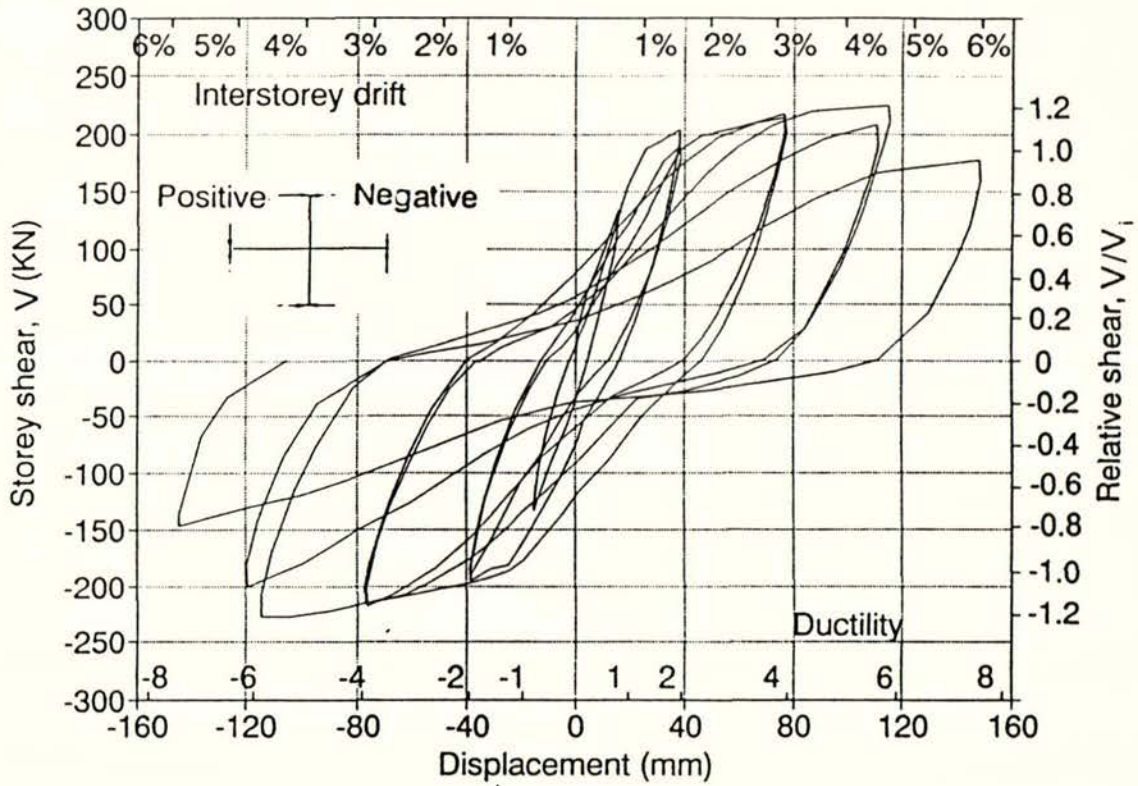


Fig.5.11 Storey shear versus displacement loops, Unit 5

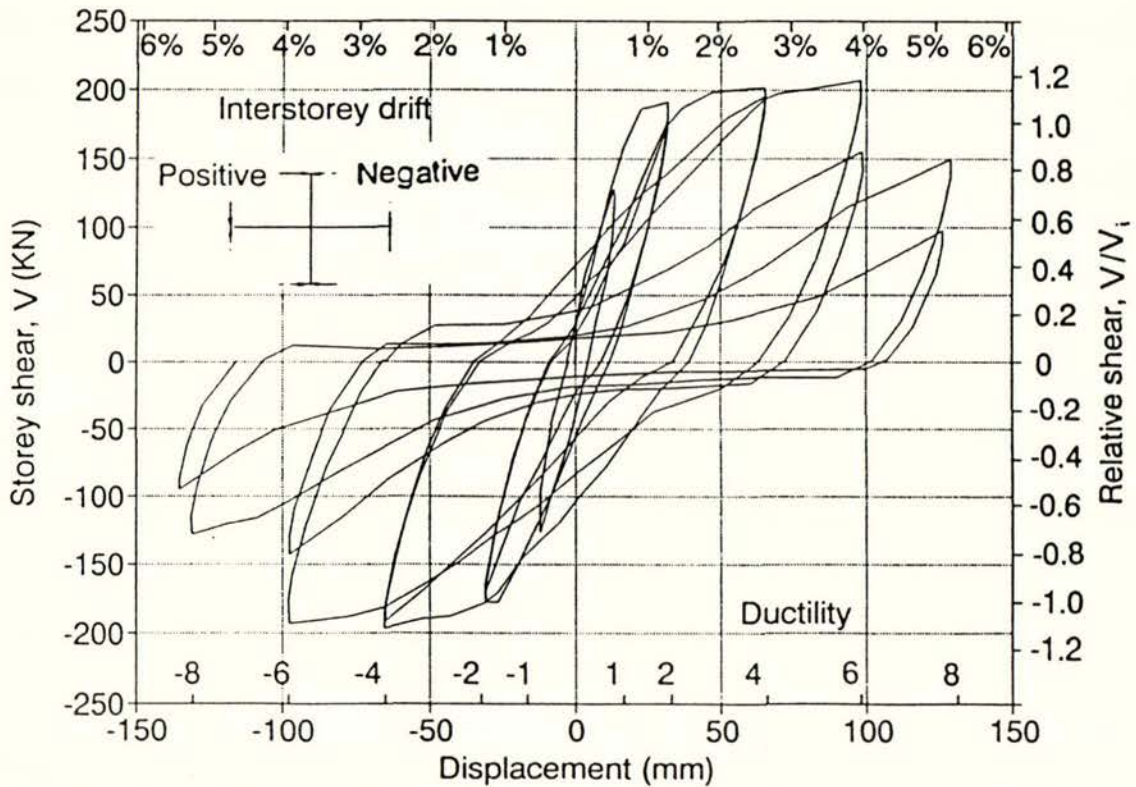


Fig.5.12 Storey shear versus displacement loops, Unit 6

5.4 COMPONENTS OF DISPLACEMENT

The storey displacement mainly consists of the deformation due to flexural and shear of the beam, flexural and shear of the column and the joint shear distortion as below,

$$\Delta = \Delta_b + \Delta_c + \Delta_j \quad (5.1)$$

The measured contributions to the storey displacement due to the deformation of the beam, the column, and the joint core are displayed for various load stages in Fig. 5.19(a) to Fig. 5.24(a). With increase in the number of loading cycles, the rate of contribution to the storey displacement due to deformation of the column reduced in all units. The contribution to the storey displacement due to the joint shear distortion was around 15% to 20% of total storey displacement for Unit 1, 3 and 5, and less than 10% of total storey displacement for Unit 2, 4 and 6.

Fig. 5.19(b) to Fig. 5.24(b) show the measured contribution of each part of the beam to the beam deformation. The deformation due to Segment 1 was the largest and includes both the slip and the elongation of the beam bars. The contribution of the slip of the beam bars to the beam deformation is also presented in these figures.

The measured distributions of curvature for all units along the beam are illustrated in Fig. 5.25 to Fig. 5.30. The value of the curvature within Segment 1 (Segments are defined in above figures) is several many times that of Segment 2. The major reason is that for Segment 1 it consists of the elongation and slip of the beam bars. Therefore, it could be accepted that the deformation within Segment 1 is approximately equal to be total accumulation of the elongation and slip of the beam bars.

It was found that the measured joint shear distortion was unsymmetric during cyclic load in the course of a test, as shown in Fig. 5.31 to Fig. 5.36. This phenomenon was caused by the different widths of the main diagonal cracks in the two diagonal directions.

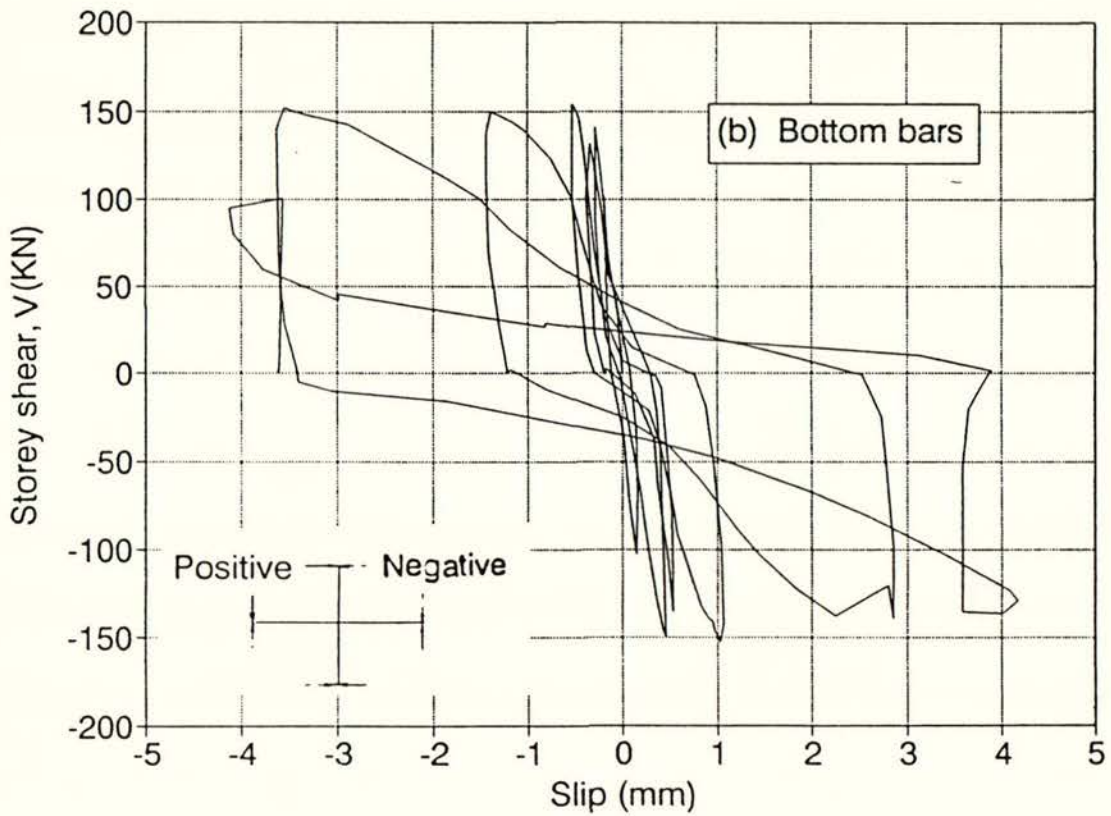
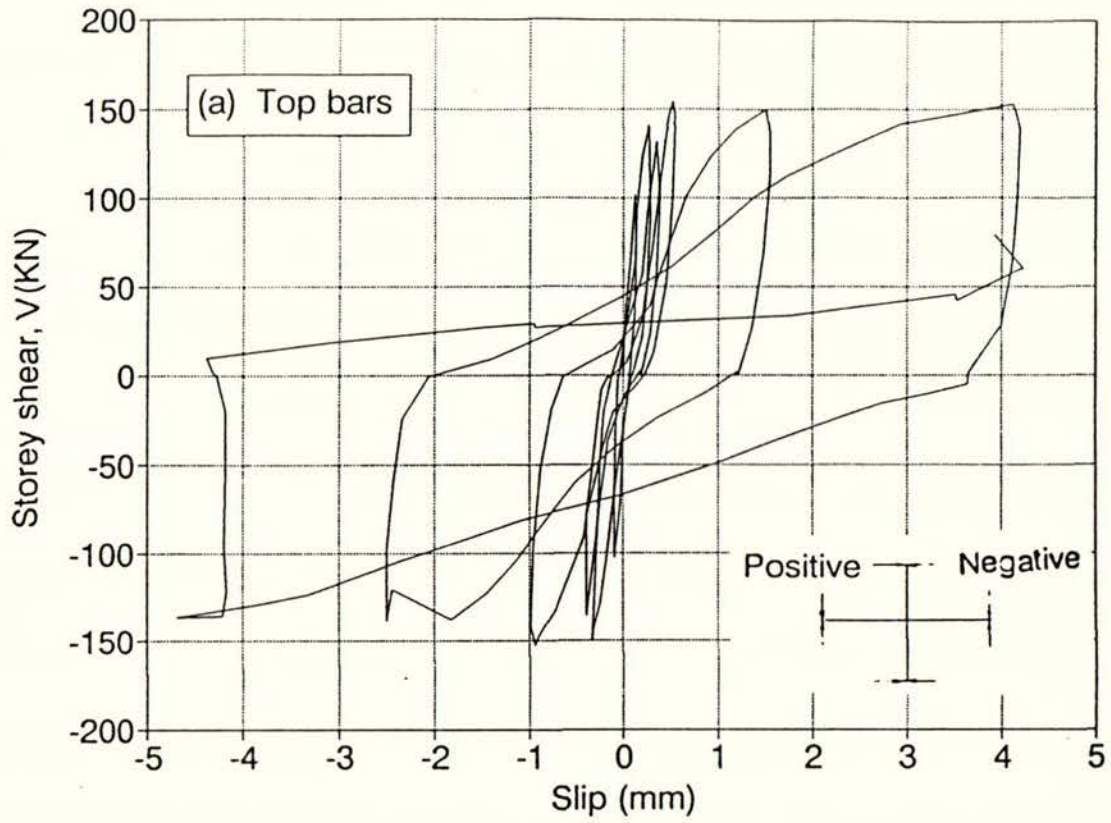


Fig. 5.13 Slip of beam bars within the joint core, Unit 1

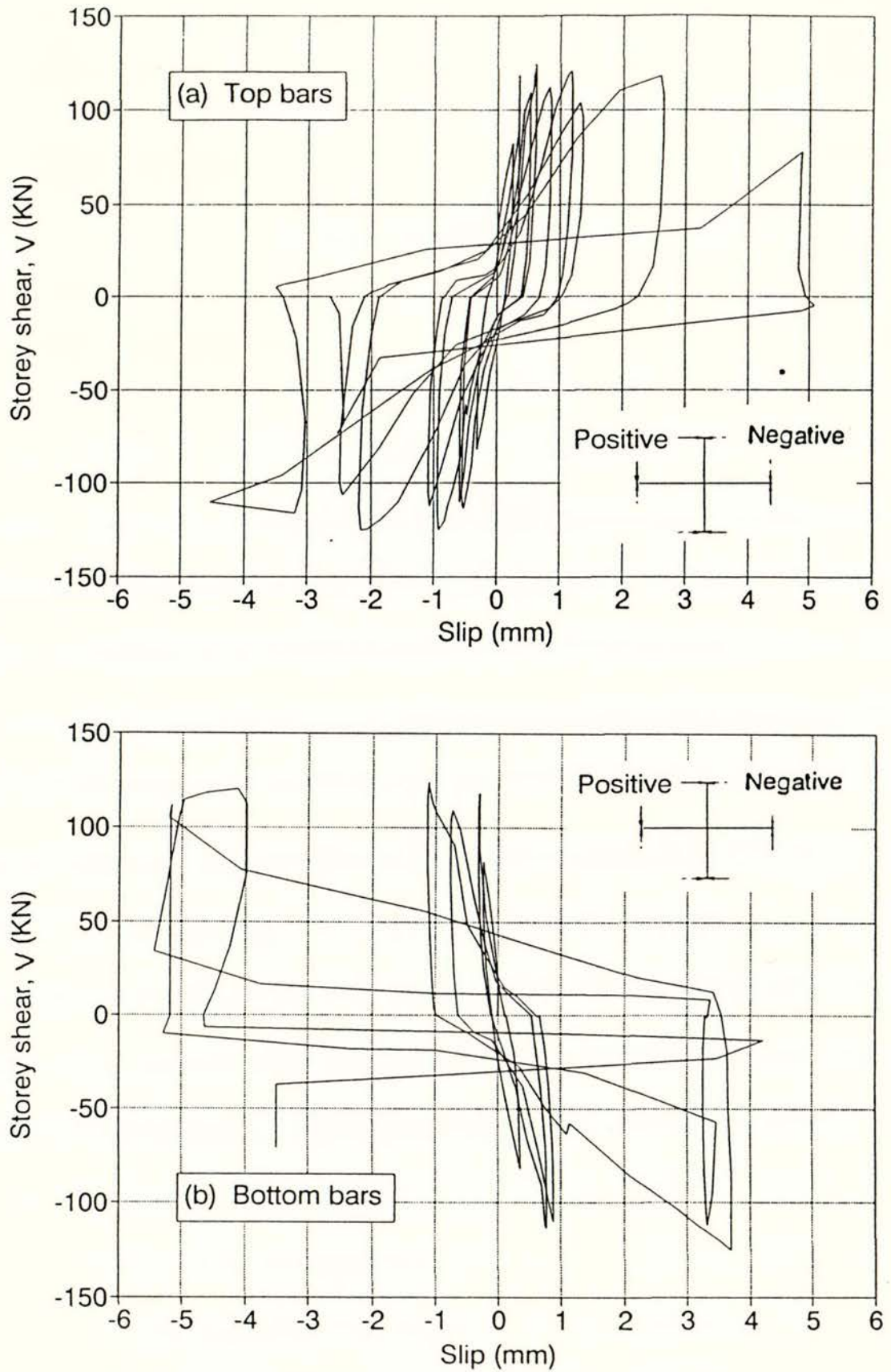


Fig. 5.14 Slip of beam bars within the joint core, Unit 2

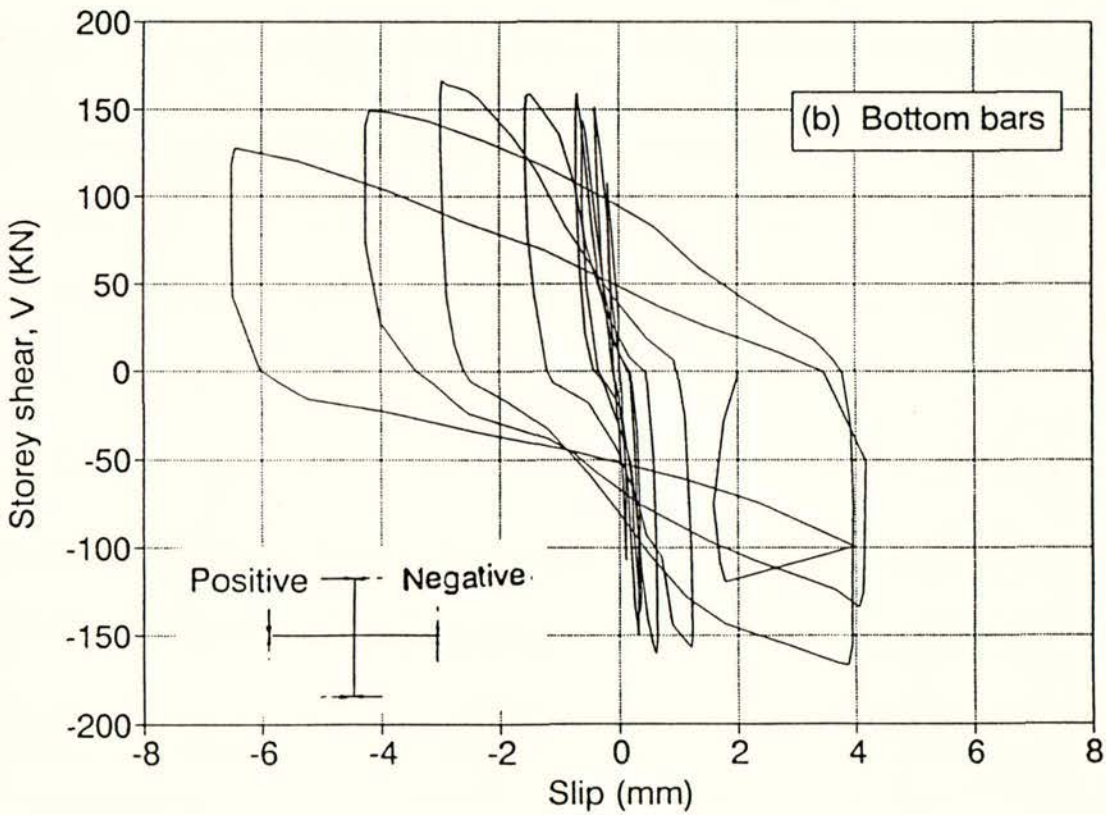
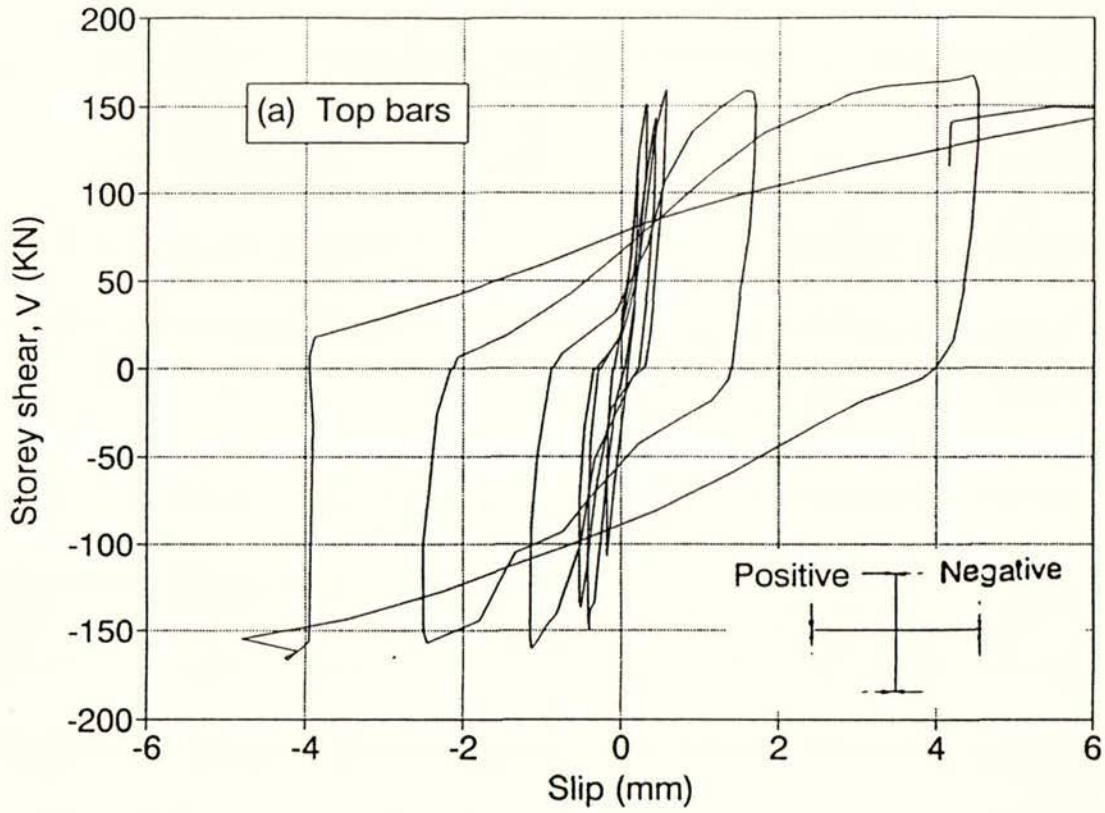


Fig. 5.15 Slip of beam bars within the joint core, Unit 3

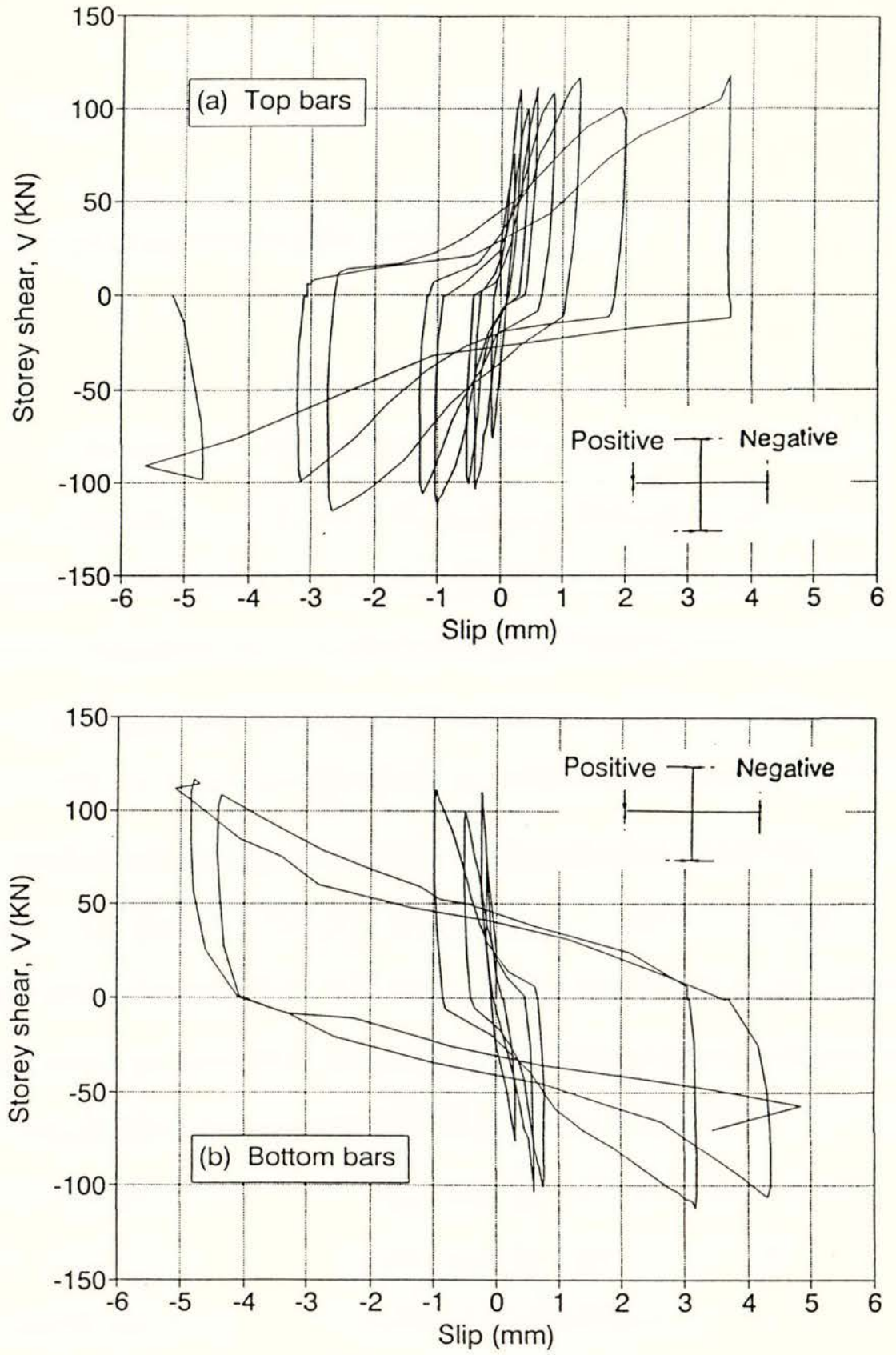


Fig. 5.16 Slip of beam bars within the joint core, Unit 4

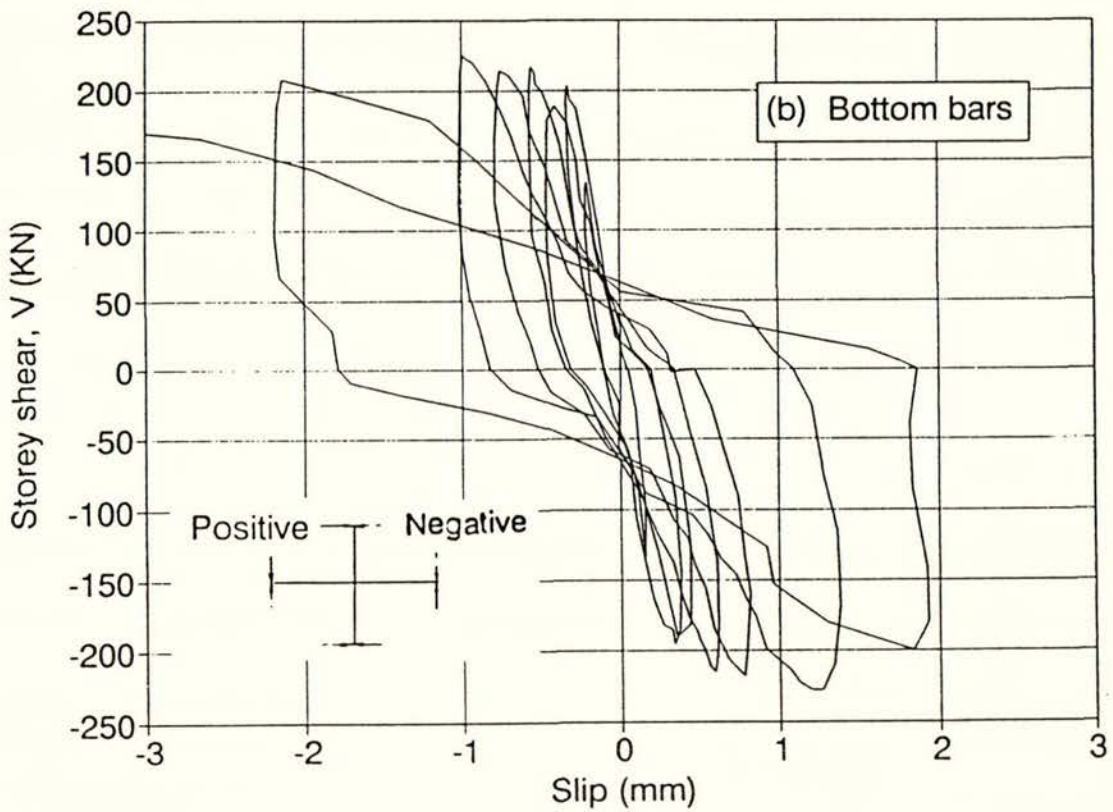
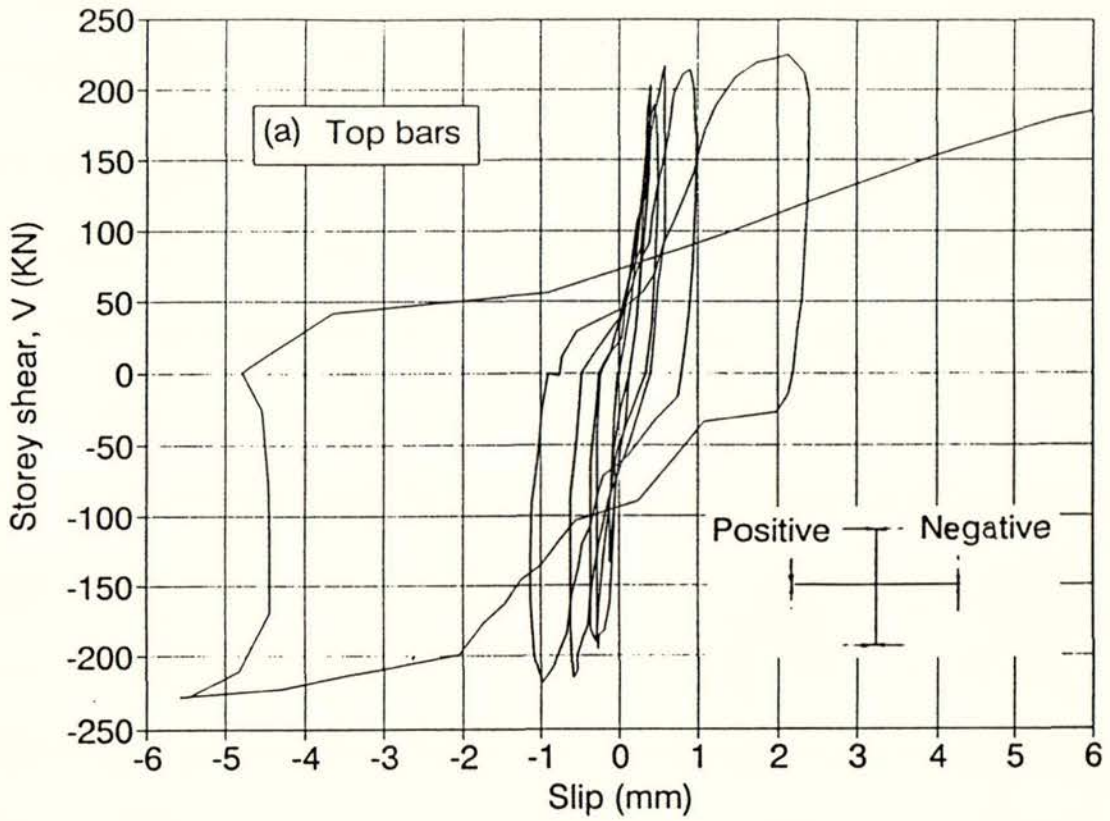


Fig. 5.17 Slip of beam bars within the joint core, Unit 5

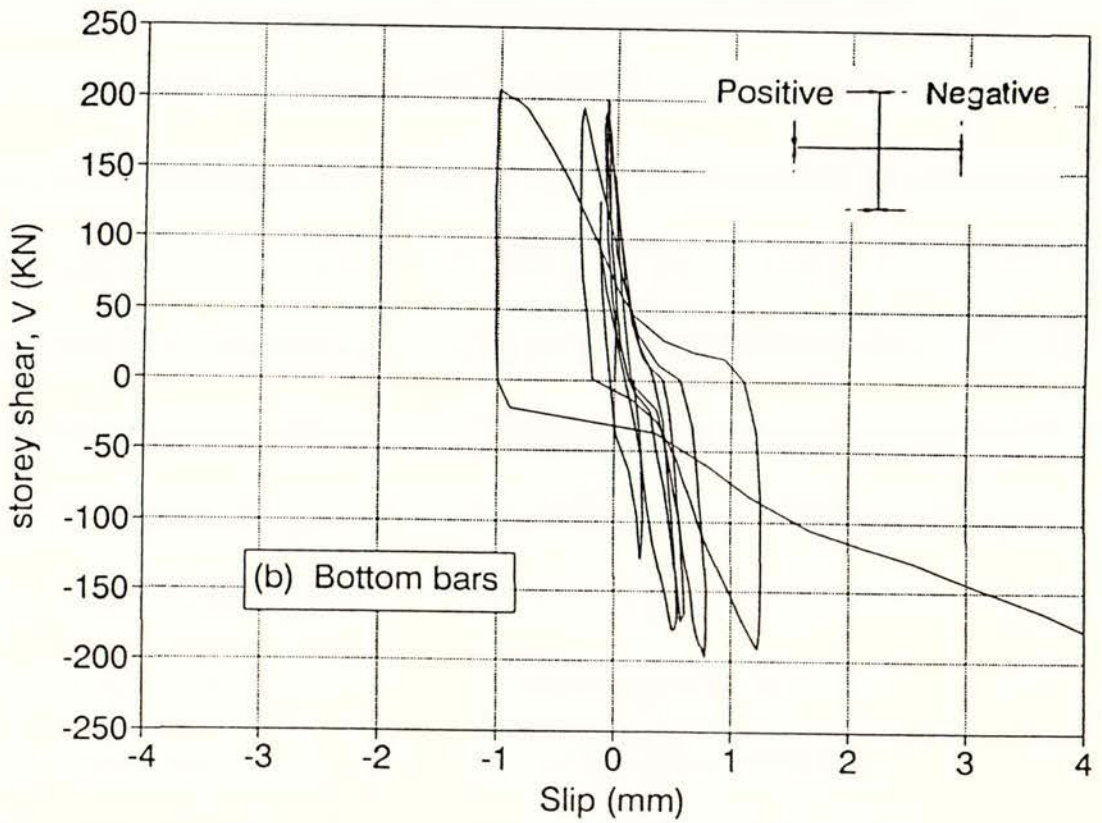
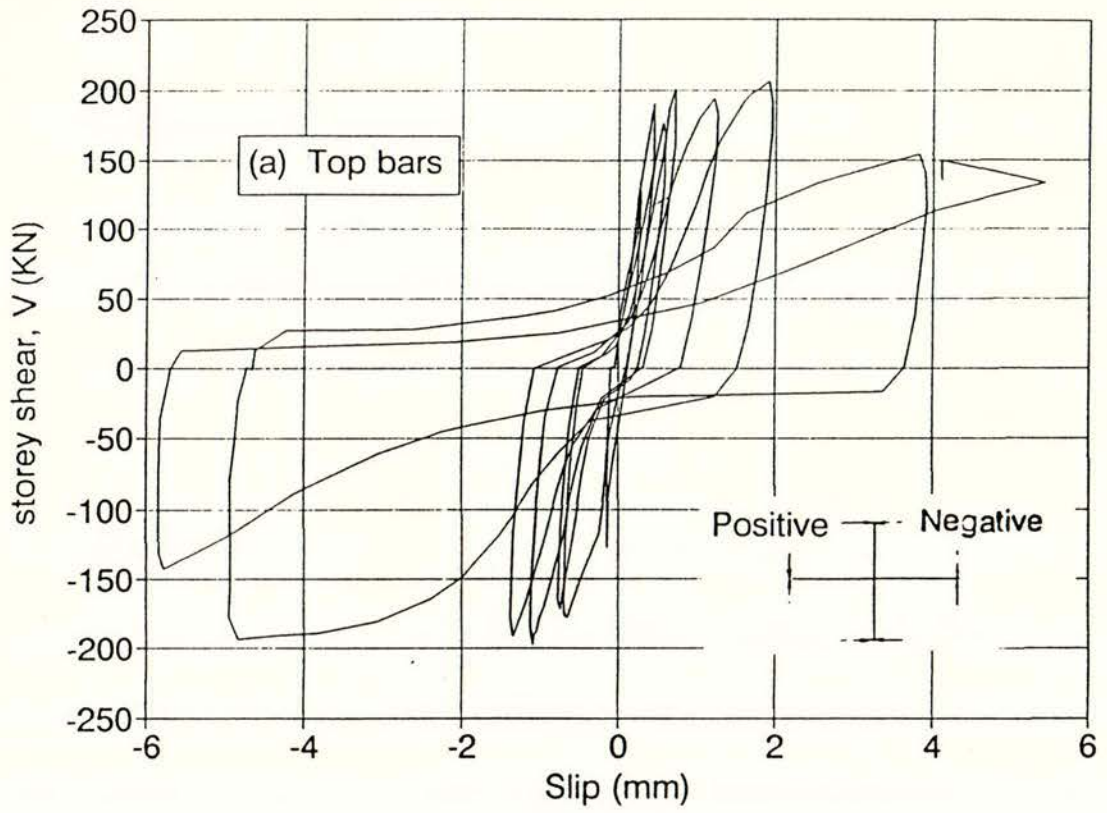


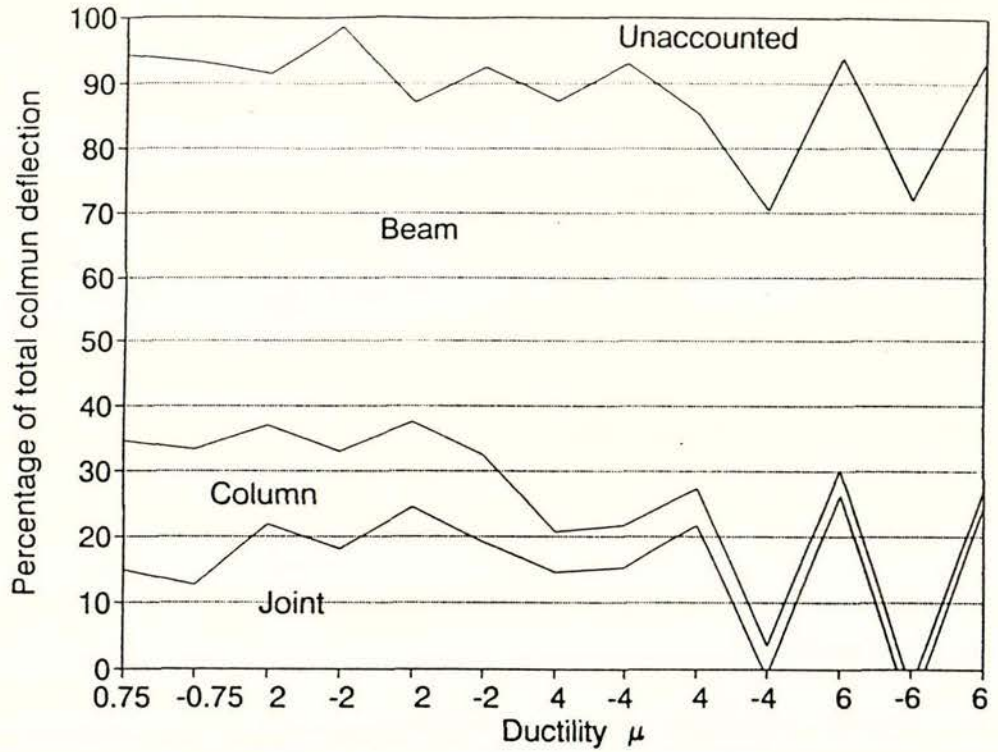
Fig. 5.18 Slip of beam bars within the joint core, Unit 6

5.5 STRAIN VARIATION ALONG BEAM BAR

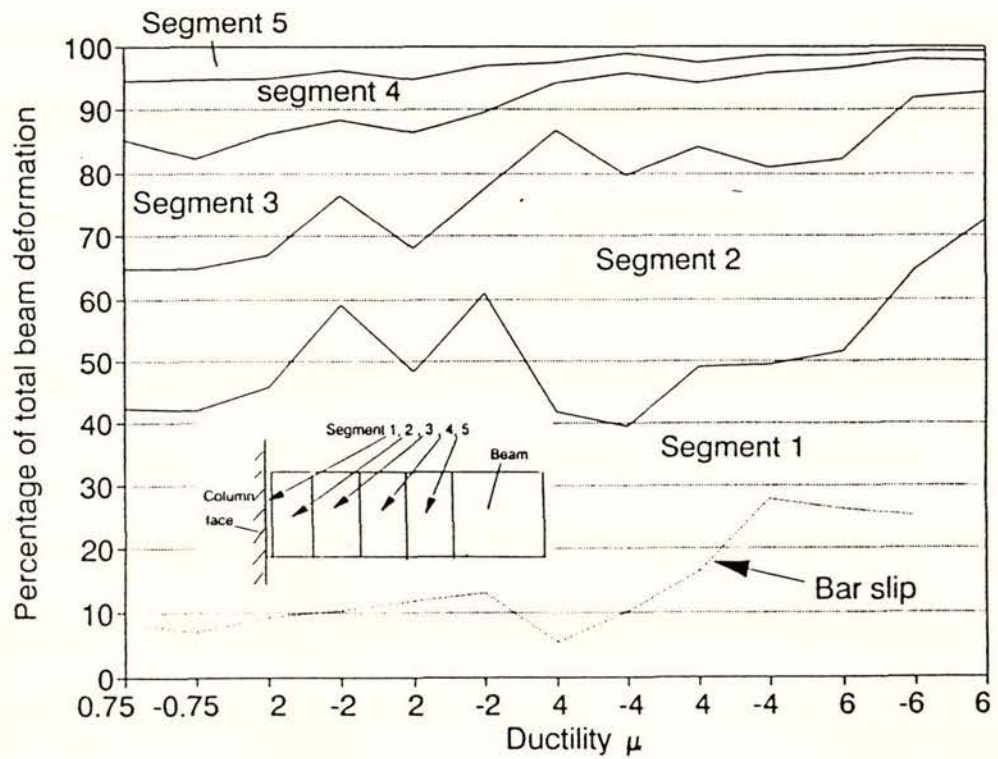
Fig. 5.37 to Fig. 5.42 illustrate the variation of strain measured on the longitudinal top and bottom bars of the beam of all six units. After a displacement ductility factor of 2, the beam bars in tension yielded at the face of the column. With further increase in the level of the displacement ductility, the strain became larger. This meant that there was the bond degradation in the joint core. In Units 2 and 4, in which more slip occurred, the yield and slip of the bottom bars occurred almost at the same time. The strain gauges at the middle of the joint core on the beam bars generally failed because of slip of beam bars in the joint at high ductility levels. So the reading of those measured points was not correct but indicated that slip of beam bars indeed occurred there.

5.6 STRAIN VARIATION IN JOINT CORE HOOPS

Fig. 5.43 to Fig. 5.48 show the variation of strain measured on the horizontal rectangular and diamond joint hoops of all six units. The yield strain of the joint core hoops was reached at higher displacement ductility factors in those units with good bond conditions for longitudinal bars, as Unit 1, 3 and 5. During the test, the joint cores tended to swell.

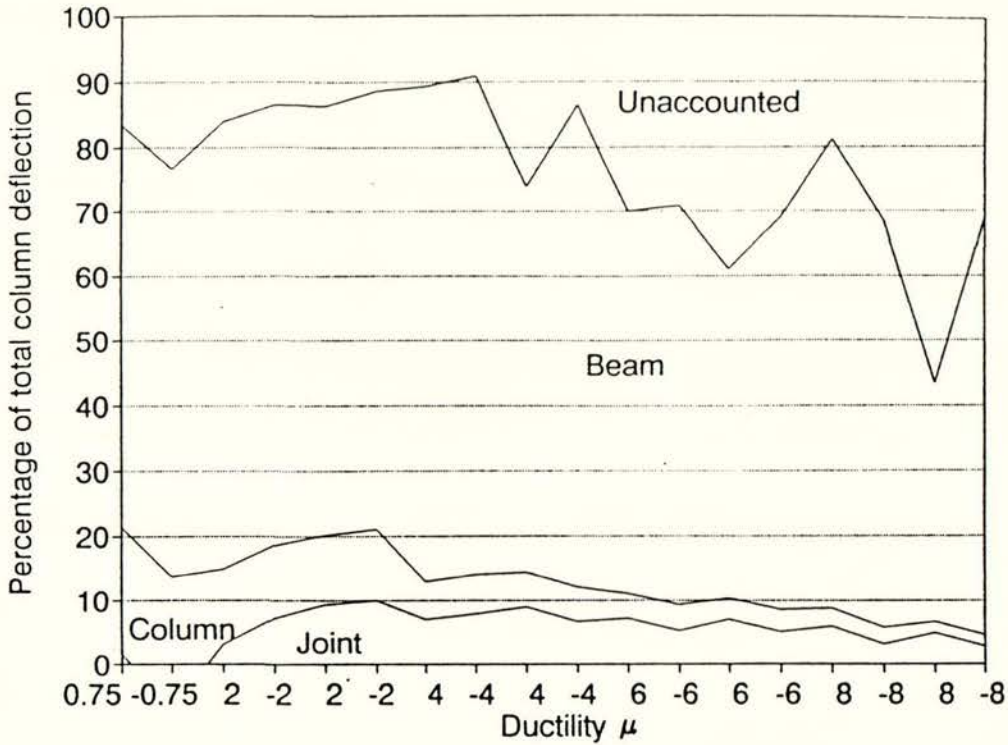


(a) Contribution to interstorey displacement from joint, column & beam deformation

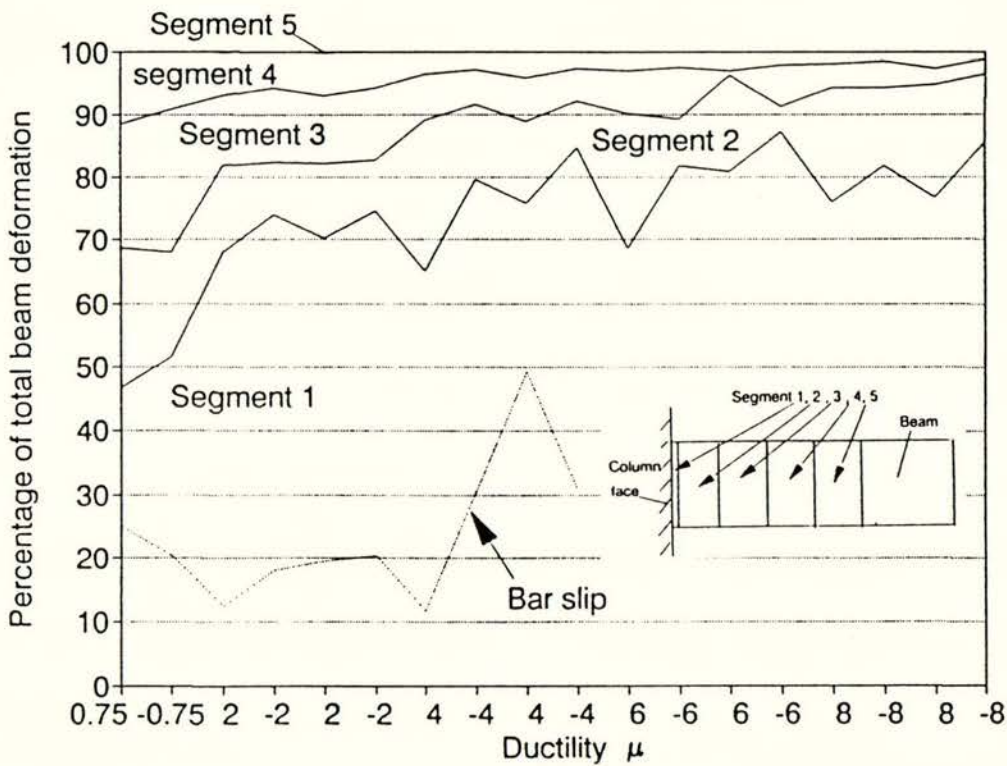


(b) Contribution to total beam deformation from segments on the beam

Fig. 5.19 Components of displacement, Unit 1

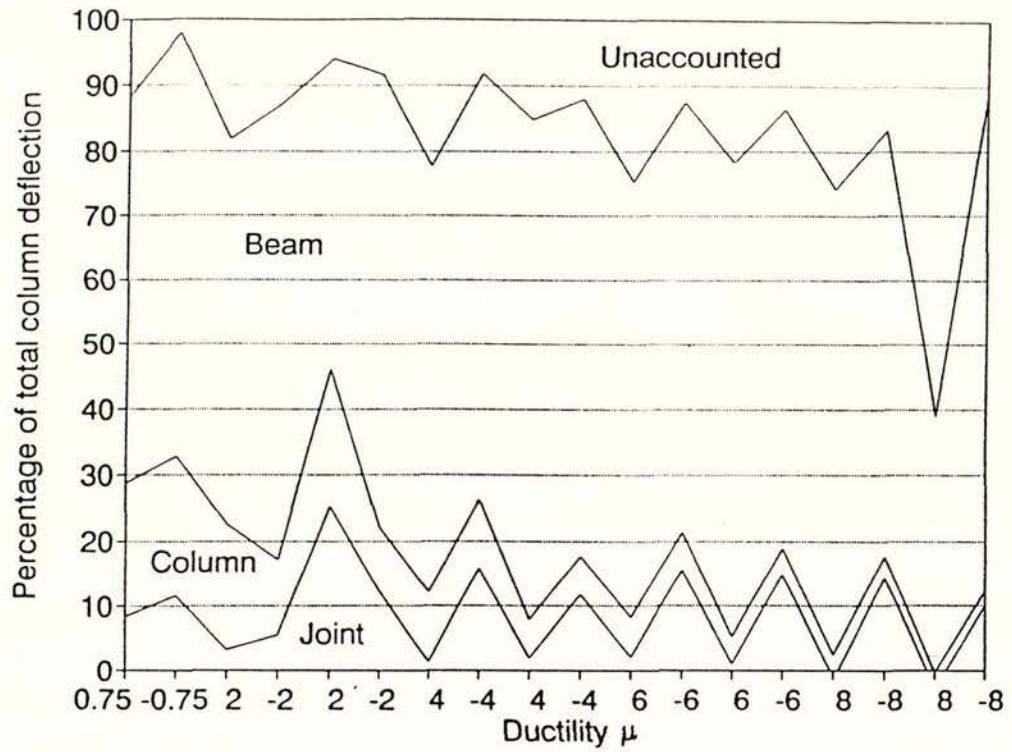


(a) Contribution to interstorey displacement from joint, column & beam deformation

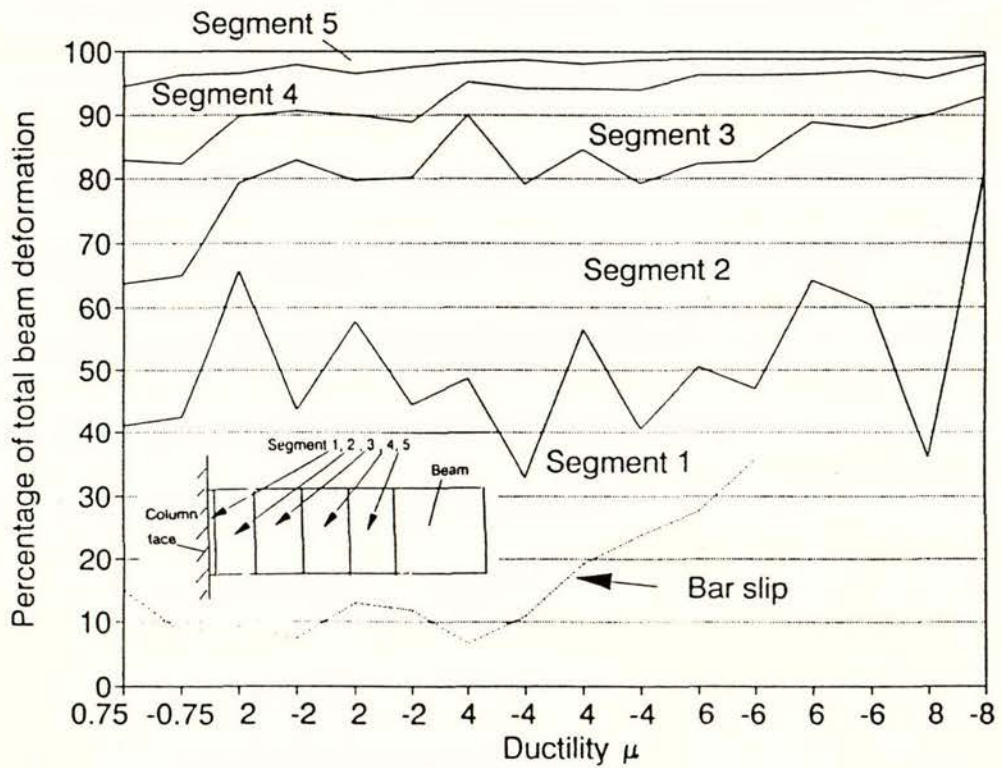


(b) Contribution to total beam deformation from segments on the beam

Fig. 5.20 Components of displacement, Unit 2

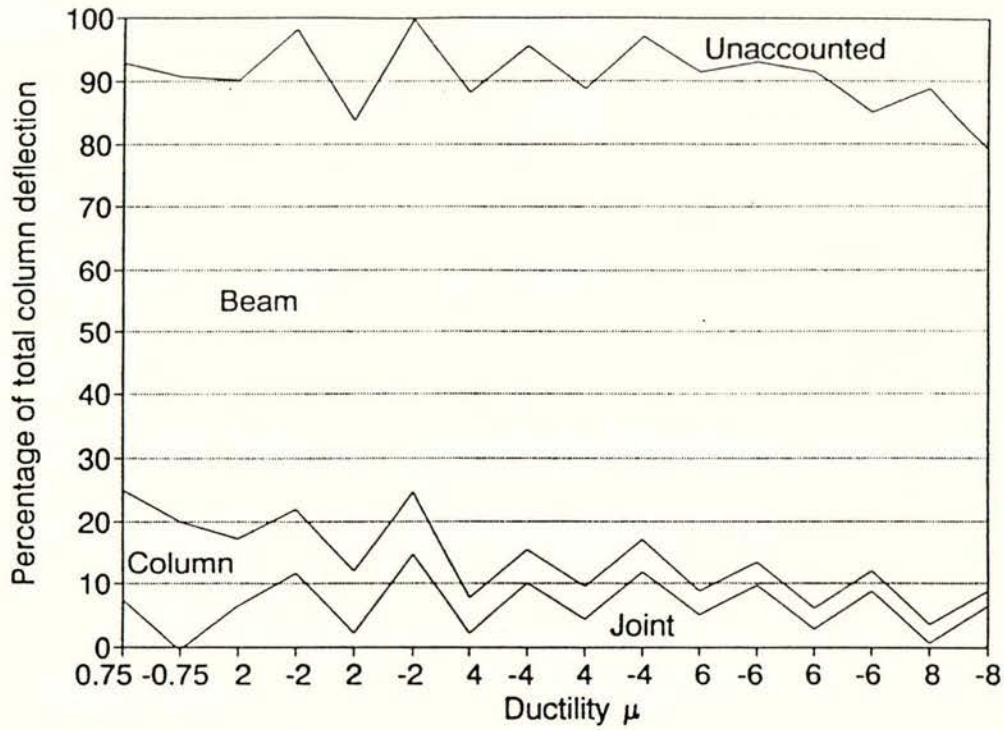


(a) Contribution to interstorey displacement from joint, column & beam deformation

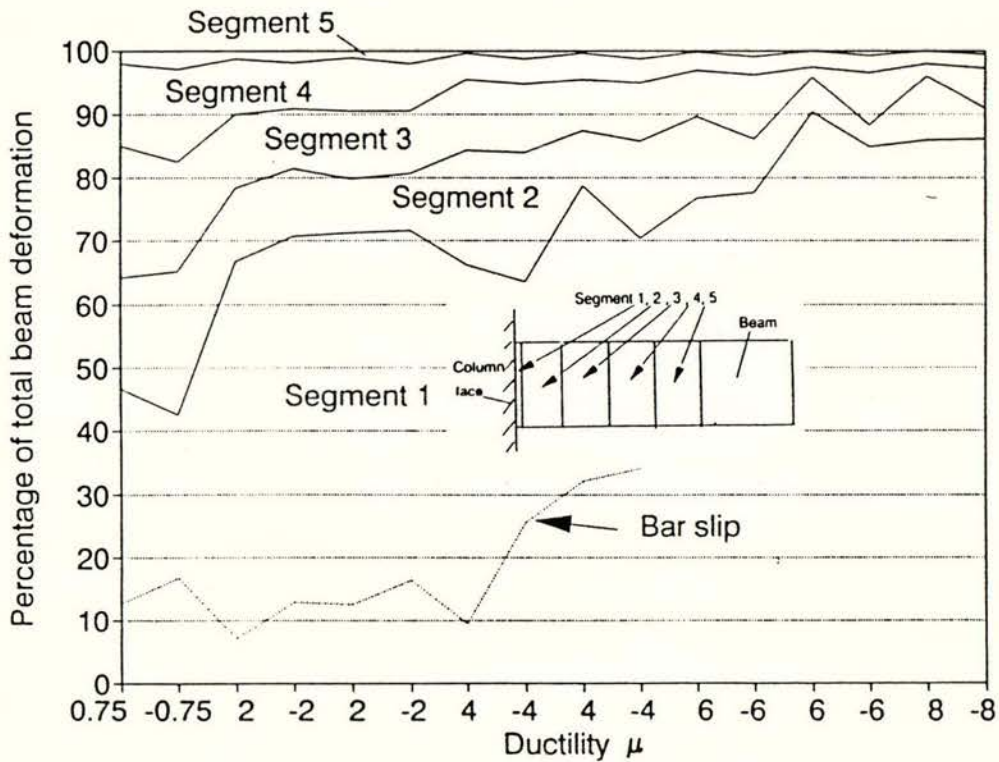


(b) Contribution to total beam deformation from segments on the beam

Fig. 5.21 Components of displacement, Unit 3

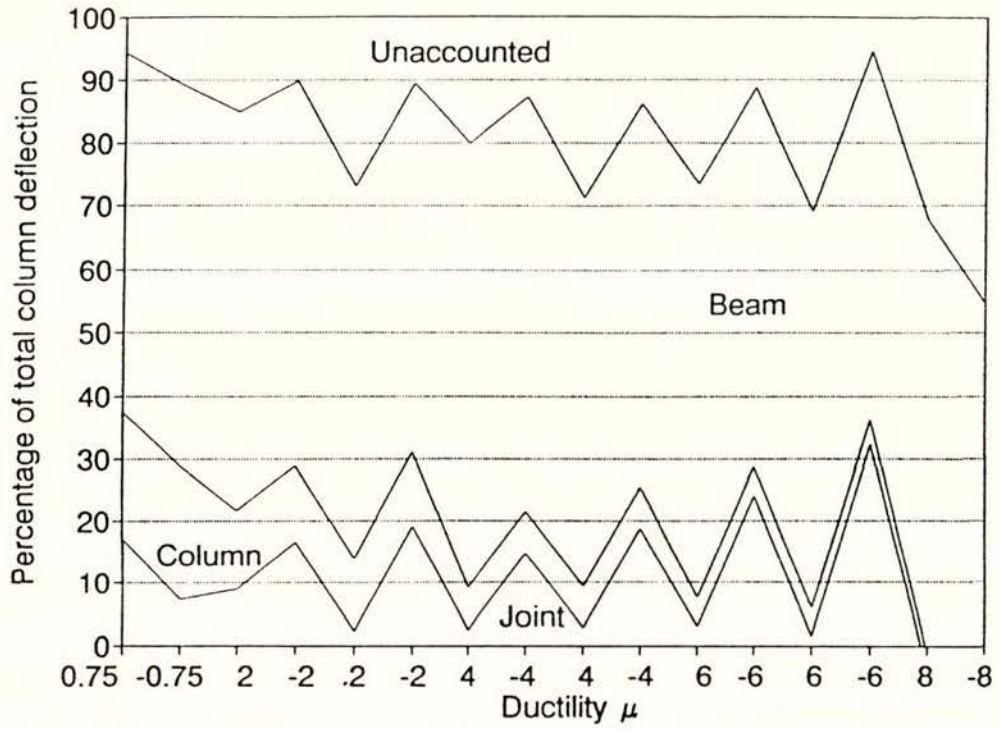


(a) Contribution to interstorey displacement from joint, column & beam deformation

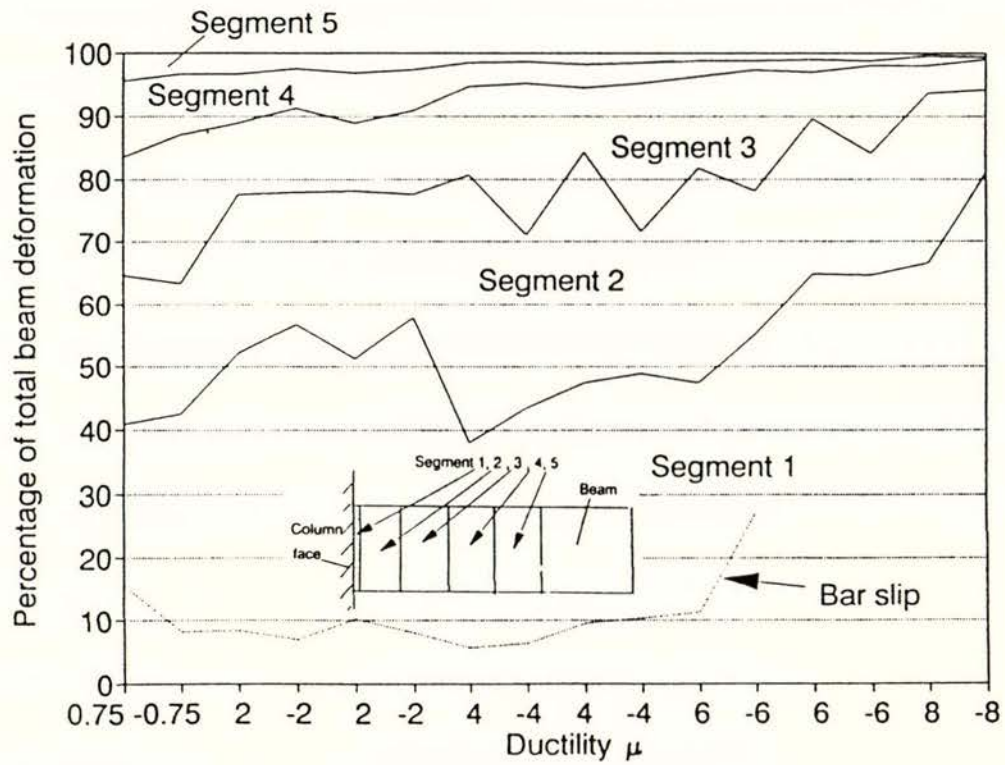


(b) Contribution to total beam deformation from segments on the beam

Fig. 5.22 Components of displacement, Unit 4

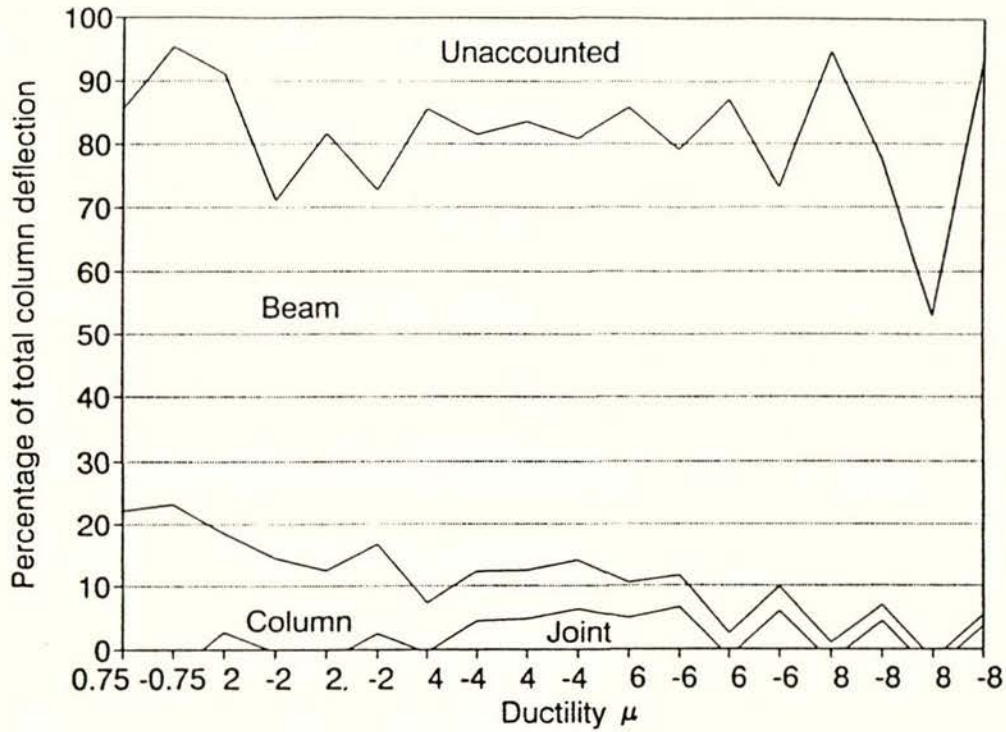


(a) Contribution to interstorey displacement from joint, column & beam deformation

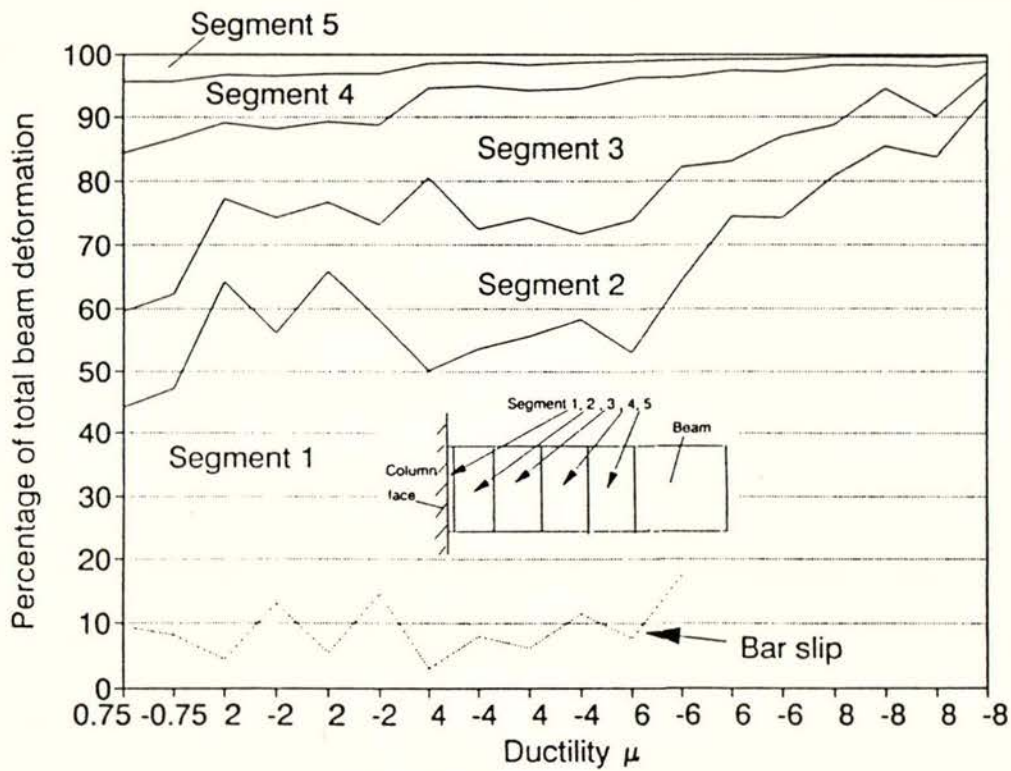


(b) Contribution to total beam deformation from segments on the beam

Fig. 5.23 Components of displacement, Unit 5



(a) Contribution to interstorey displacement from joint, column & beam deformation



(b) Contribution to total beam deformation from segments on the beam

Fig. 5.24 Components of displacement, Unit 6

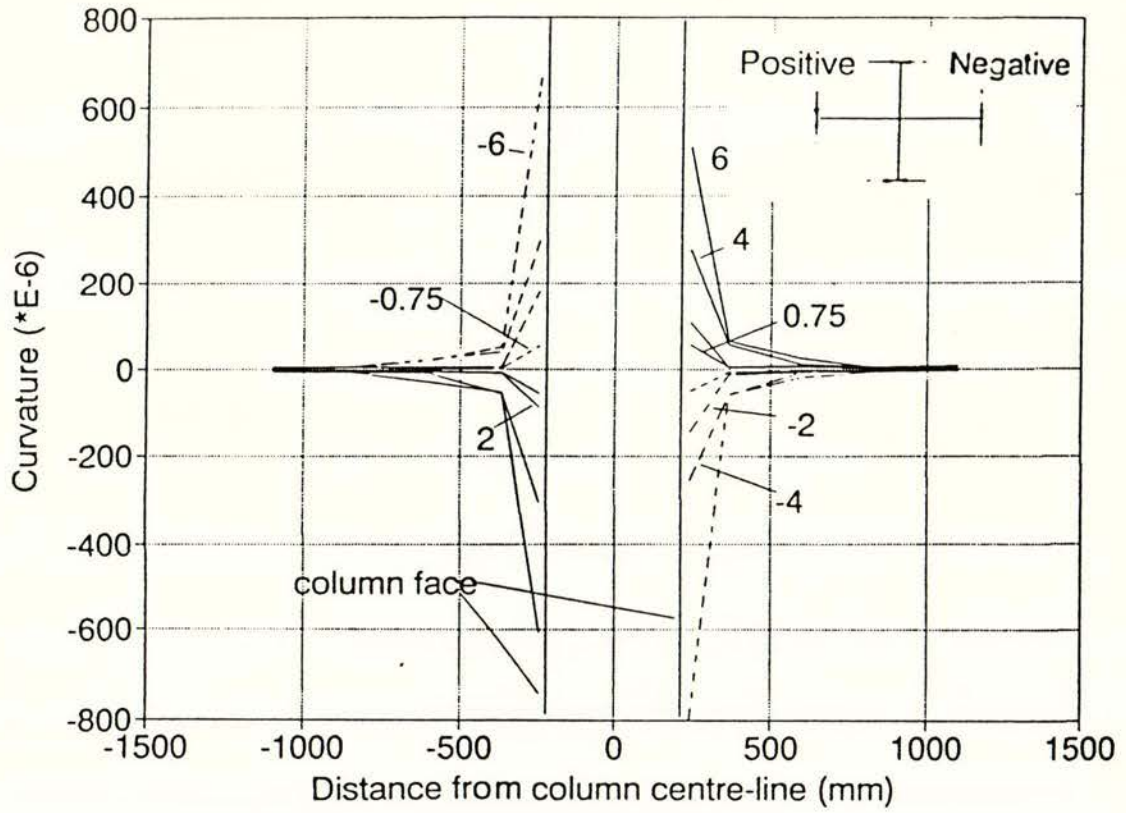


Fig.5.25 Distribution of curvature along the beam, Unit 1

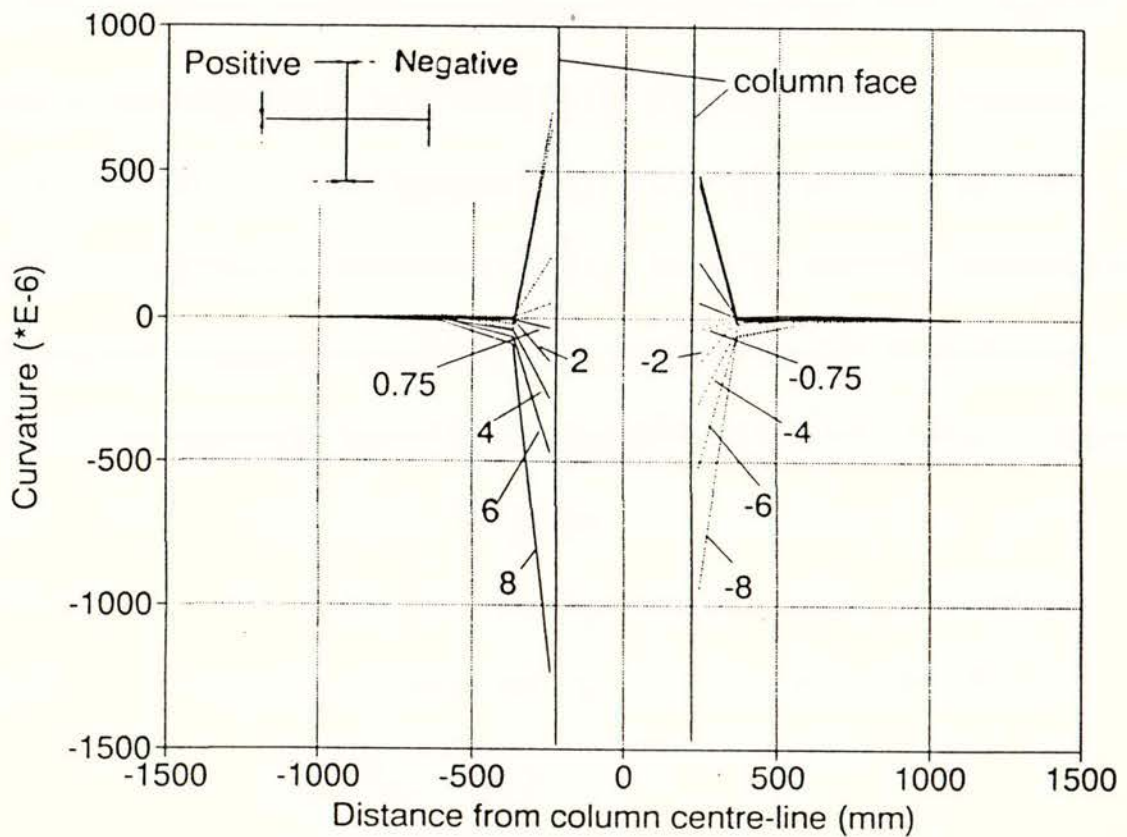


Fig.5.26 Distribution of curvature along the beam, Unit 2

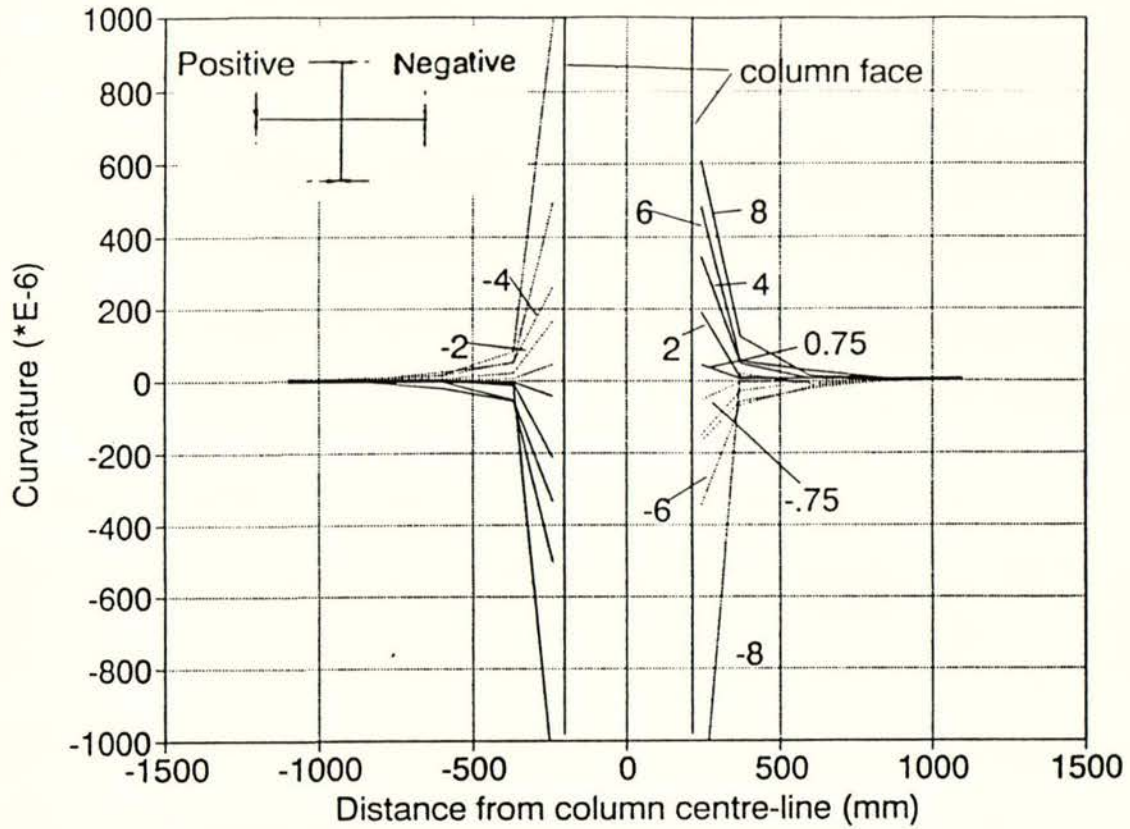


Fig.5.27 Distribution of curvature along the beam, Unit 3

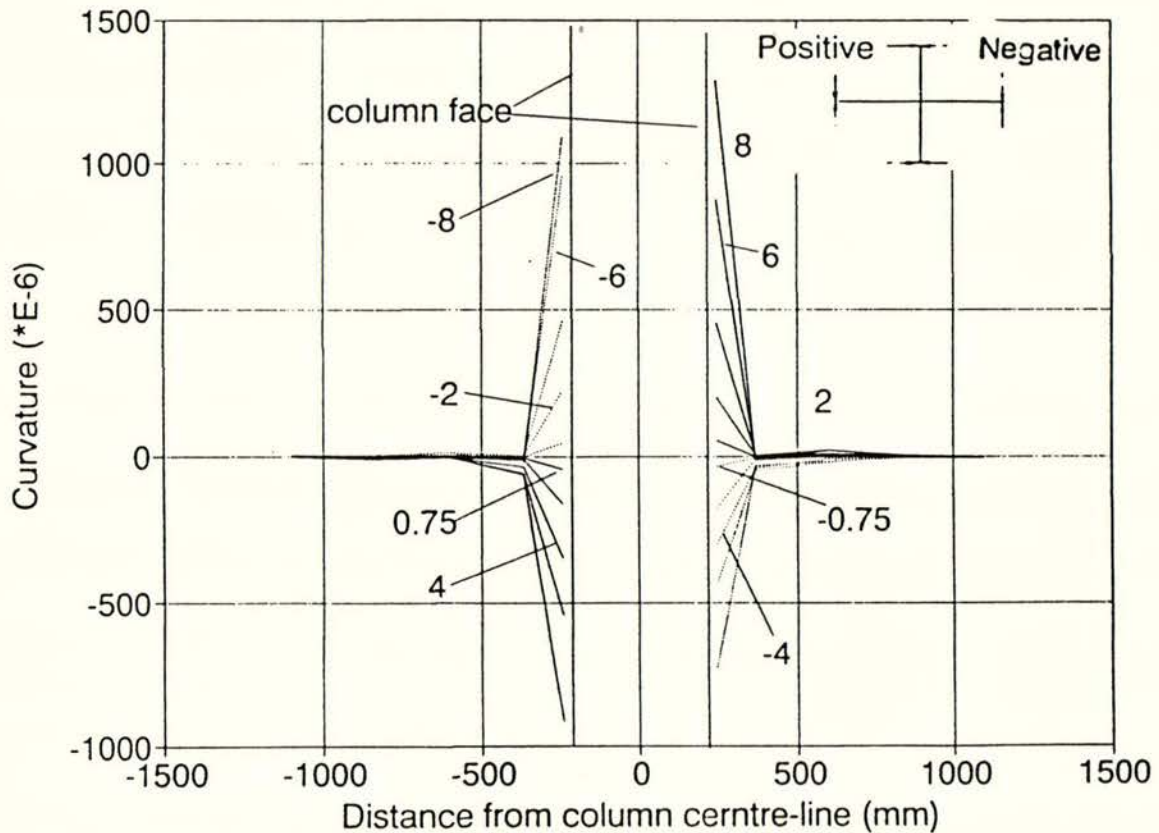


Fig.5.28 Distribution of curvature along the beam, Unit 4

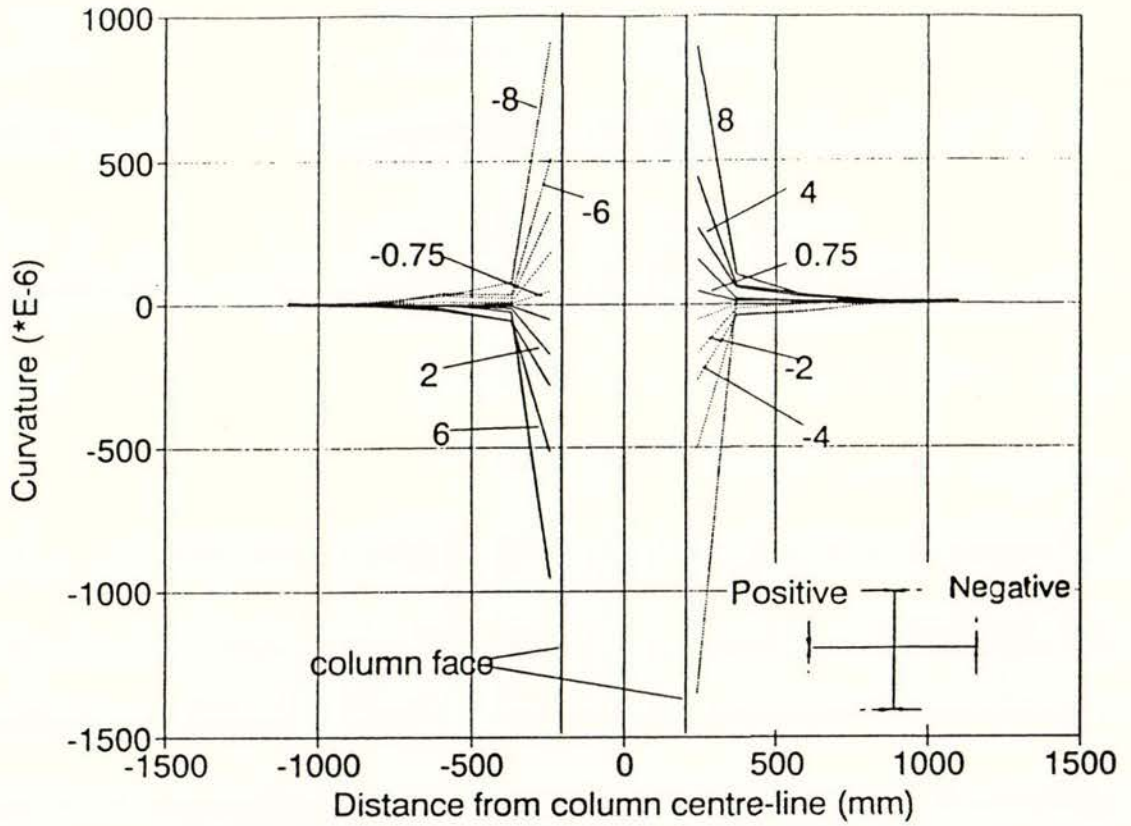


Fig.5.29 Distribution of curvature along the beam, Unit 5

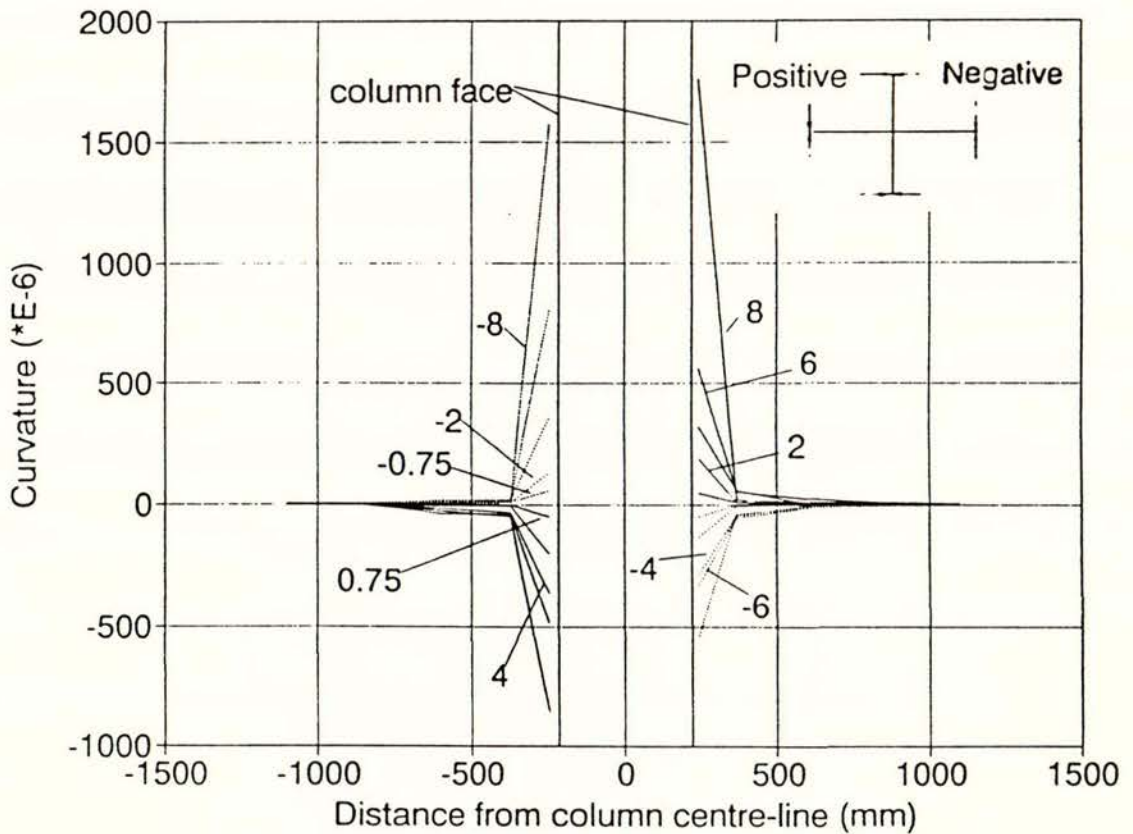


Fig.5.30 Distribution of curvature along the beam, Unit 6

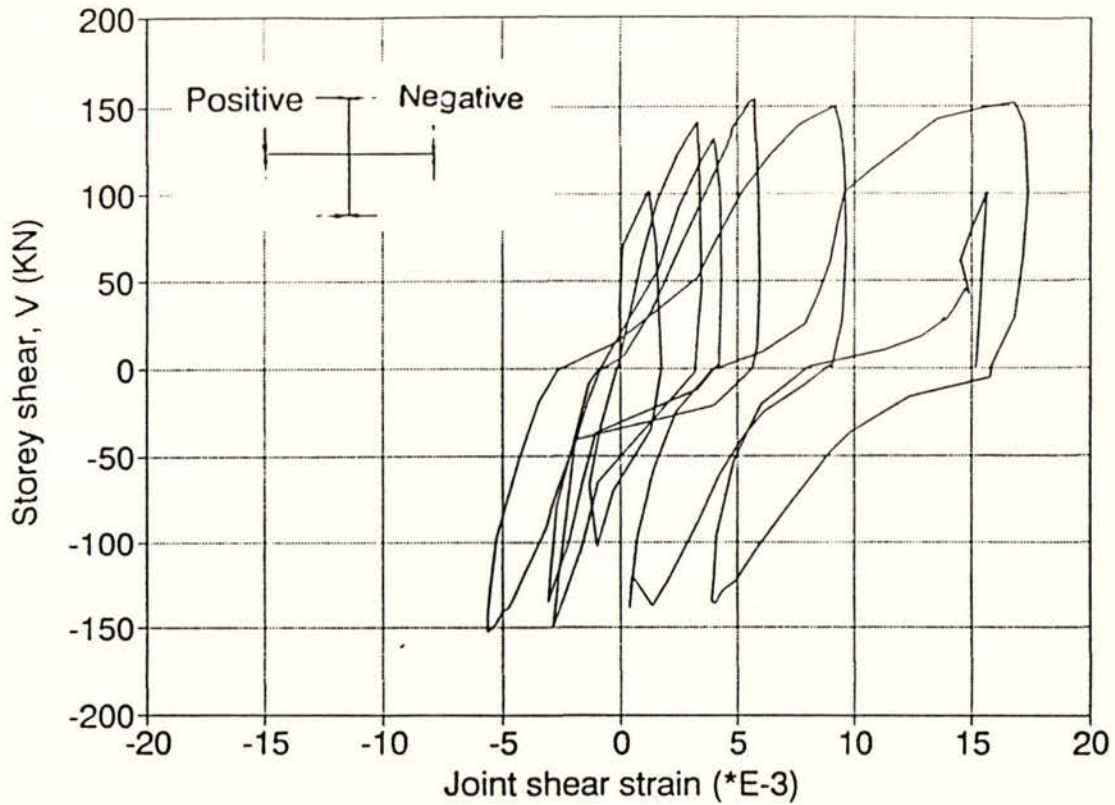


Fig.5.31 Shear deformation of the joint core, Unit 1

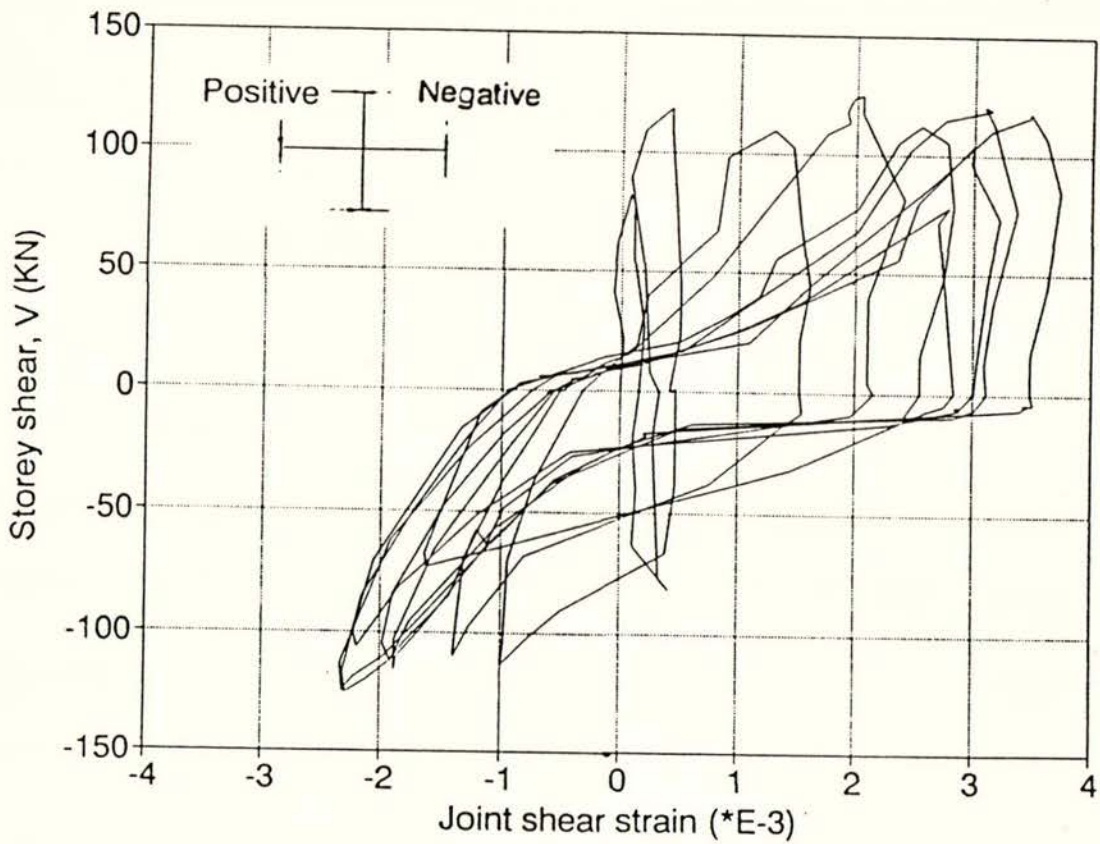


Fig.5.32 Shear deformation of the joint core, Unit 2

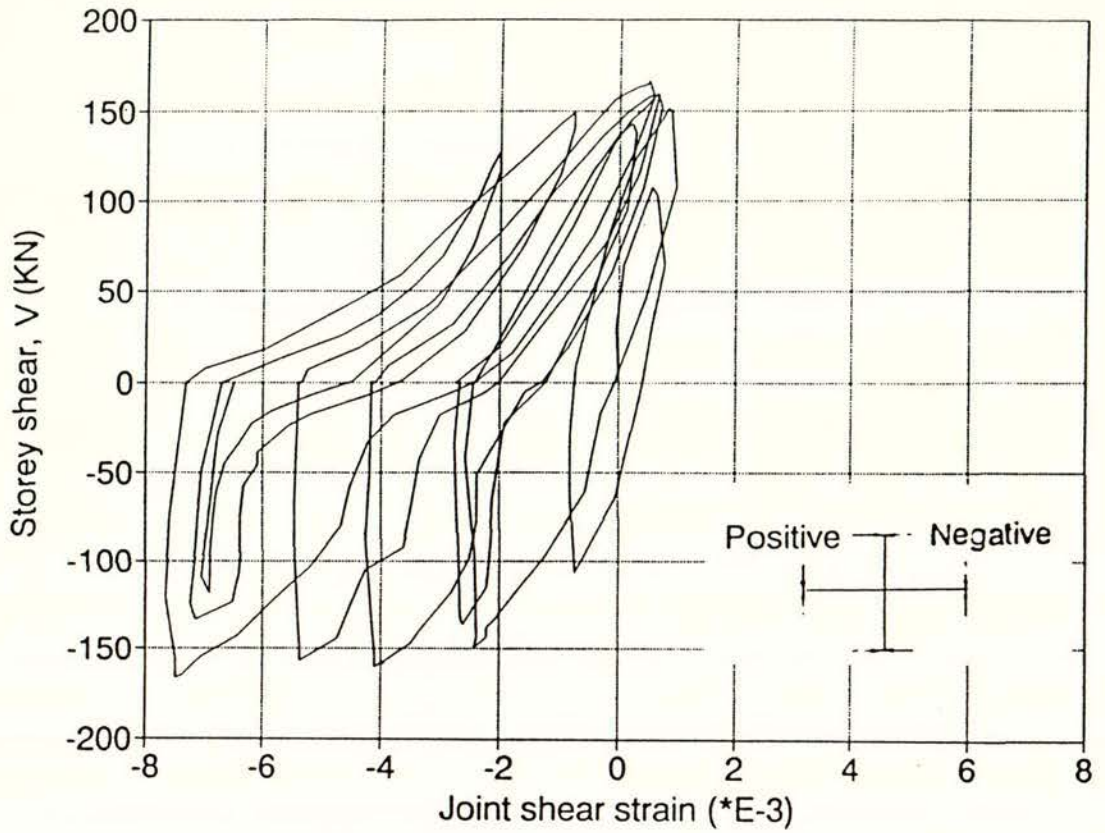


Fig.5.33 Shear deformation of the joint core, Unit 3

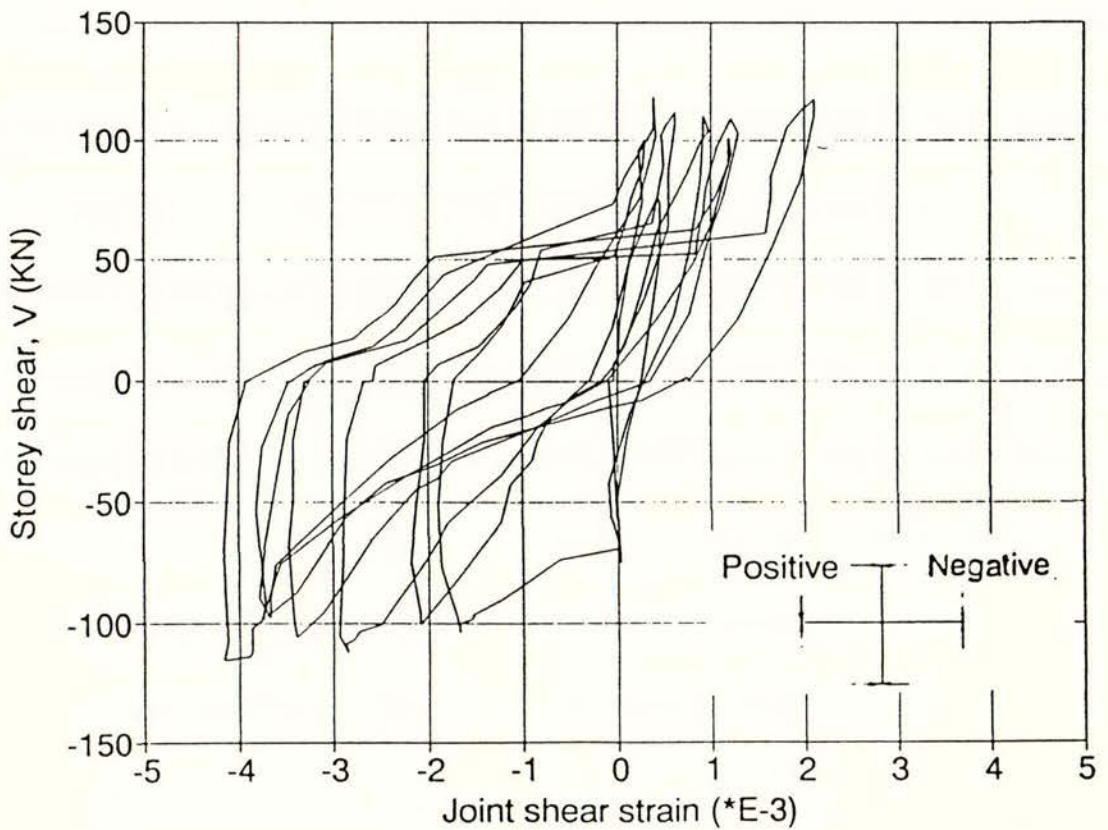


Fig.5.34 Shear deformation of the joint core, Unit 4

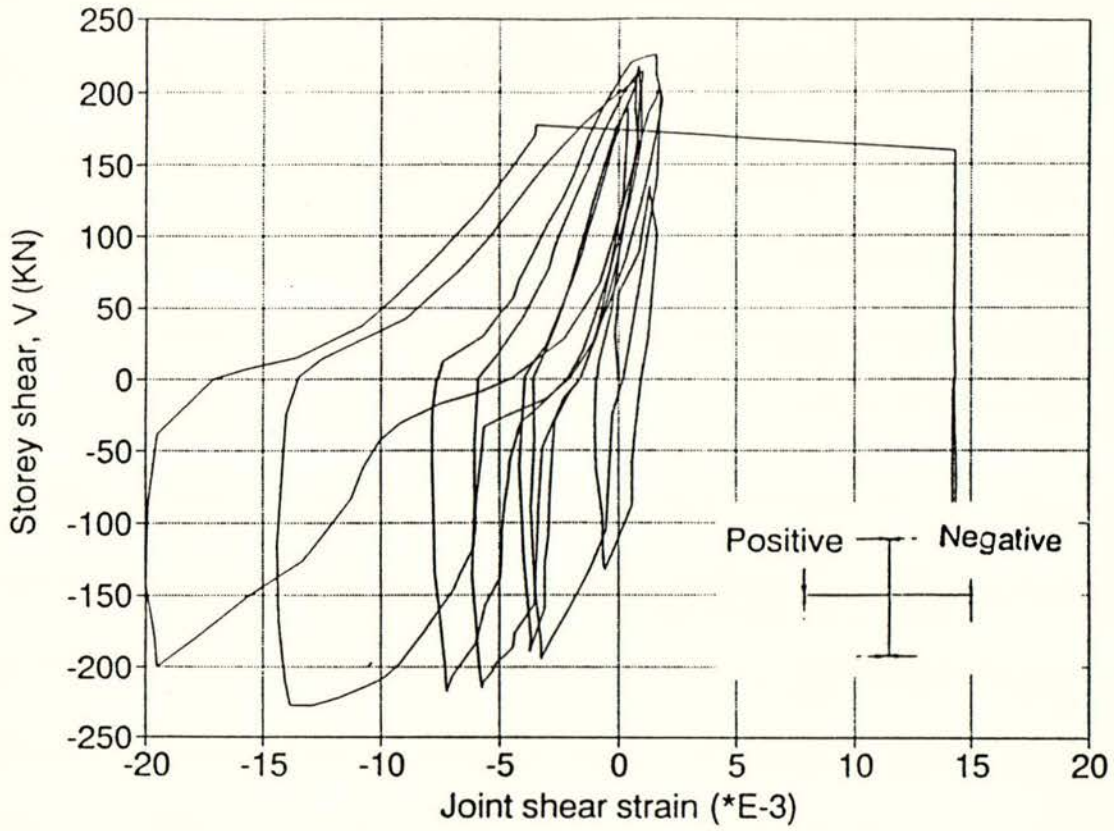


Fig.5.35 Shear deformation of the joint core, Unit 5

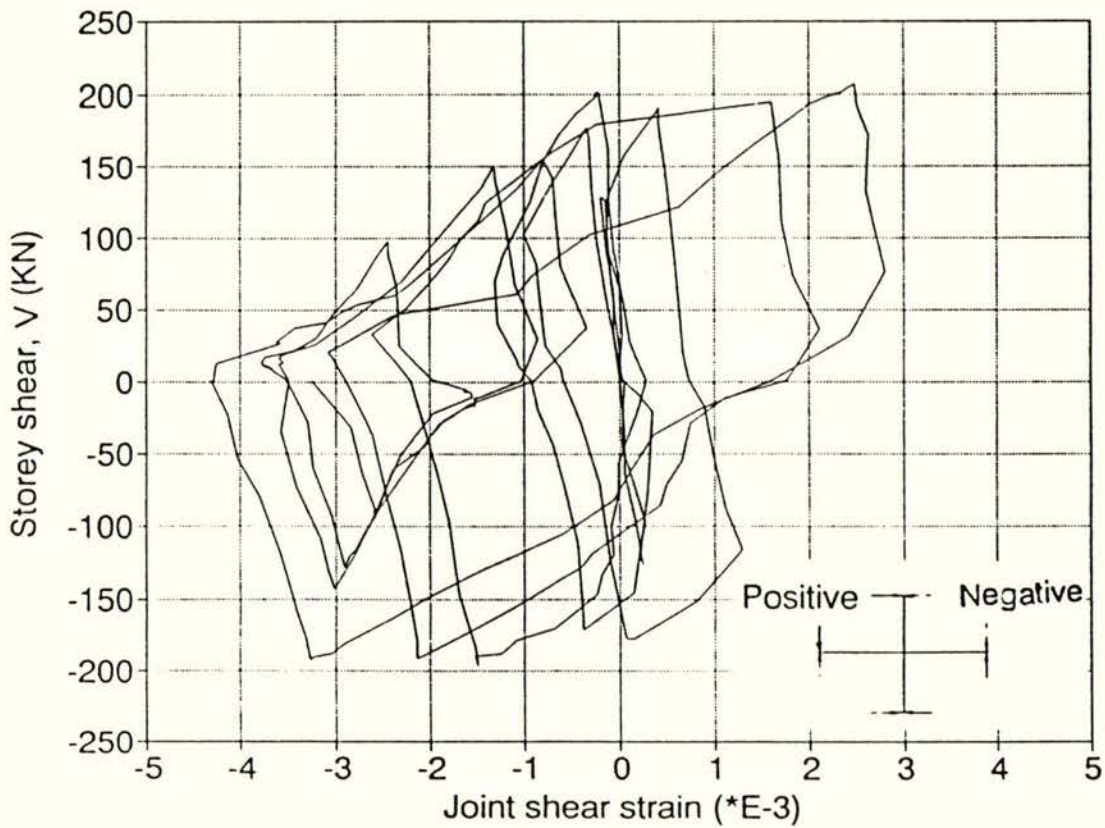


Fig.5.36 Shear deformation of the joint core, Unit 6

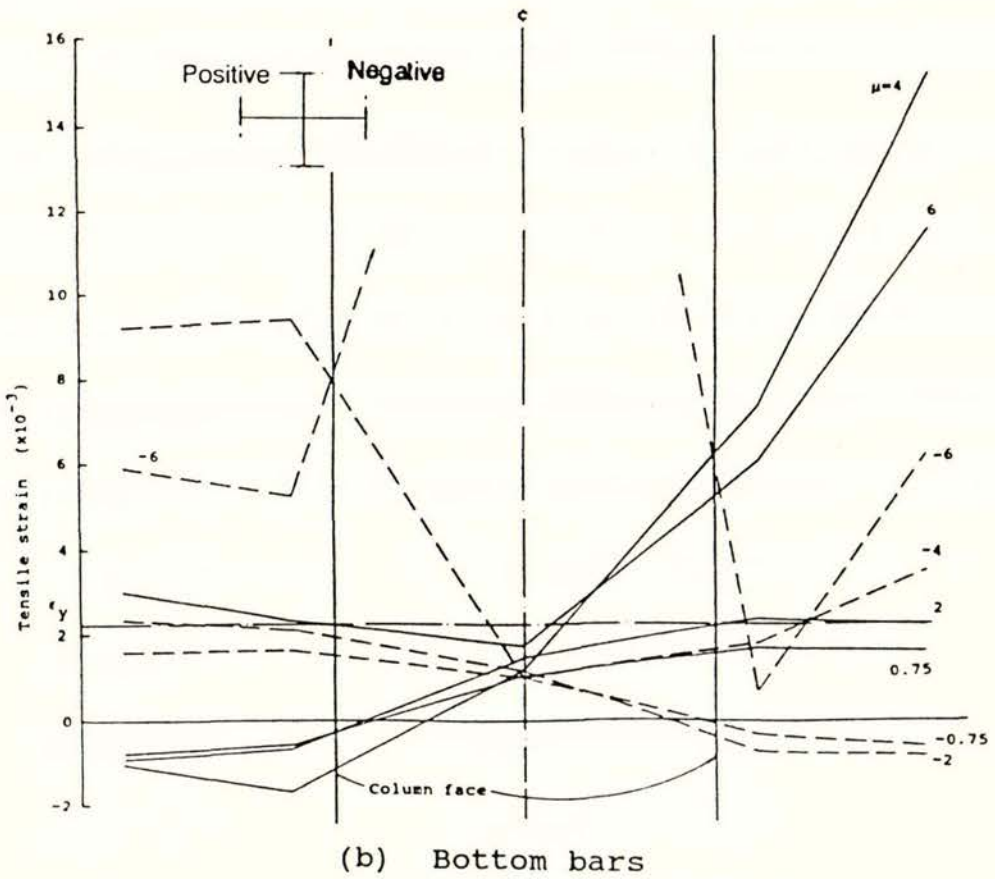
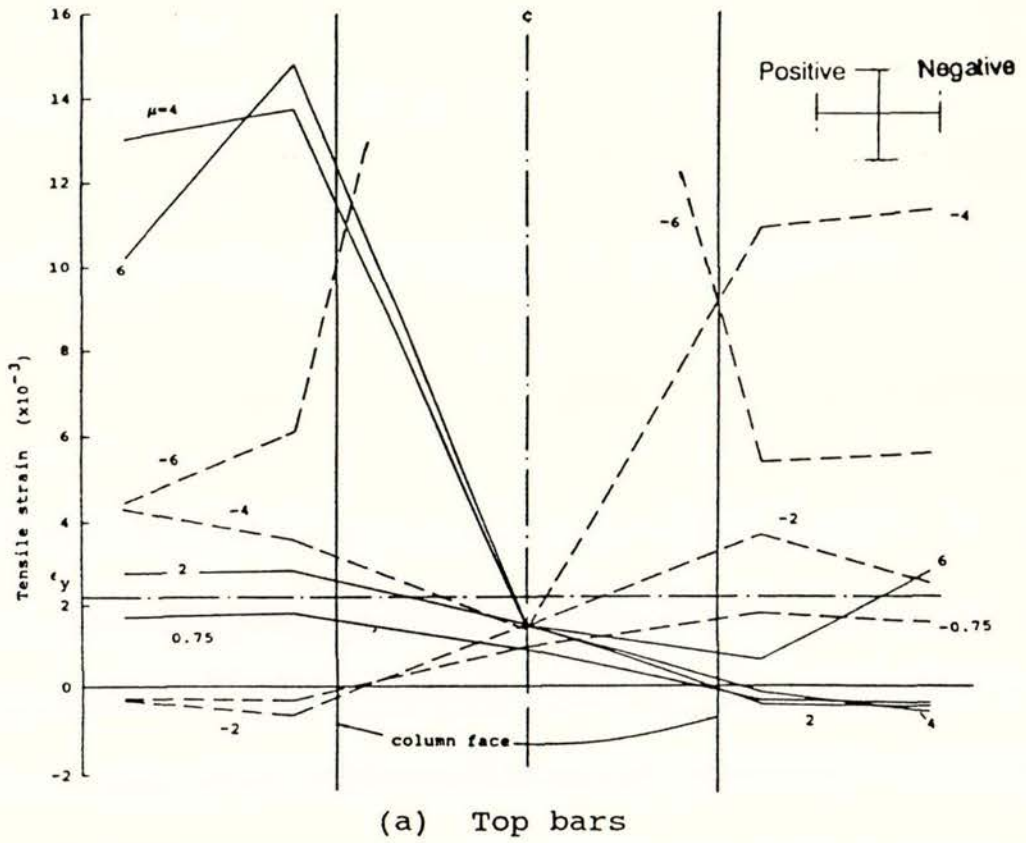


Fig. 5.37 Strain variation along beam bars, Unit 1

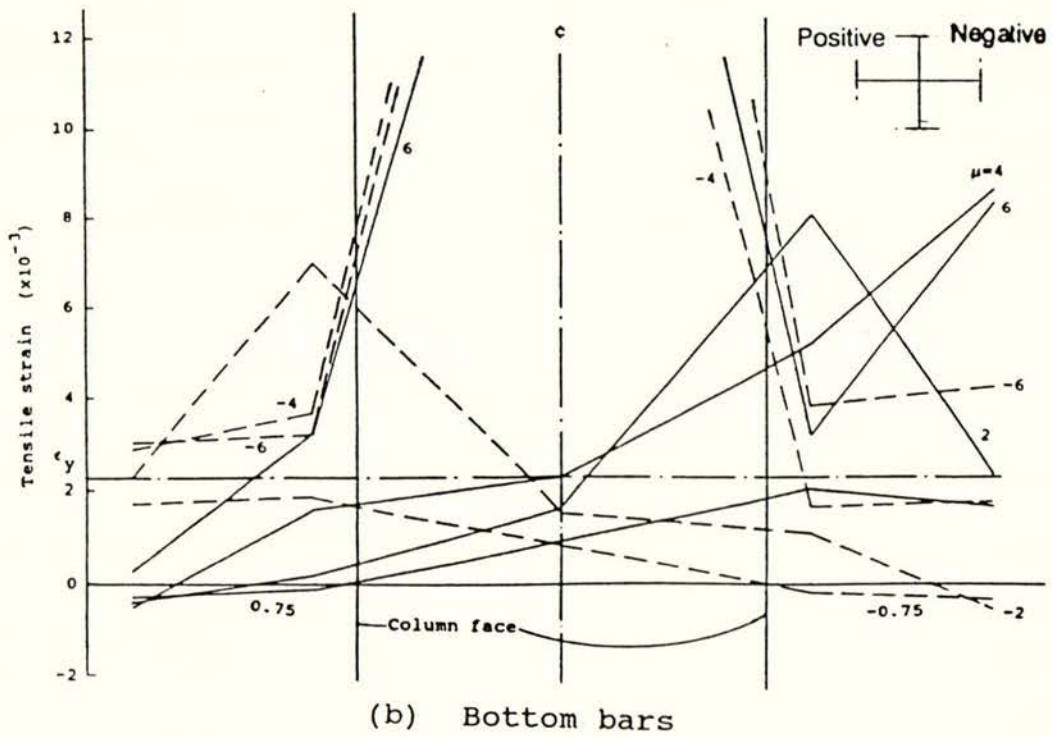
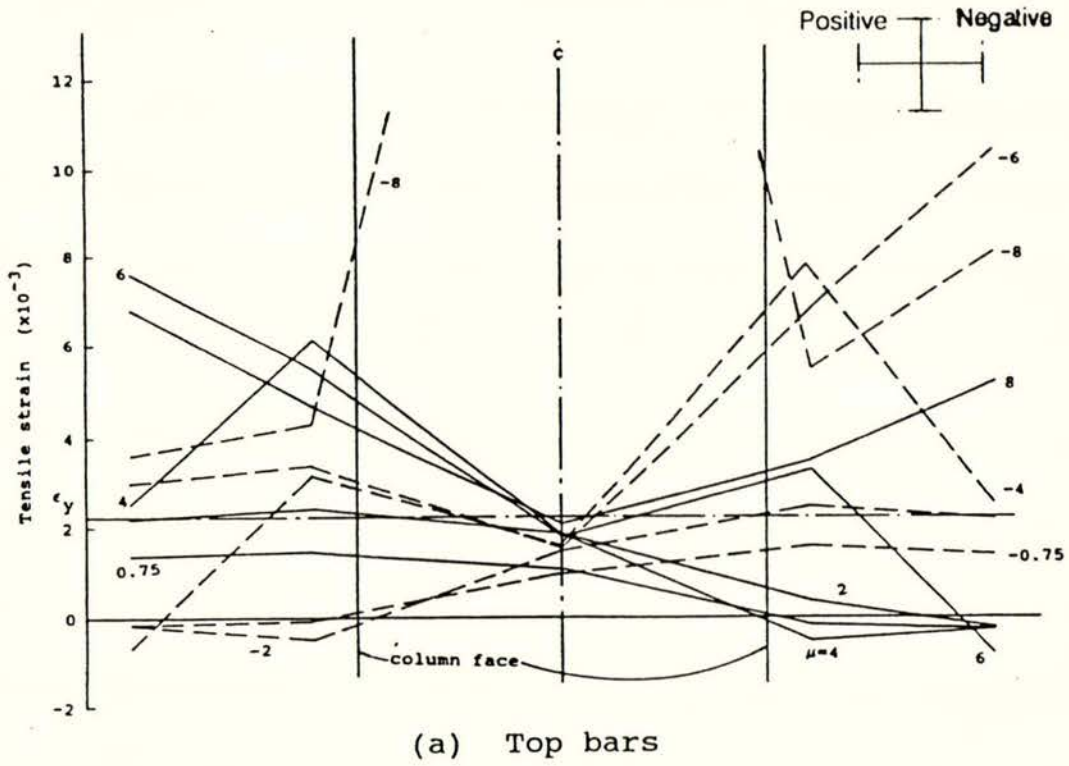


Fig. 5.38 Strain variation along beam bars, Unit 2

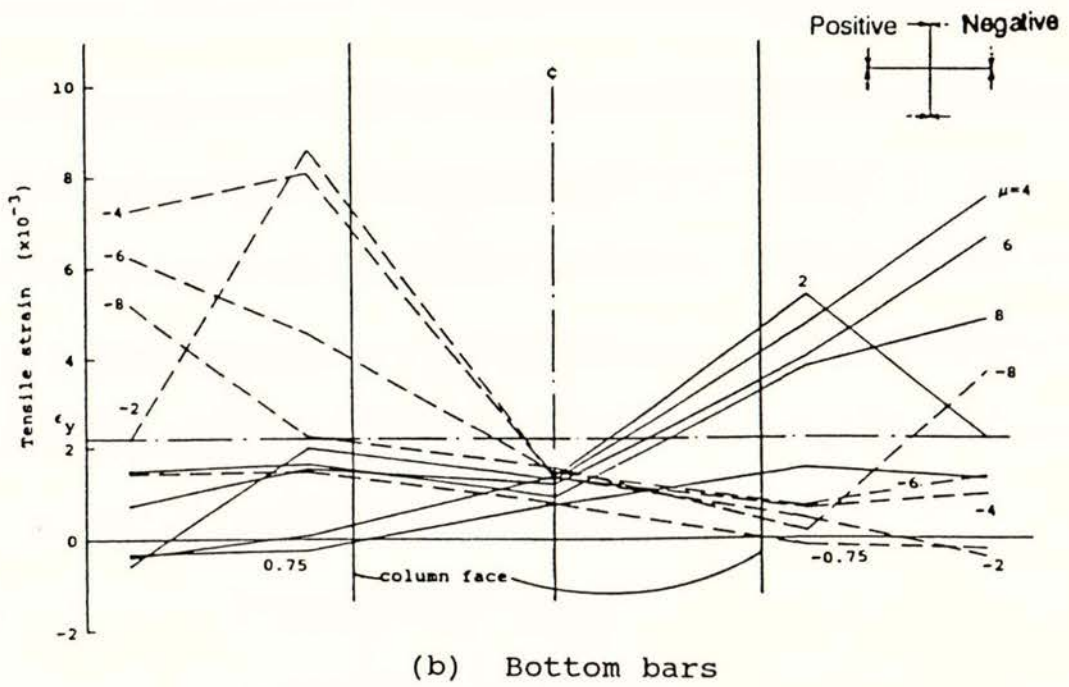
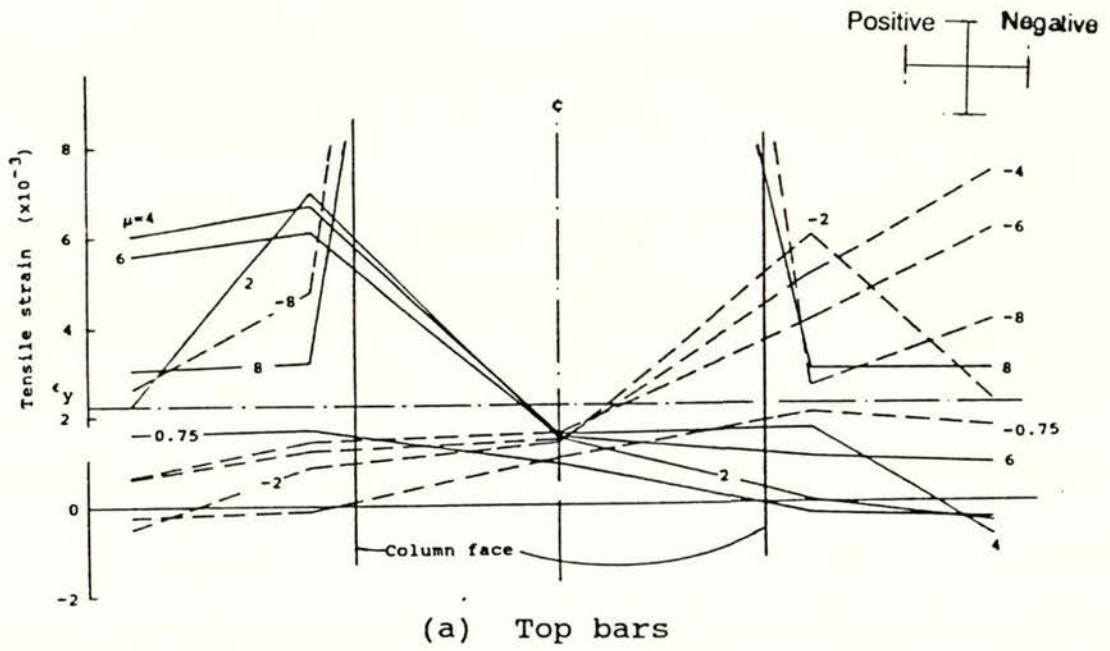
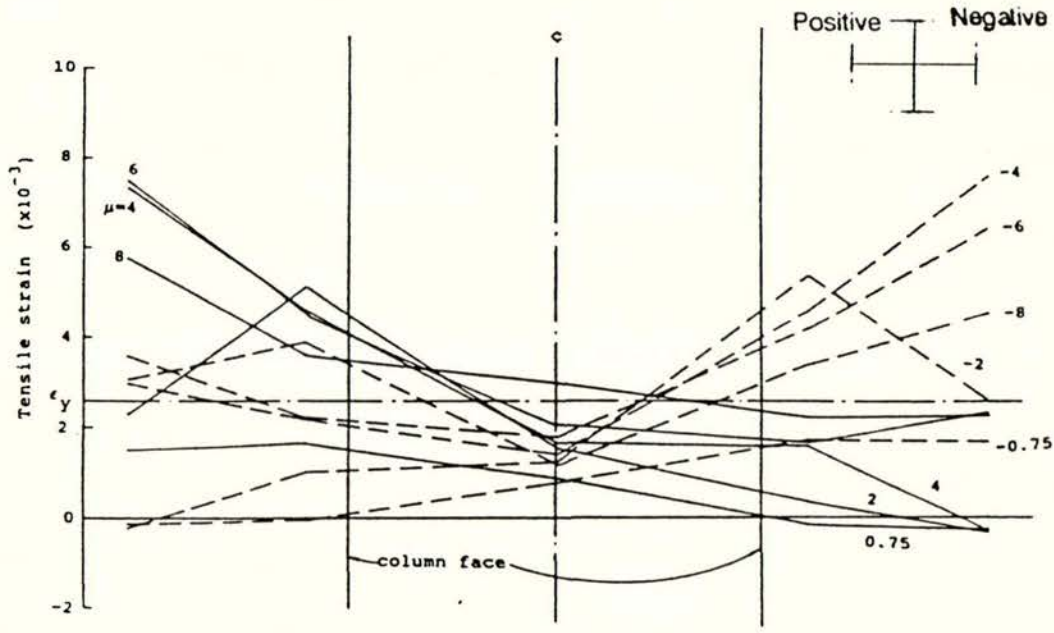
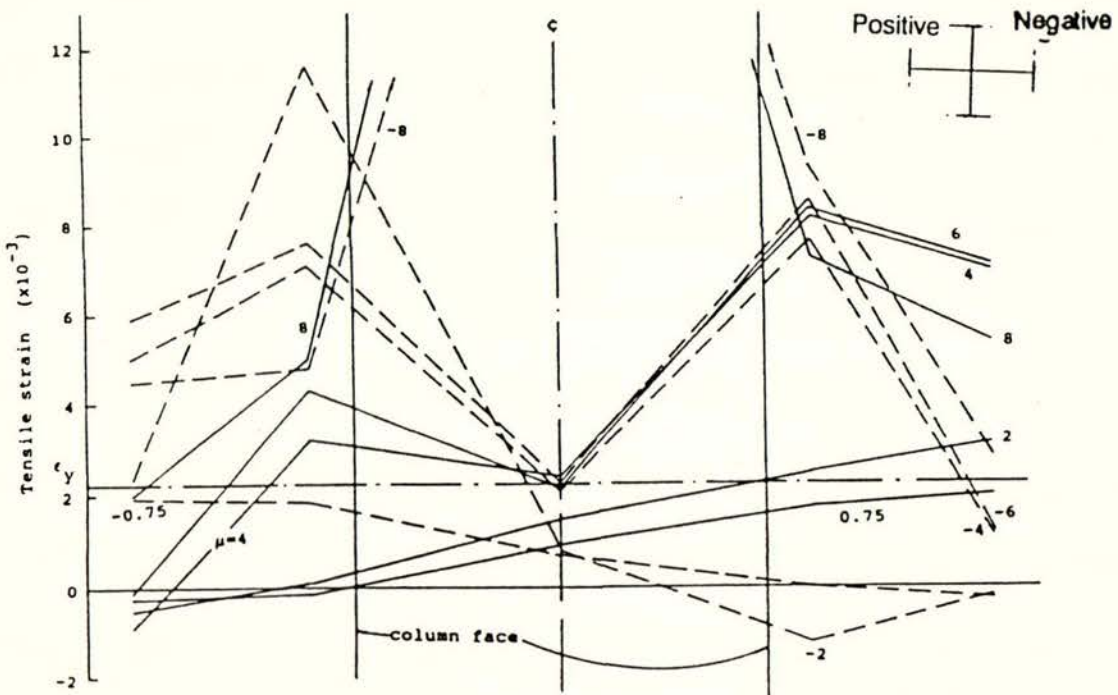


Fig. 5.39 Strain variation along beam bars, Unit 3



(a) Top bars



(b) Bottom bars

Fig. 5.40 Strain variation along beam bars, Unit 4

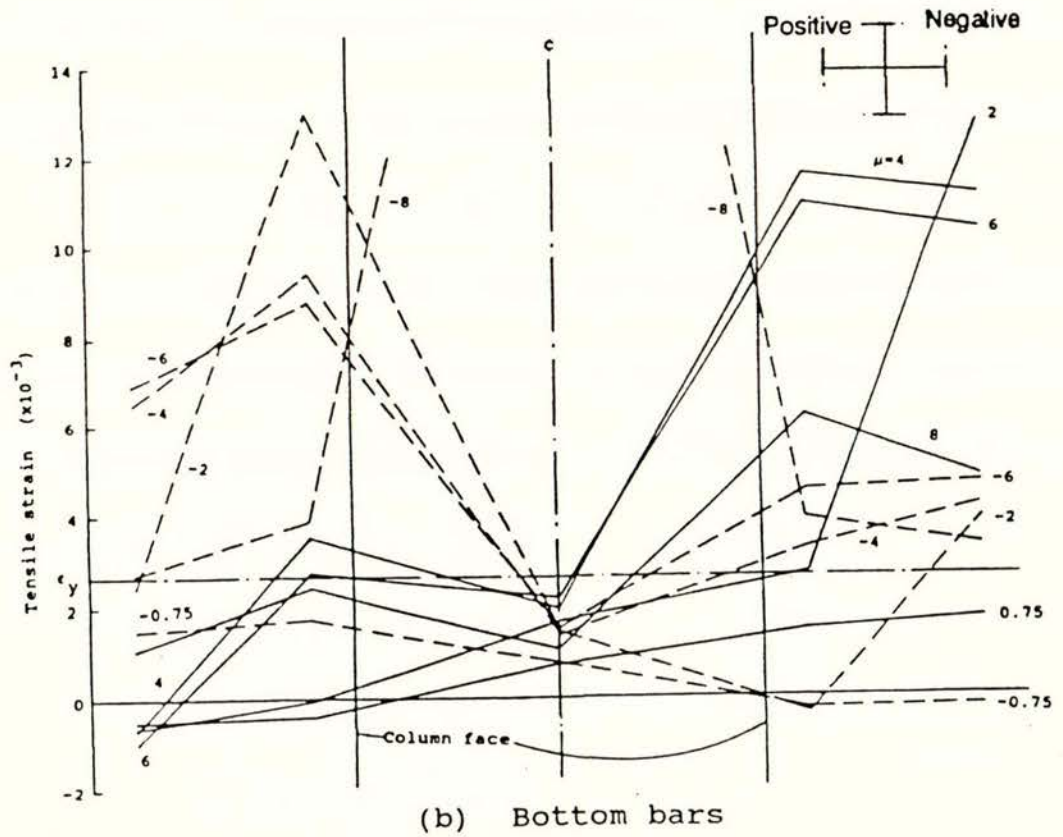
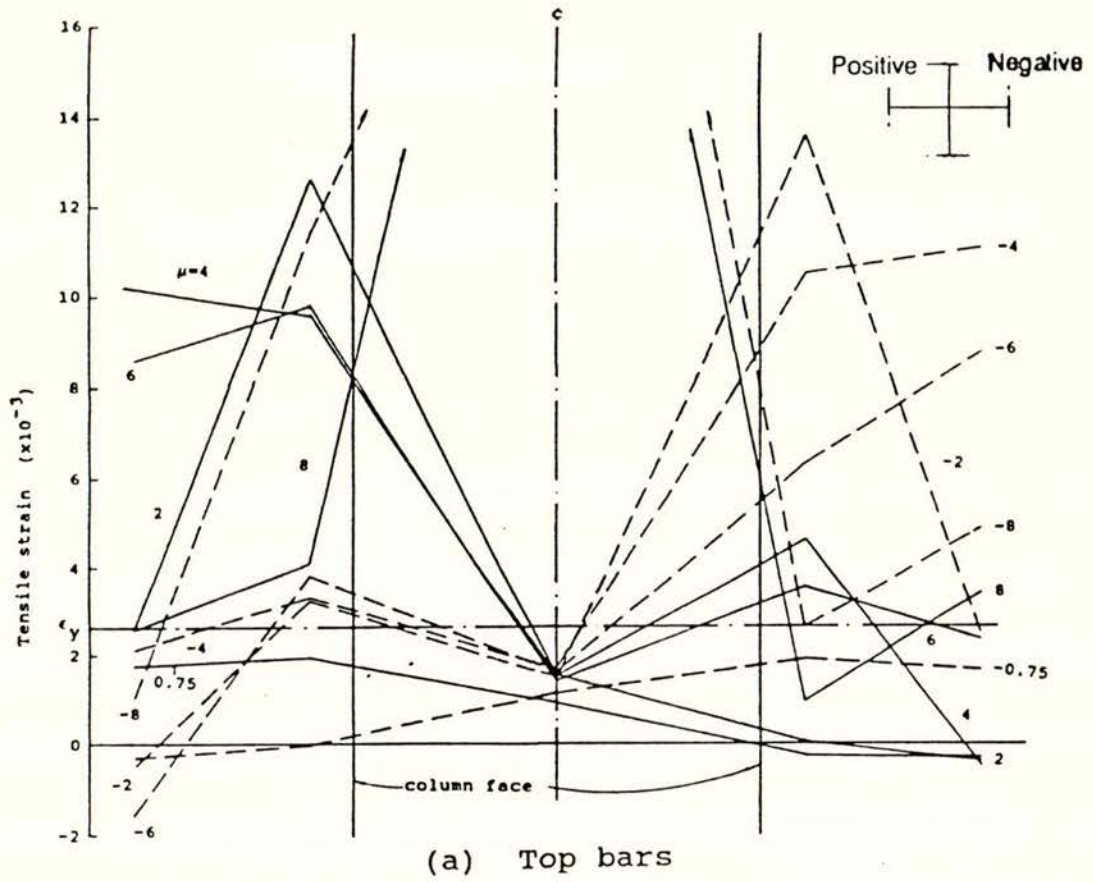


Fig. 5.41 Strain variation along beam bars, Unit 5

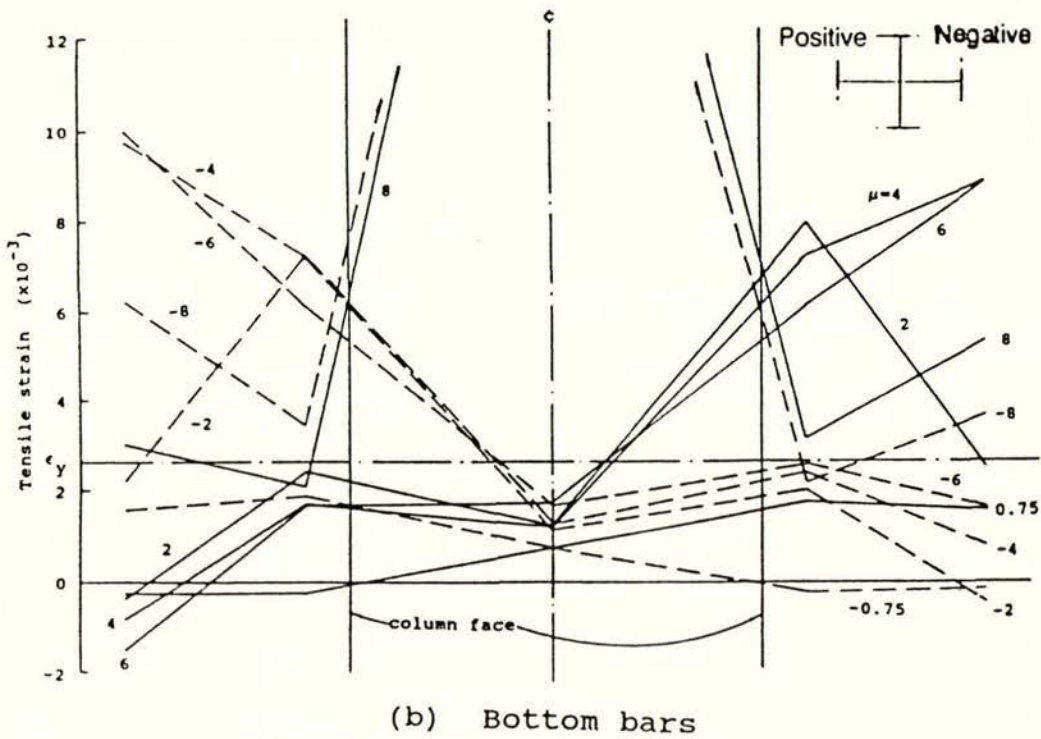
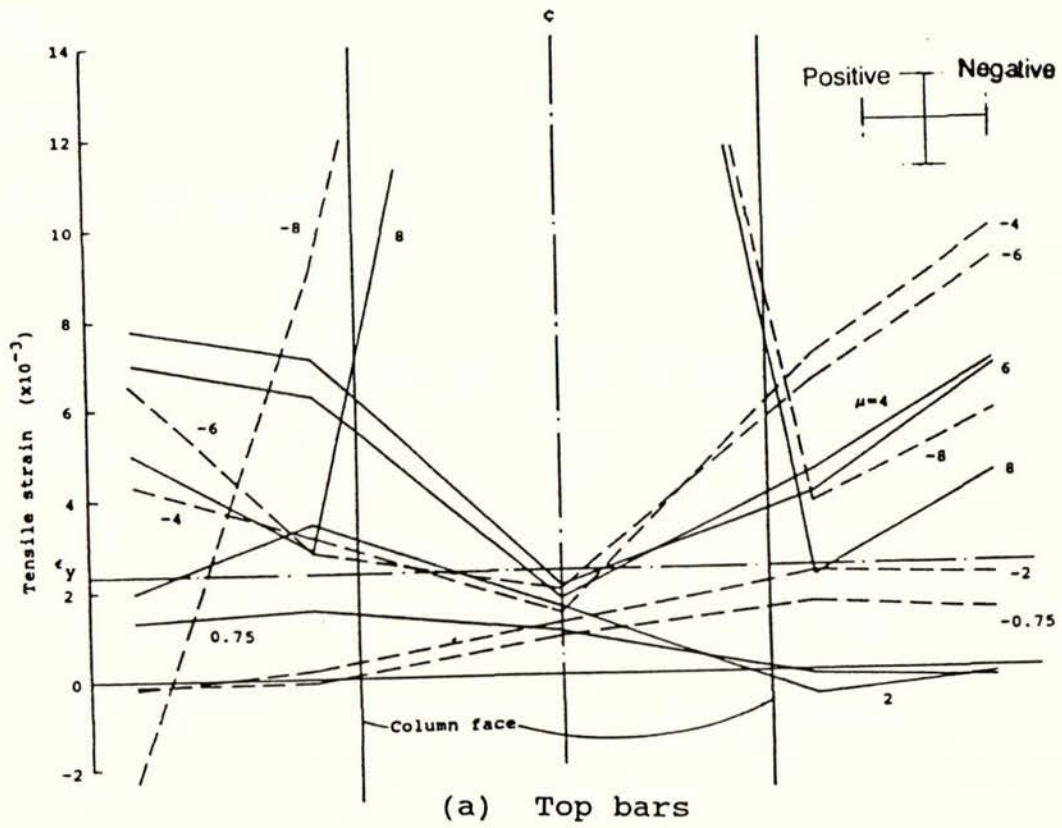


Fig. 5.42 Strain variation along beam bars, Unit 6

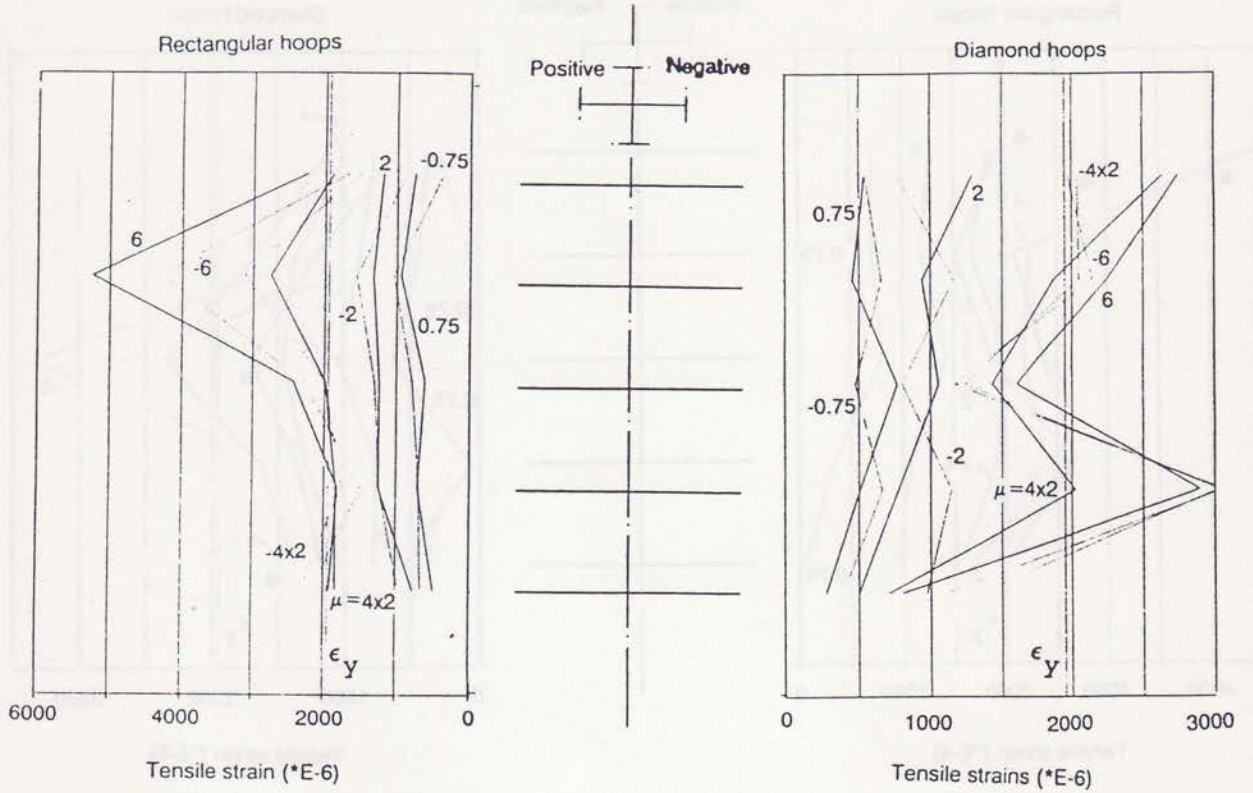


Fig. 5.43 Strain variation of joint core hoops, Unit 1

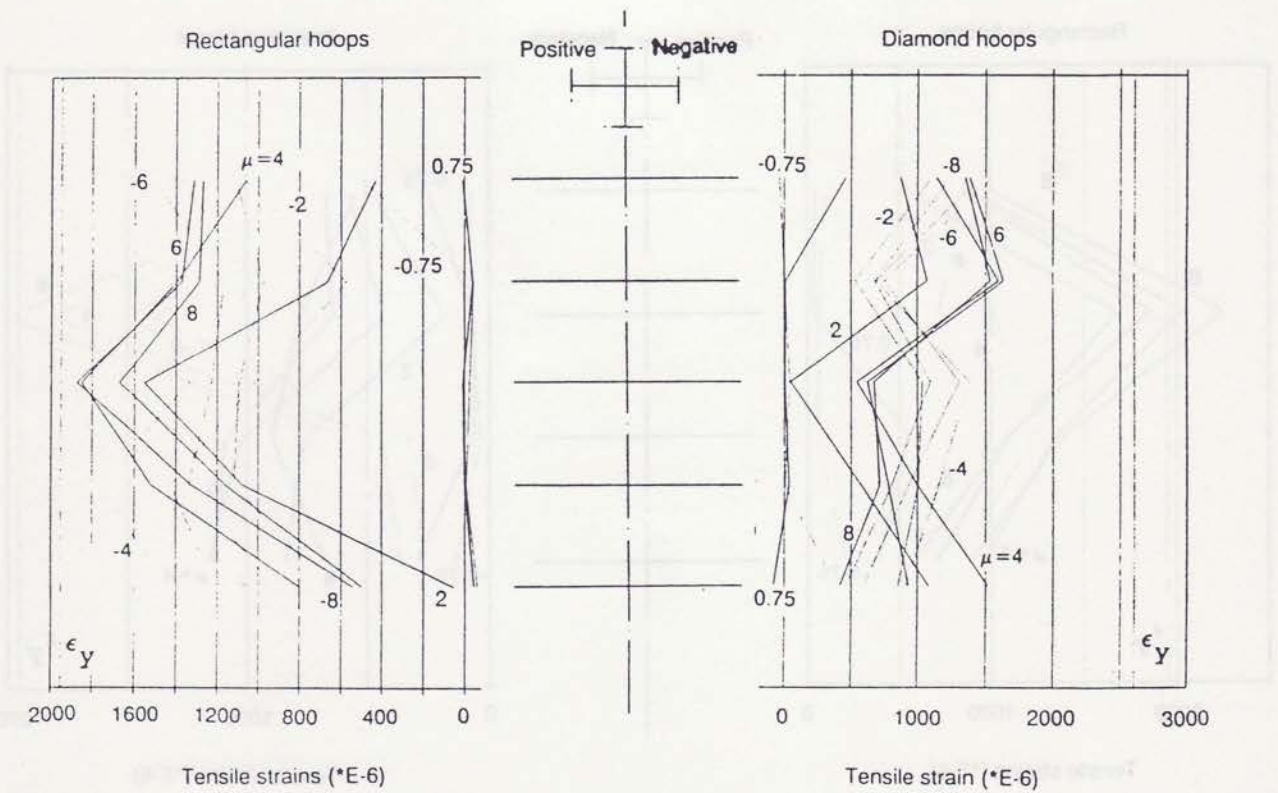


Fig. 5.44 Strain variation of joint core hoops, Unit 2

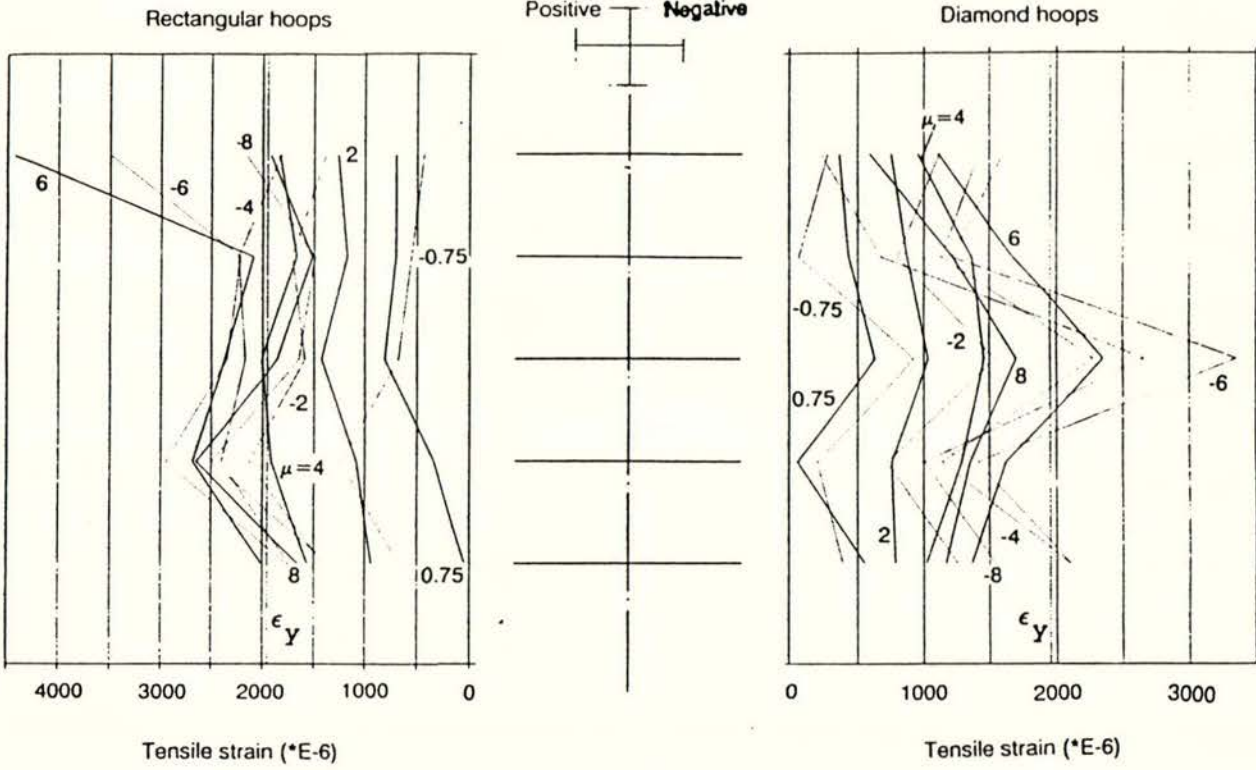


Fig. 5.45 Strain variation of joint core hoops, Unit 3

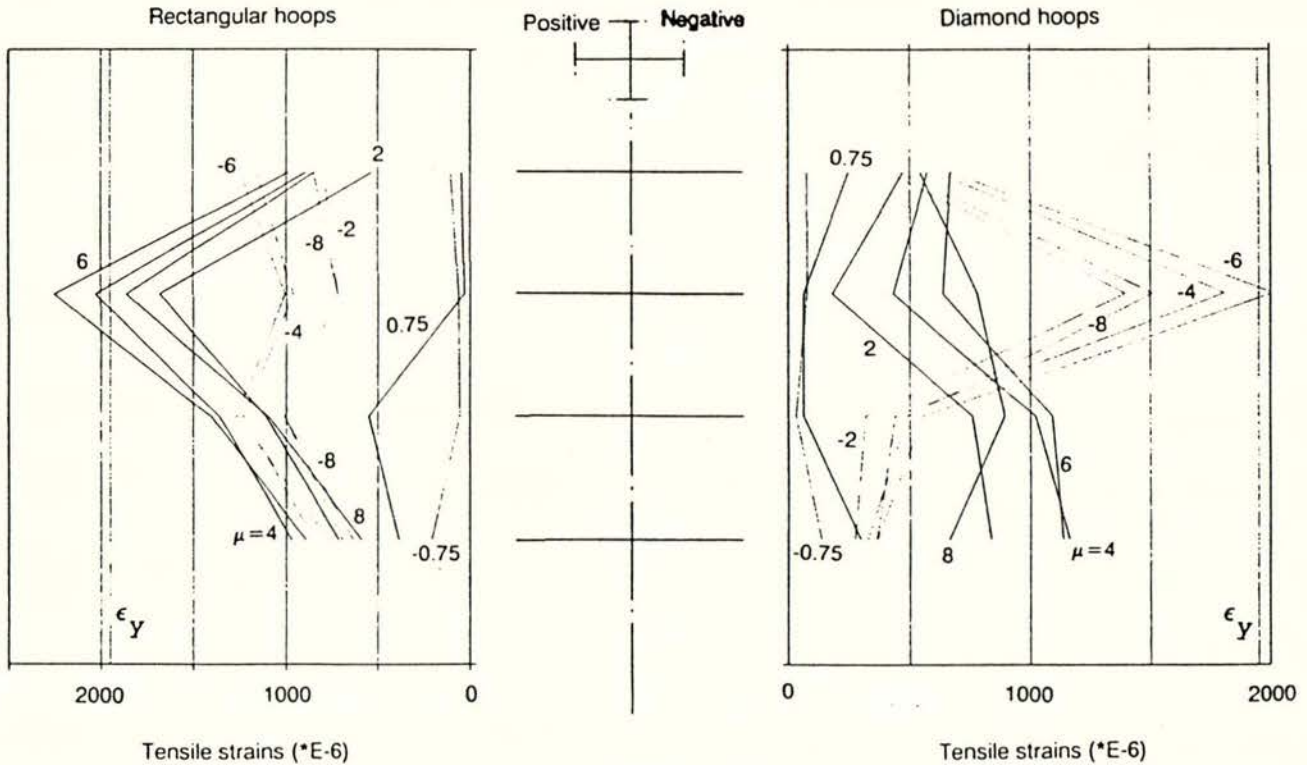


Fig. 5.46 Strain variation of joint core hoops, Unit 4

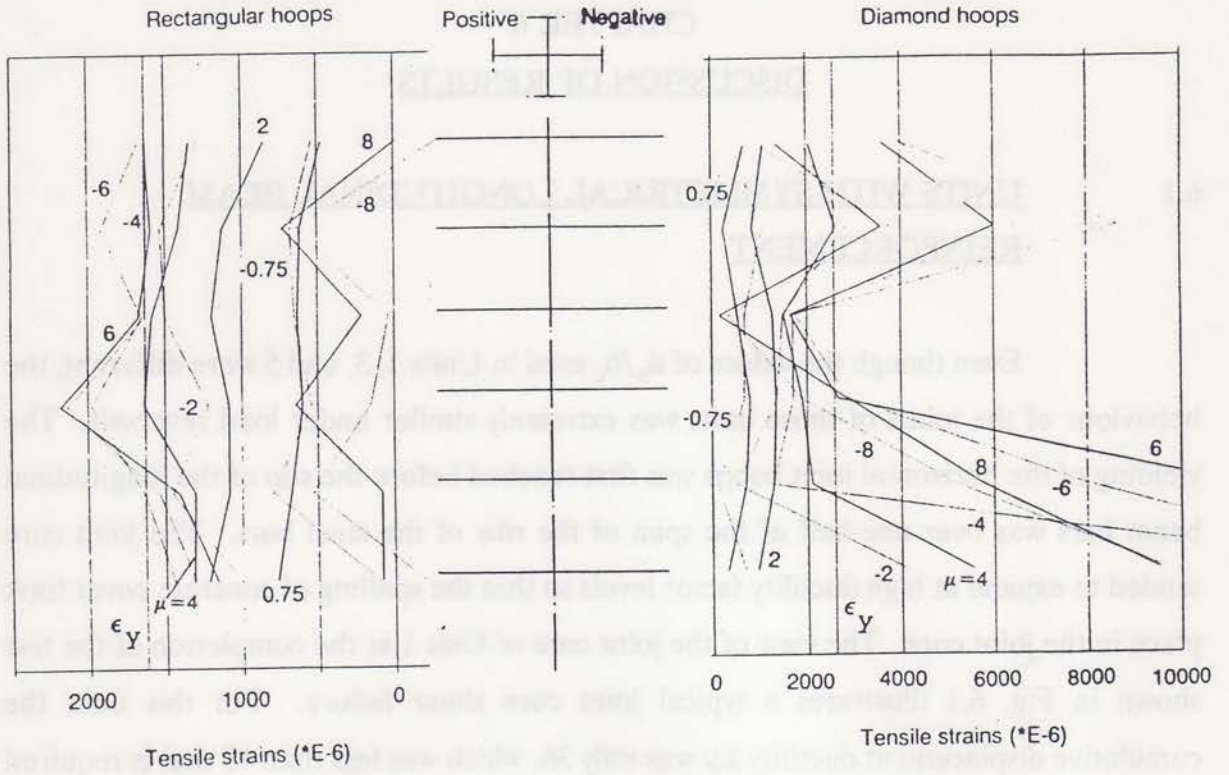


Fig. 5.47 Strain variation of joint core hoops, Unit 5

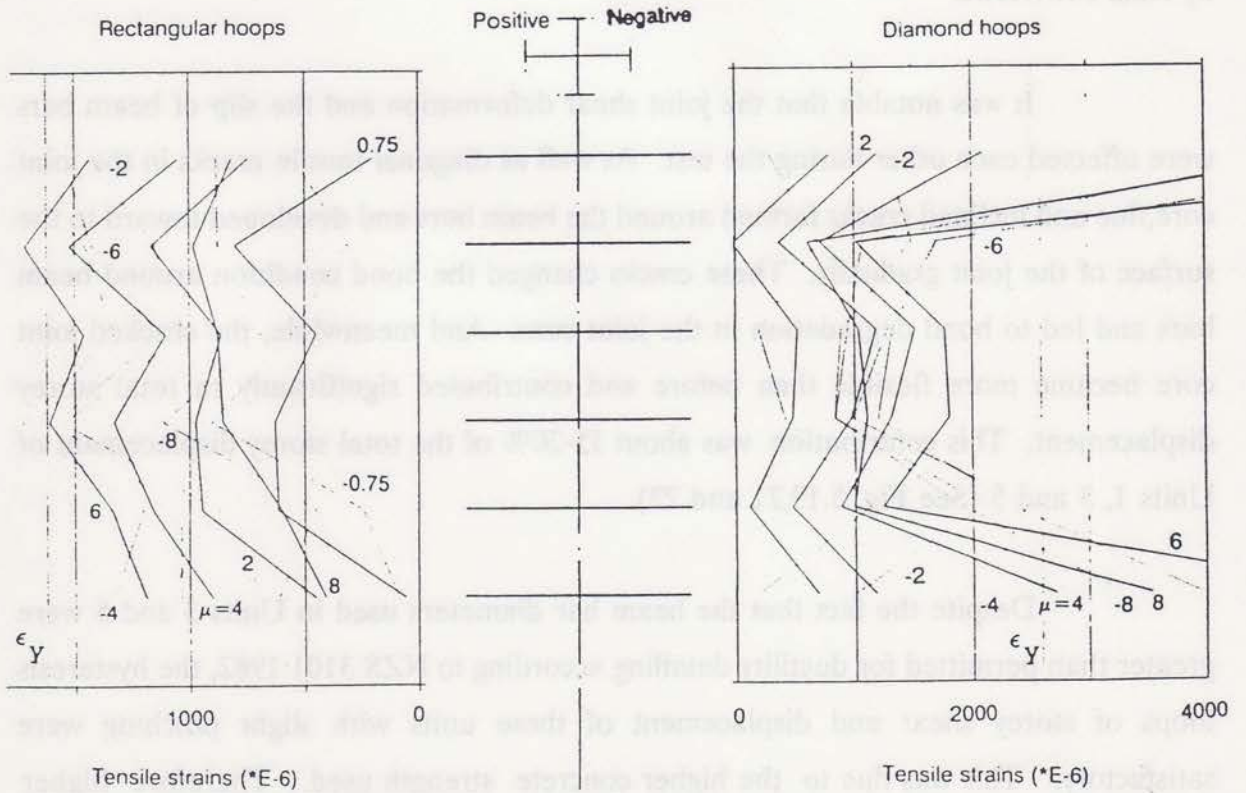


Fig. 5.48 Strain variation of joint core hoops, Unit 6

CHAPTER 6
DISCUSSION OF RESULTS

6.1 UNITS WITH SYMMETRICAL LONGITUDINAL BEAM
REINFORCEMENT

Even though the values of d_b/h_c used in Units 1, 3, and 5 were different, the behaviour of the joints of those units was extremely similar under load reversals. The yielding of the horizontal joint hoops was first reached before the slip of the longitudinal beam bars was over one-half of the span of the ribs of the steel bars. The joint core tended to expand at high ductility factor levels so that the spalling of concrete cover took place in the joint core. The view of the joint core of Unit 1 at the completion of the test shown in Fig. 6.1 illustrates a typical joint core shear failure. For this unit, the cumulative displacement ductility $\Sigma\mu$ was only 36, which was less than 48 that is required for ductile moment resisting reinforced concrete frames before the load carrying capacity reducing by more than 20% according to 2/DZ 4203 [24]. Unit 1, 3, 5 contained 60% and 75%, respectively, of the horizontal and vertical joint shear reinforcement required by NZS 3101:1982.

It was notable that the joint shear deformation and the slip of beam bars were affected each other during the test. As well as diagonal tensile cracks in the joint core, fine and inclined cracks formed around the beam bars and developed toward to the surface of the joint gradually. These cracks changed the bond condition around beam bars and led to bond degradation in the joint core. And meanwhile, the cracked joint core became more flexible than before and contributed significantly to total storey displacement. This contribution was about 15-20% of the total storey displacement of Units 1, 3 and 5 (See Fig. 5.19,21 and 23).

Despite the fact that the beam bar diameters used in Units 3 and 5 were greater than permitted for ductility detailing according to NZS 3101:1982, the hysteresis loops of storey shear and displacement of these units with slight pinching were satisfactory. This was due to the higher concrete strength used. Therefore higher

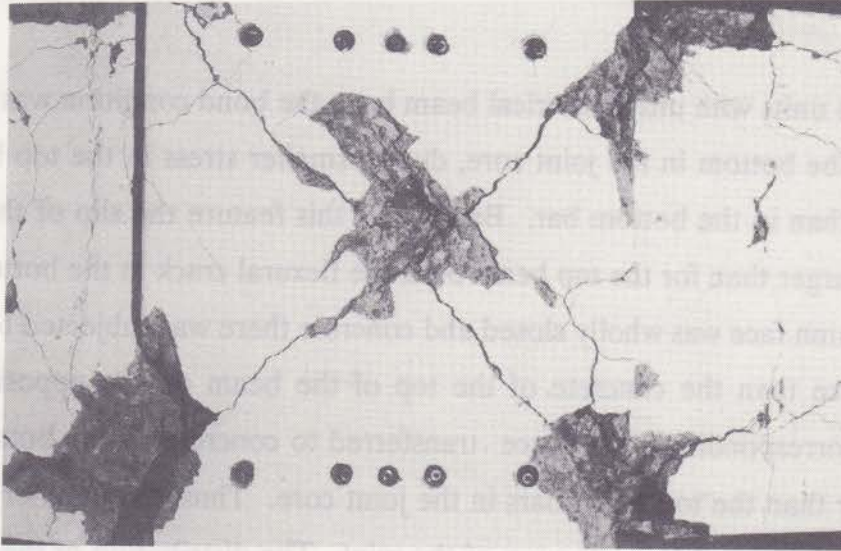


Fig. 6.1 Feature of shear failure in the joint core, unit 1

concrete strength is of benefit to the bond conditions of beam bars in the beam-column joint core. It should be pointed out that slip of beam bars occurred in the joint core from the beginning of loading, as shown in Fig. 5.13 to Fig. 5.18. The process of the slip of the beam bars was an progressive. With increasing of the storey displacement, the slip of beam bars in the joint core became larger. After the yielding of the horizontal joint hoops was reached, the bond strength around the beam bars drastically dropped. This phenomenon was observed in the curves of storey shear and slip of the beam bars.

6.2 UNITS WITH UNSYMMETRICAL LONGITUDINAL BEAM REINFORCEMENT

The ratio of total area of bottom beam bars to top beam bars β was 0.50, 0.64 and 0.50 for Unit 2, 4 and 6, respectively. After yielding of the longitudinal steel, the failure of Units 2, 4 and 6 were due to loss of the bond strength in the joint core under simulated lateral load reversals. Though the horizontal and vertical joint

reinforcement provided of Units 2, 4 and 6 were same as Units 1, 3 and 5 to be respectively 60% and 75% of the requirement in NZS 3101:1982, the joint core region was intact when the slip of bottom beam bars occurred. The contribution to the storey displacement due to the joint shear distortion was about 10% in the core of Units 2, 4 and 6 (See Fig. 5.20, 22 and 24).

The units with unsymmetrical beam bars, the bond condition was better in the top than in the bottom in the joint core, due to smaller stress in the top beam bar in compression than in the bottom bar. Because of this feature the slip of the bottom beam bars was larger than for the top beam bars, the flexural crack at the bottom of the beam at the column face was wholly closed and concrete there was subjected to a larger compression force than the concrete of the top of the beam on the opposite of the column face. Correspondingly, the force transferred to concrete by the bottom beam bars was smaller than the top beam bars in the joint core. Thus, the number of cracks was fewer on the bottom than on the top of the joint. The distribution of the cracks of Unit 2 in the joint region is illustrated in Fig. 5.2(k).

The significant pinching of the hysteresis loops resulted in a reduction in the dissipated energy after the bottom beam bars lost bond strength. The storey displacement suddenly increased without any change in resistance until the crack in the beam at the column face was completely closed at the bottom. Fig. 5.19(b) through Fig. 5.24(b) show that the contribution to the deformation of the beam due to the slip of the beam bars was basically steady in the proportion before the bond was lost wholly. After the loss of the bond, the component due to the slip of the beam bars quickly increased.

The yielding of the bottom beam bars at the middle of the joint and the slip of the bottom beam bars occurred at nearly the same stage. This meant that yield penetration was a major factor leading to the loss of bond strength around beam bars.

Considering the hysteresis loops of Units 2, 4 and 6, it is evident that higher concrete strength can improve the bond condition of beam bars in the beam-column joint

region. The value of β plays an important role and has an effect on the shape of the hysteresis loops.

6.3 COMPARISON OF THE RESULTS

Comparing the hysteresis loops of Units 2 and 3, the effect of the value of β is evident. The smaller the value of β , the more significant is the pinching of the hysteresis loops.

Comparing the hysteresis loops of Units 2 and 6, it is observed that the higher concrete strength, the better the bond condition is in the joint core.

From Table 5.2 and Fig. 5.13 through Fig. 5.18, it is seen that the bond condition is almost same for the top beam bars and for the bottom beam bars in the joint core when $\beta=1$, and that is, better for the top beam bars than for the bottom beam bars in the joint core when $\beta < 1$.

6.4 BOND REQUIREMENT OF BEAM BAR IN AN INTERIOR BEAM-COLUMN JOINT

When bond deterioration progresses in beam bars passing through an interior beam-column joint under severe seismic loading, serious pinching may be observed in horizontal load-deflection curves of the beam-column joint assemblage. Some tests [30] have shown that bond deterioration in those beam bars as a result of yield penetration into the joint core could contribute up to 50% of the overall deflections in beam-column assemblages. To prevent such excessive bond deterioration, when plastic hinges form in the beams at the column faces, the current concrete design code NZS 3101:1982[12] limits the diameter of the beam bar d_b passing through an interior beam-column joint as

$$d_b \leq 12h_c/f_y \quad (6.1)$$

where h_c = column depth parallel to the longitudinal beam bars being considered

f_y = specified yield strength of a beam bar

The above code limit expressed by Eq. 6.1 was derived considering the most severe stress condition attained when beam bars were subjected to overstrength simultaneously in tension at one column face and in compression at the opposite column face [31]. That is, it was assumed that the resultant forces of steel T_1 and C_{s2} in Fig. 6.2 could reach $\alpha f_y A_s$ at the same time, where α = overstrength factor of steel. This situation can occur if the bond condition is extremely good and hence the beam bars do not slip during cyclic loading.

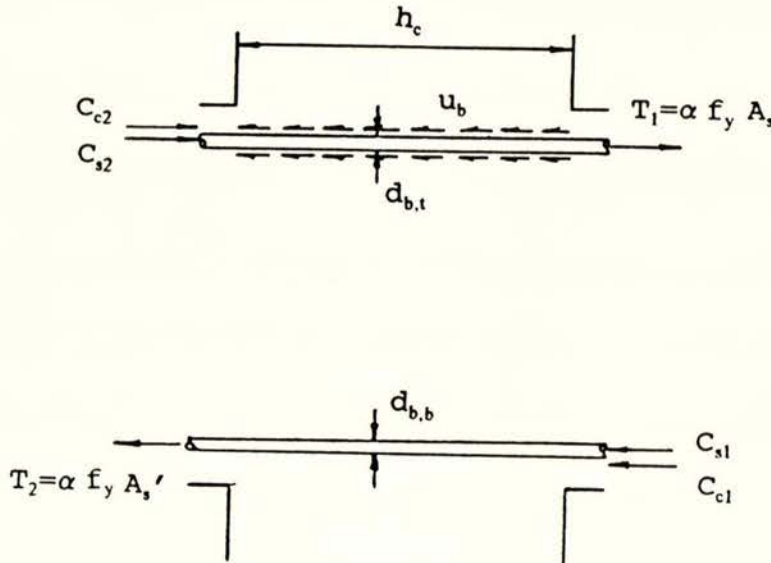


Fig. 6.2 Force acting on the beam bars across an interior beam-column joint core

It is notable that the effect of concrete strength on bond performance is neglected in Eq. 6.1. This is mainly because Eq. 6.1 was based on the experimental studies prior to 1980 in which the specified compressive strength of concrete f'_c had been mostly in a narrow range from 20 MPa to 30 MPa.

Park and Dai [20] have recently conducted tests on one-way beam-column joints subjected to severe simulated seismic loading. Based on these test results, they concluded that some relaxation in the current NZS 3101 [12] requirement for beam bar anchorage in interior beam-column joints would still lead to acceptable performance. The same conclusion has also been reached from the test results obtained in this study as mentioned in Sections 6.1 and 6.2. The main aspects which gave the legitimacy of that conclusion were:

- (a) Although the beam bar diameters used for the test specimens, except for Units 1, 1' and 3', were 32 to 139% larger than those permitted by the current code (see Table 6.2), the observed hysteresis loops of the test units were satisfactory up to the storey drift of at least 3%, which corresponded to displacement ductility factors of 4 to 6.
- (b) In the tests, the compression stress in the beam bars was not likely to exceed f_y , due to bond slip with acceptable magnitude, even in the case that $\beta = A'_s/A_s = 1.0$, where A'_s is the total area of bottom beam bars and A_s is the total area of the top beam bars. As a matter of course, when $\beta \leq 1/\alpha$, the requirements of equilibrium indicate that the compression stress in the top beam bars cannot exceed f_y .
- (c) Some yield penetration into the joint core, as a result of bond deterioration, should be acceptable as long as slip of beam bars in the joint core is not excessive. This is because the effect of pinching of the hysteresis loops of beam-column joint assemblages on the dynamic response of moment resisting frames has been found to be relatively small [eg. 21].
- (d) Bond strength increases approximately in proportion to $\sqrt{f'_c}$ [20,23]. Hence, the higher the compressive strength of concrete is, the better the anchorage condition of beam bars.

Based on the above aspects, design recommendations for the anchorage of

beam bars in interior beam column joints may be derived as follows. Consider a longitudinal beam bar with diameter d_b passing through a column with depth h_c as shown in Fig. 6.2. The tension stress f_s in the beam bars at a column face is considered to reach the over strength αf_y . The compression stress f'_s in the same bars at the opposite column face is considered not to exceed the yield strength of steel f_y , that is, $f'_s = \gamma f_y$ where $\gamma \leq 1.0$. The average ultimate bond stress u_b is assumed to be proportional to the square root of the compressive strength of concrete f'_c , that is, $u_b = K\sqrt{f'_c}$ MPa [20,23], where K is a factor which is determined taking account of the transverse stress condition on the beam bars and the location of those bars as mentioned later. For the equilibrium of the top beam bar shown in Fig. 6.2,

$$T_1 + C_{s2} = \pi d_b h_c u_b \quad (6.2)$$

Eq. 6.2 can be rewritten as

$$(\alpha + \gamma) f_y \frac{\pi}{4} d_b^2 = \pi d_b h_c K\sqrt{f'_c} \quad (6.3)$$

For design use, Eq. 6.3 is written as

$$\frac{d_b}{h_c} \leq \frac{4}{(\alpha + \gamma)} \frac{K\sqrt{f'_c}}{f_y} \quad (6.4)$$

where the values for α , γ and K need to be found. In this stage, those values were determined based on the following consideration.

(A) α Value

The overstrength factor α for Grades 300 and 430 steels may be estimated as 1.25 as specified in the Amendment No. 1:1989 to NZS 3101 Part 2. As an alternative, α may be determined by conducting tensile tests on the steel used. Actually, α values obtained from the tensile tests on Grade 430 steel units for Units 1 to 6 were all higher than the value specified in the code, and were 1.35 in average (see Table 6.1).

(B) γ Value

It is not necessary to take γ value as more than 1.0 and $\gamma - 1.0$ may be used for simplicity in Eq. 6.4. However, a smaller value of γ may be used by taking the following aspects into account.

Cheung, Paulay and Park [22,23] have conducted severe seismic loading tests on interior beam-column-slab assemblages. They found that the compression stress in the top beam bars was unlikely to exceed $0.7 f_y$ due to bond slip with acceptable magnitude after a few cycles of stress reversals. Based on this finding, it could be assumed that $\gamma \leq 0.7$ for the top beam bars. In addition, since $C_{s2} = \gamma f_y A_s \leq T_2 = \alpha f_y A_s'$ in Fig. 6.2,

$$\gamma \leq \alpha\beta$$

From the above, for top beam bars

$$0.7 \geq \gamma \leq \alpha\beta \quad (6.5)$$

If the yield strengths and the overstrength factors are different between top and bottom bars as in the case listed in Table 6.1, Eq. 6.5 is modified as

$$0.7 \geq \gamma \leq \alpha_b \beta f_{yb}/f_{yt} \quad (6.6)$$

where α_b = overstrength factor of bottom bar steel
 f_{yb} = yield strength of bottom bar steel
 f_{yt} = yield strength of top bar steel

The bottom beam bars can be subjected to higher stress in compression, when β is much less than unity, from the equilibrium. Hence, γ for the bottom bars may be approximated as 1.0 when β is, say, less than 0.75. When β is more than 0.75, γ may be reduced to 0.7 in inverse proportion to β . Hence, for the bottom beam bars,

$$\gamma = 1.0 \text{ when } \beta \leq 0.75 \quad (6.7)$$

may be assumed.

$$\gamma = 0.7 + 1.2 (1-\beta) \text{ when } 1 \geq \beta > 0.75 \quad (6.8)$$

(C) K Value

In this study, a basic value of K denoted as K_o is estimated based on the average ultimate bond stress u_b implicitly assumed in Eq. 6.1. It can be assumed that Eq. 6.1 corresponds to Eq. 6.4 when f'_c is as low as 25 MPa and γ is equal to 1 [23]. In this case, substituting $f'_c = 25$ MPa, $\alpha = 1.25$ and $\gamma = 1$ into Eq. 6.4, $d_b/h_c \leq 8.89 K/f_y$ and the right hand term is equivalent to $12/f_y$ in Eq. 6.1. Thus, $K = K_o = 12/8.89 = 1.35$ is obtained. In this study, K_o is used as a basic value of K for the bottom beam bars passing through the joint core and K is modified by taking the following factors into account.

Normally concrete placed in-situ is cast up to the level of the top surface of beams including the beam-column joint area. Hence, the bond condition of top beam bars are worse than that of bottom beam bars due to sedimentation of concrete. To take this factor into account for the top beam bars, K is reduced by multiplying $\xi_t = 0.85$ when more than 300 mm of fresh concrete is cast underneath those bars, based on the previous studies [23,31].

When axial loads of columns are high, such loads will effectively confine the beam bars in the joint core and, as a result, increase the bond strength. To take this factor into account, the value of K can be increased by multiplying by ξ_p [31] where

$$1.0 \leq \xi_p = \frac{P_u}{2f'_c A_g} + 0.95 < 1.25 \quad (6.9)$$

In the case of a two-way frame, the detrimental effects resulting from the formation of simultaneous plastic hinges in the beams at all four faces of a column may need to be taken into account [23]. However, this factor is not included in this study which considered one-way frames.

By combining the above factors, K is expressed as

$$K = \xi_t \xi_p K_o \quad (6.10)$$

Thus Eq. 6.4 can be rewritten as

$$\frac{d_b}{h_c} \leq \frac{4}{(\alpha+\gamma)} \frac{\xi_t \xi_p K_o \sqrt{f'_c}}{f_y} \quad (6.11)$$

For simplicity, Eq. 6.11 may be expressed as

$$\frac{d_b}{h_c} \leq \frac{\xi_t \xi_p K_m \sqrt{f'_c}}{\xi_m \alpha f_y} \quad (6.12)$$

$$\text{where } K_m = 4 K_o$$

$$\xi_m = \left(1 + \frac{\gamma}{\alpha}\right)$$

K_m is approximated as 5.4 assuming $K_o = 1.35$.

The above bond criteria for top and bottom beam bars given by Eq. 6.12 were applied to Units 1 to 6 tested in this study and also Units 1' to 4' tested by Park and Dai [20]. As can be seen from Table 6.2, the use of Eq. 6.12 in design would result in satisfactory performance during severe seismic loading. That is, for the test units which satisfied Eq. 6.12, no significant pinching of the hysteresis loops were observed before ductility displacement factors of 6 were reached.

As a reference, the values of d_b/h_c limited by the bond criterion proposed by Kitayama et al [21] are also listed in Table 6.2. This bond criterion appears to be inadequate to ensure satisfactory behaviour of beam-column joints designed for full ductility.

TABLE 6.1 Steel and Concrete Properties of Test Units

Investigator	Test Unit	f'_c in MPa	Top Beam Bars f_{yt} in MPa (α_t)	Bottom Beam Bars f_{yb} in MPa (α_b)	β (A'_s/A_s)
Xian Zuo Xin	Unit 1	30.9	453 (1.36)	453 (1.36)	1.0 (7HD12/7HD12)
	Unit 2	40.8	445 (1.36)	445 (1.36)	0.5 (2HD16/4HD16)
	Unit 3	42.5	445 (1.35)	445 (1.36)	1.0 (4HD16/4HD16)
	Unit 4	47.2	492 (1.35)	445 (1.36)	0.64 (2HD16/2HD20)
	Unit 5	60.7	492 (1.35)	492 (1.35)	1.0 (3HD20/3HD20)
	Unit 6	59.3	463 (1.33)	492 (1.35)	0.51 (2HD20/2HD28)
Dai Ruitong	Unit 1'	45.9	294 (1.48)	294 (1.48)	0.4 (2D16/5D16)
	Unit 2'	36.0	314 (1.54)	300 (1.49)	0.51 (2D20/2D28)
	Unit 3'	36.2	294 (1.48)	294 (1.48)	0.4 (2D16/5D16)
	Unit 4'	40.1	314 (1.54)	300 (1.49)	0.51 (2D20/2D28)

TABLE 6.2 Performance and Bond Conditions of Test Units

Investigator	Test Unit	Shape of Hysteresis Loops	Actual d_b/h_c		$\frac{d_b}{h_c} = \frac{\xi_p \xi_t K_m}{\xi_m \alpha} \frac{\sqrt{f'_c}}{f_y}$		NZ Code		$\frac{d_b}{h_c} = 3.2 \frac{\sqrt{f'_c}}{f_y}$	
			(a) Top Beam Bars (b) Bottom Beam Bars	(a) Top Beam Bars (b) Bottom Beam Bars	(a) Top Beam Bars (b) Bottom Beam Bars	(a) Top Beam Bars (b) Bottom Beam Bars	(a) Top Beam Bars (b) Bottom Beam Bars			
Xian Zuo Xin	Unit 1	Slight pinching after $\mu = 6$	(a) 1/37.5 (b) 1/37.5	(a) 1/31.0 (b) 1/31.0	(a) 1/37.8 (b) 1/37.8	(a) 1/25.5 (b) 1/25.5				
	Unit 2	Significant pinching after $\mu = 4$	(a) 1/28.1 (b) 1/28.1	(a) 1/26.4 (b) 1/30.5	(a) 1/37.1 (b) 1/37.1	(a) 1/21.8 (b) 1/21.8				
	Unit 3	Slight pinching after $\mu = 6$	(a) 1/28.1 (b) 1/28.1	(a) 1/26.0 (b) 1/26.0	(a) 1/37.1 (b) 1/37.1	(a) 1/21.3 (b) 1/21.3				
	Unit 4	Significant pinching after $\mu = 6$	(a) 1/22.5 (b) 1/28.1	(a) 1/27.2 (b) 1/28.5	(a) 1/41.0 (b) 1/37.1	(a) 1/22.4 (b) 1/20.2				
	Unit 5	Slight pinching after $\mu = 6$	(a) 1/22.5 (b) 1/22.5	(a) 1/24.0 (b) 1/24.0	(a) 1/38.6 (b) 1/41.0	(a) 1/18.8 (b) 1/20.0				
	Unit 6	Significant pinching after $\mu = 6$	(a) 1/16.1 (b) 1/22.5	(a) 1/22.7 (b) 1/27.8	(a) 1/38.6 (b) 1/41.0	(a) 1/18.8 (b) 1/20.0				
Dai Ruitong	Unit 1'	Spindle type fat loops	(a) 1/25.4 (b) 1/25.4	(a) 1/16.7 (b) 1/20.0	(a) 1/24.5 (b) 1/24.5	(a) 1/13.6 (b) 1/13.6				
	Unit 2'	Slight pinching after $\mu = 5$	(a) 1/14.5 (b) 1/20.3	(a) 1/21.7 (b) 1/23.0	(a) 1/26.2 (b) 1/25.0	(a) 1/16.4 (b) 1/15.6				
	Unit 3'	Spindle type fat loops	(a) 1/25.4 (b) 1/25.4	(a) 1/18.7 (b) 1/22.5	(a) 1/24.5 (b) 1/24.5	(a) 1/13.6 (b) 1/13.6				
	Unit 4'	Slight pinching after $\mu = 5$	(a) 1/14.5 (b) 1/20.3	(a) 1/20.5 (b) 1/21.9	(a) 1/26.2 (b) 1/25.0	(a) 1/16.4 (b) 1/15.6				

Note: The test units were all cast in the horizontal position and hence the depth of fresh concrete cast underneath the top and bottom beam bars was all less than 300 mm.

CHAPTER 7

CONCLUSIONS AND SUGGESTIONS7.1 CONCLUSIONS

(1) The effect of the concrete cylinder strength on the bond-slip of longitudinal beam bars passing through the joint core is very significant. With an increase in concrete strength, the requirement for limitation of bar diameter of longitudinal beam bars in the interior beam-column joint can be relaxed.

(2) With the change of the ratio of total area of longitudinal bottom beam bars to top beam bars, the bond condition of the top and bottom beam bar in the joint core will be changed. It is necessary that the limitation of beam bar diameters required for the top and bottom beam bars may be different.

(3) Higher strength of steel does not lead to the serious bond-slip of beam bars in an interior beam-column joint under load reversals if higher concrete strength and a suitable value of β are used. It is suggested that the concrete cylinder strength be not lower than 30 MPa when $f_y = 430$ MPa. Otherwise, the smaller beam bar diameter needed may cause undue construction difficulties.

(4) When plastic hinges form in the beams close to the column faces, and the column axial load is zero or less than $0.1f'_c A_g$, where $A_g =$ gross area of the column and $f'_c =$ concrete compressive cylinder strength, it is recommended that the following equation be used for the limitation of the diameter of the longitudinal beam bars passing through interior joints of ductile frames.

$$\frac{d_b}{h_c} \leq \frac{\xi_t \xi_p K_m \sqrt{f'_c}}{\xi_m \alpha f_y}$$

The symbols are explained in Section 6.4 and Notation.

7.2 SUGGESTIONS FOR FUTURE RESEARCH

- (1) The optimum value of β an interior beam-column joint of a reinforced concrete moment-resisting ductile frame, from the point of view of reducing serious bond-slip of beam bars in the joint and minimizing construction cost needs further investigate.
- (2) Further study is needed to determine how much force of beam bars can be transferred to a joint core by concrete in the compressive zone after full depth beam cracks have occurred adjacent to the column faces.
- (3) Study of deformation shapes to reduce bond-slip of deformed longitudinal bars in interior beam-column joints during cycle loading reversals is needed.

APPENDIX A: THEORETICAL PREDICTION OF THE STRENGTH AND FIRST YIELD DISPLACEMENT OF TEST UNITS

A.1 THEORETICAL STRENGTHS OF UNITS

Fig. 4.2 to 4.7 show the dimensions and reinforcing details for six test units. Measured material properties are listed in Table 4.1 and 4.2 also. The theoretical strengths of units were calculated based on the measured material strengths but ignoring strain hardening of steel, and assuming an extreme fibre concrete compressive strain of 0.003, a rectangular concrete compressive stress block with a mean stress of $0.85f'_c$ and a strength reduction factor $\phi = 1.0$. The design procedure of NZS 3101 for the beam-column joint was fully followed.

The theoretical flexural strengths of the beams and theoretical storey shear strength are given for each unit in Table A.1. The nominal horizontal shear stress in the joint was $0.17f'_c$, $0.1f'_c$, $0.12f'_c$, $0.08f'_c$, $0.11f'_c$, and $0.11f'_c$, respectively.

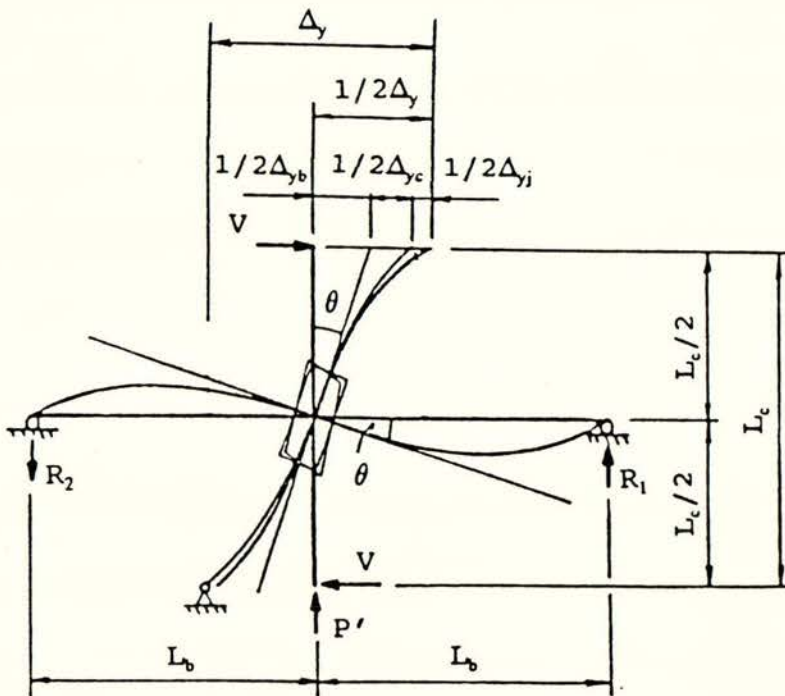


Fig. A.1 Components contribution to storey displacement of the unit

Table A.1 Theoretical flexural and shear strengths of units

Unit	1	2	3	4	5	6
M_{u1} KNm	146	81	154	82	200	137
M_{u2} KNm	146	154	154	135	200	243
V_i KN	136	109	143	101	186	176

A.2 CALCULATION OF FIRST YIELD DISPLACEMENT [19]

As outlined in Section 5.4, the storey displacement consists of three components, namely the deformations of the beam, column and joint core as shown in Fig. A.1. Thus, the first storey displacement is expressed by following,

$$\Delta_{1y} = \Delta_{yb} + \Delta_{yc} + \Delta_{yj} \quad (\text{A.1})$$

(a) Δ_{yb} is component due to flexural and shear deformations of the beam. It is evident from Fig. A.1 that

$$\Delta_{yb} = \theta L_c \quad (\text{A.2})$$

where

$$\theta = \frac{M_{u2} L_b (1 + \beta_i^b)}{3E_c I_{cr}^b} \quad (\text{A.3})$$

$$\beta_i^b = \frac{6\kappa E_c I_{cr}^b}{GA^b L_b^2} \quad (\text{A.4})$$

where I_{cr}^b is moment of inertia of cracked beam section, assumed to be $0.5I^b$ where I^b is the moment of inertia of the gross (uncracked) beam section. G is shear modulus of concrete which can be assumed to be $0.4E_c$. Hence Δ_{yb} is given by

$$\Delta_{yb} = \frac{M_{u2} L_b L_c (1 + \beta_i^b)}{3E_c I_{cr}^b} \quad (A.5)$$

(b) Δ_{yc} is the component due to flexural and shear deformations of the column. It is evident from Fig.A.1 that

$$\Delta_{yc} = \frac{V_i L_c^3 (1 + \beta_i^c)}{12E_c I_{cr}^c} \quad (A.6)$$

where

$$\beta_i^c = \frac{24\kappa E_c I_{cr}^c}{GA^c L_c^2} \quad (A.7)$$

and I_{cr}^c is moment of inertia of cracked column section, assumed to be $0.6I^c$ where I^c is the moment of inertia of the gross (uncracked) column section.

(c) Δ_{yj} is the component due to shear distortion of the joint core. Fig.A.2 shows that

$$\Delta_{yj} = \gamma(L_c - h_b) \quad (A.8)$$

where

$$\gamma = \frac{(\delta + \delta')d'}{2h'b'} \quad (A.9)$$

and δ , δ' , d' , h , and b , are shown in Fig.A.2, and h_b is depth of the beam section. The value of δ and δ' were found from measurements made on the joint core during testing.

A.3 THEORETICAL FIRST YIELD DISPLACEMENT

Table A.2 lists the values of the theoretical first yield displacement Δ_y for all units. The component due to shear distortion of the joint core was estimated to be 20% of total first yield displacement, i.e., $\Delta_{yj} = 0.2\Delta_y$.

Table A.2 Values of the theoretical first yield displacement

Unit	1	2	3	4	5	6
Δ_{yb} (mm)	5.77	5.45	5.21	4.56	5.74	7.01
Δ_{yc} (mm)	4.27	3.24	3.89	2.75	4.44	4.21
Δ_{yj} (mm)	2.512	2.172	2.274	1.826	2.546	2.804
Δ_y (mm)	12.56	10.86	11.37	9.13	12.73	14.02

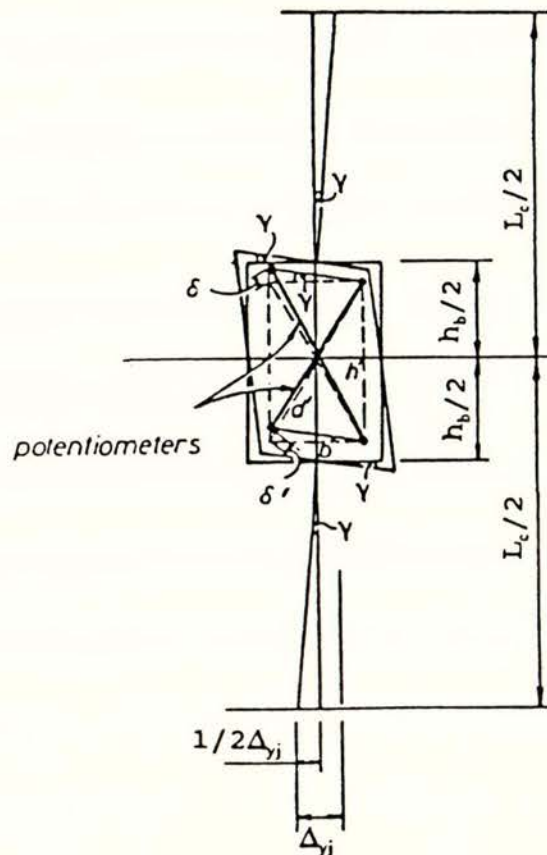


Fig.A.2 Component of displacement due to distortion of the joint core

APPENDIX B: ESTIMATED DEFORMATION OF THE BEAM

The contribution to the 1 storey displacement from the deformation of beams is determined from the measured average curvatures over segments of the beam of 2 times the beam depth, i.e. 1000 mm. In this project, each beam was divided into six segments. Five pairs of linear potentiometers and clip gauges were arranged on Segment 1 to Segment 5 to measure curvatures over the plastic hinge region. A value of an average rotation θ_n of any segment is given by the following equation,

$$\theta_n = \frac{\Delta S_n - \Delta S_n'}{h_n} \quad (\text{B.1})$$

The deformation of any segment is

$$\Delta_{b,n} = \frac{L_c}{L_b} l_n \theta_n \quad (\text{B.2})$$

The component Δ_b due to deformation of beams is calculated as below,

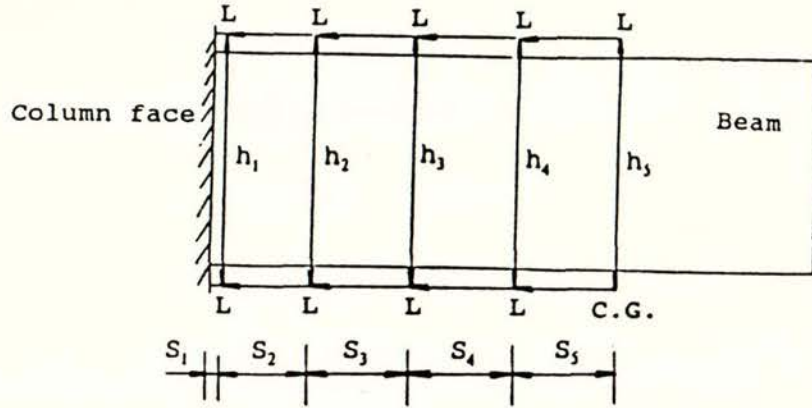
$$\Delta_b = \frac{L_c}{L_b} \left(\sum_{n=1}^5 l_n \theta_n \right) \quad (\text{B.3})$$

The symbols in above equations are defined in section of NOTATION and in Fig. B.1.

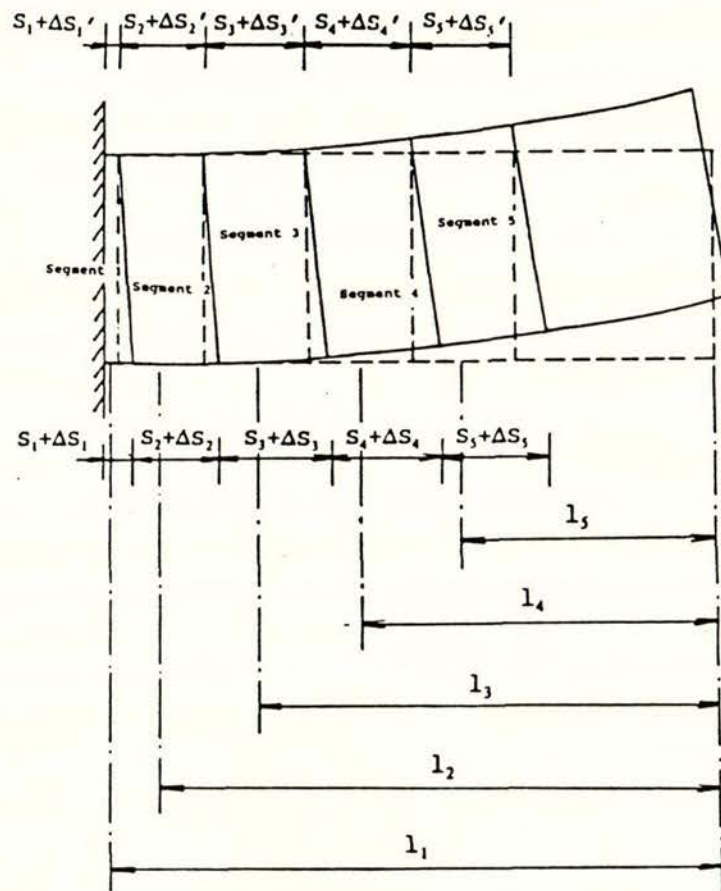
In above, it is considered that the contribution of Segment 1 to the storey displacement is mainly from the elongation of the beam bar and local slip or slip of the beam bar from the joint core.

C.G. - Clip gauge

L ---- Linear potentiometre



(a) before deformation of beam



(b) after deformation of beam

Fig. B.1 Deformation of beam